

# Transportation Research Center



"An Industry, Agency & University Partnership"



Mississippi Department  
of Transportation



U.S. Department  
of Transportation  
Federal Highway  
Administration

## Chip and Scrub Seal Field Test Results for Hwy 17 and Hwy 35

Final Report

FHWA/MS-DOT-RD-09-202-Vol II

Written and Performed By:

Isaac L. Howard, PhD-Mississippi  
State University

December 9, 2009



CIVIL & ENVIRONMENTAL  
ENGINEERING

## Technical Report Documentation Page

1. Report No. FHWA/MS-DOT-RD-09-202-Vol II	2. Government Accession No.	3. Recipient's Catalog No.	
4. Title and Subtitle Chip and Scrub Seal Field Test Results for <i>Hwy 17</i> and <i>Hwy 35</i>		5. Report Date December 9, 2009	
		6. Performing Organization Code	
7. Author Isaac L. Howard, PhD, Assistant Professor, Mississippi State University		8. Performing Organization Report No.	
9. Performing Organizations Name and Address Mississippi State University Civil and Env. Engineering Dept. 501 Hardy Road: P O Box 9546 Mississippi State, MS 39762		10. Work Unit No. (TRAIS)	
		11. Contract or Grant No.	
12. Sponsoring Agency Name and Address Mississippi Department of Transportation Research Division PO Box 1850 Jackson, MS 39215-1850		13. Type of Report and Period Covered  Final Report	
		14. Sponsoring Agency Code	
Supplementary Notes: Work performed under Mississippi State University research project titled: Laboratory and Field Study of Chip and Scrub Seals for Development of Asphalt Pavement Maintenance Toolbox. The project was performed under Mississippi Department of Transportation State Study 202. The results of the research are contained in multiple volumes, of which this report is Volume II (Vol II).			
16. Abstract  This report contains field test results from two pavements located in Mississippi containing chip seals and scrub seals. Limestone aggregate from the same source was used with PASS-CR emulsion. The pavements were tested at three intervals. One or both of the pavements were tested for: aggregate retention, skid resistance, cracking, bleeding/flushing, rutting, roughness, and structural integrity via a Falling Weight Deflectometer (FWD). Analysis consisted of data interpretation focusing on trends and statistical analysis using existing methods with exception of FWD data. FWD data was analyzed with a method developed for this research that combined key elements from methods of Arkansas, North Carolina, and Texas. Test results showed scrub seals to out perform chip seals. Test results also provided information related to construction practices that were compared to best practices recently released in the form of a national synthesis			
17. Key Words Chip Seals, Scrub Seals, Field Performance, FWD, Falling Weight Deflectometer, Skid Resistance, Aggregate Retention		18. Distribution Statement Unclassified	
19. Security Classif. (of this report) Unclassified	20. Security Classif. (of this page) Unclassified	21. No. of Pages 118	22. Price

## **NOTICE**

The contents of this report reflect the views of the author, who is responsible for the facts and accuracy of the data presented herein. The contents do not necessarily reflect the views or policies of the Mississippi Department of Transportation or the Federal Highway Administration. This report does not constitute a standard, specification, or regulation.

This document is disseminated under the sponsorship of the Department of Transportation in the interest of information exchange. The United States Government and the State of Mississippi assume no liability for its contents or use thereof.

The United States Government and the State of Mississippi do not endorse products or manufacturers. Trade or manufacturer's names appear herein solely because they are considered essential to the object of this report.

# TABLE OF CONTENTS

LIST OF FIGURES.....	vi
LIST OF TABLES.....	viii
ACKNOWLEDGEMENTS.....	ix
<b>CHAPTER 1 - INTRODUCTION.....</b>	<b>1</b>
1.1 General and Background Information.....	1
1.2 Objectives.....	3
1.3 Scope.....	3
<b>CHAPTER 2 - LITERATURE REVIEW.....</b>	<b>4</b>
2.1 General Information.....	4
2.2 Chip Seals.....	4
2.3 Skid Resistance.....	5
2.4 Field Evaluated Aggregate Retention.....	6
2.5 Seal Treatment Performance.....	6
2.6 Structural Integrity Benefits of Seal Treatments.....	8
<b>CHAPTER 3 - EXPERIMENTAL PROGRAM.....</b>	<b>13</b>
3.1 Experimental Program Overview.....	13
3.2 Test Sections.....	13
3.2.1 Hwy 17 Test Section.....	14
3.2.2 Hwy 35 Test Section.....	19
3.3 Aggregate Retention.....	22
3.4 Skid Resistance.....	24
3.5 Structural Deterioration.....	24
3.6 Manual Rut Measurements.....	25
3.7 Automated Distress Measurements.....	26
3.8 Visual Assessments.....	27

<b>CHAPTER 4 - TEST RESULTS AND DATA ANALYSIS.....</b>	<b>28</b>
4.1	General Field Test Results.....28
4.2	Bleeding/Flushing Test Results.....28
4.2.1	<i>Hwy 17</i> Bleeding/Flushing Test Results.....28
4.2.2	<i>Hwy 35</i> Bleeding/Flushing Test Results.....30
4.3	Skid Resistance Test Results.....31
4.4	Aggregate Retention Test Results.....33
4.4.1	<i>Hwy 17</i> Aggregate Retention Test Results.....33
4.4.2	<i>Hwy 35</i> Aggregate Retention Test Results.....36
4.5	Rutting Test Results.....38
4.5.1	<i>Hwy 17</i> Rutting Test Results.....38
4.5.2	<i>Hwy 35</i> Rutting Test Results.....39
4.6	Roughness Test Results.....42
4.6.1	<i>Hwy 17</i> Roughness Test Results.....42
4.6.2	<i>Hwy 35</i> Roughness Test Results.....44
4.7	Cracking Test Results.....45
4.7.1	<i>Hwy 17</i> Cracking Test Results.....45
4.7.2	<i>Hwy 35</i> Cracking Test Results.....47
4.8	Structural Integrity Analysis and Test Results.....48
4.8.1	<i>FWD</i> Backcalculation and Structural Integrity Assessment.....48
4.8.1.1	Moisture Content During <i>FWD</i> Testing.....48
4.8.1.2	Temperature Prediction for use With <i>FWD</i> Measurements.....49
4.8.1.3	<i>FWD</i> Deflection Adjustments to Reference Temperature.....50
4.8.1.4	Structural Integrity Calculations.....52
4.8.2	<i>FWD</i> Test Results and Data Analysis.....53
4.8.2.1	Analysis of <i>FWD</i> Corrected Deflections.....53
4.8.2.2	Analysis of $SN_{eff}$ Data .....56
4.8.2.3	Analysis of Backcalculated $M_r$ Values .....63
4.8.2.4	Analysis of $SN_{New}$ Data.....65

**CHAPTER 5 - SUMMARY CONCLUSIONS AND RECOMMENDATIONS.....66**

5.1 Summary.....66

5.2 Conclusions.....66

5.3 Recommendations.....68

**CHAPTER 6 - REFERENCES.....69**

**APPENDIX A - PHOTOS OF TEST SECTIONS.....73**

## LIST OF FIGURES

Figure 1.1.	Photos of Chip and Scrub Seal Treatments.....	2
Figure 3.1.	Location of Testing Coordinates.....	14
Figure 3.2.	<i>Hwy 17</i> Test Section Layout.....	15
Figure 3.3.	<i>Hwy 17</i> Seal Characteristics Immediately After Rolling.....	16
Figure 3.4.	Coring of Pavement for Determination of Thickness and Moisture Content.....	16
Figure 3.5.	Coring Photos Within <i>Hwy 17</i> Highlighting Base/Subbase Materials.....	17
Figure 3.6.	Average Viscosity Data of <i>Hwy 17</i> .....	18
Figure 3.7.	Coring of <i>Hwy 17</i> After Test Phases.....	19
Figure 3.8.	<i>Hwy 35</i> Test Section Layout.....	20
Figure 3.9.	Coring Photos of <i>Hwy 35</i> .....	21
Figure 3.10.	Photos of <i>Hwy 35</i> Prior to Sealing Activities.....	22
Figure 3.11.	Aggregate Retention Testing.....	23
Figure 3.12.	Locked Wheel Skid Trailer.....	24
Figure 3.13.	Falling Weight Deflectometer Used for Testing.....	25
Figure 3.14.	Manual Rut Measurements.....	25
Figure 3.15.	Schematic of Relative Depth and Rut Measurements.....	26
Figure 3.16.	Automated Data Collection Vehicle Used for Roadway Profiles.....	26
Figure 4.1.	Relative Differences in <i>Hwy 17</i> Wheel Path Aggregate Coverage (Jan 2009).....	29
Figure 4.2.	Skid Data of Individual Test Sections.....	32
Figure 4.3.	Skid Data Used to Estimate Life of <i>Hwy 35</i> Scrub Seal.....	33
Figure 4.4.	Photos of Cores Taken From Northbound <i>Hwy 17</i> .....	34
Figure 4.5.	Comparison of Chip and Scrub Seal Aggregate Loss on <i>Hwy 17</i> .....	35
Figure 4.6.	Relative Depth Profiles of <i>Hwy 35</i> Sections 1 and 2.....	39
Figure 4.7.	Relative Depth Profiles of <i>Hwy 35</i> Sections 3 and 4.....	40
Figure 4.8.	Relative Depth Profiles of <i>Hwy 35</i> Sections 5 and 6.....	41
Figure 4.9.	AASHTO (1986) Temperature Predictions for Depths of Interest.....	49
Figure 4.10.	Comparison of Deflection Correction Factors.....	51
Figure 4.11.	Comparison of $D_{1-68-TC}$ and $D_{1-68-TACA}$ .....	54
Figure 4.12.	$SN_{eff-TC}$ Results for Cored Test Sections.....	61
Figure 4.13.	$SN_{eff-TACA}$ Results for Cored Test Sections.....	62
Figure 4.14.	Comparison of Effective Structural Capacity Calculation Methods.....	63
Figure A.1.	Windshield Survey of Southern Half of <i>Hwy 17</i> During Test Phase 1: Jan 08.....	73
Figure A.2.	Windshield Survey of Northern Half of <i>Hwy 17</i> During Test Phase 1: Jan 08.....	74
Figure A.3.	Windshield Survey of Southern Half of <i>Hwy 17</i> During Test Phase 2: Aug 08.....	77
Figure A.4.	Windshield Survey of Northern Half of <i>Hwy 17</i> During Test Phase 2: Aug 08.....	76
Figure A.5.	Windshield Survey of Southern Half of <i>Hwy 17</i> During Test Phase 3: Jan 09.....	77
Figure A.6.	Windshield Survey of Northern Half of <i>Hwy 17</i>	

	During Test Phase 3: Jan 09.....	78
Figure A.7.	Windshield Survey of Northern Half of <i>Hwy 35</i> During Test Phase 1: Jan 08.....	79
Figure A.8.	Windshield Survey of Southern Half of <i>Hwy 35</i> During Test Phase 1: Jan 08.....	80
Figure A.9.	Windshield Survey of Northern Half of <i>Hwy 35</i> During Test Phase 2: Aug 08.....	81
Figure A.10.	Windshield Survey of Southern Half of <i>Hwy 35</i> During Test Phase 2: Aug 08.....	84
Figure A.11.	Visual Assessment Photos of <i>Hwy 17</i> Coordinate 5.061.....	83
Figure A.12.	Visual Assessment Photos of <i>Hwy 17</i> Coordinate 5.156.....	84
Figure A.13.	Visual Assessment Photos of <i>Hwy 17</i> Coordinate 5.251.....	87
Figure A.14.	Visual Assessment Photos of <i>Hwy 17</i> Coordinate 5.346.....	86
Figure A.15.	Visual Assessment Photos of <i>Hwy 17</i> Coordinate 5.441.....	87
Figure A.16.	Visual Assessment Photos of <i>Hwy 17</i> Coordinate 5.561.....	88
Figure A.17.	Visual Assessment Photos of <i>Hwy 17</i> Coordinate 5.656.....	89
Figure A.18.	Visual Assessment Photos of <i>Hwy 17</i> Coordinate 5.751.....	90
Figure A.19.	Visual Assessment Photos of <i>Hwy 17</i> Coordinate 5.846.....	91
Figure A.20.	Visual Assessment Photos of <i>Hwy 17</i> Coordinate 5.941.....	92
Figure A.21.	Visual Assessment Photos of <i>Hwy 17</i> Coordinate 6.061.....	93
Figure A.22.	Visual Assessment Photos of <i>Hwy 17</i> Coordinate 6.156.....	94
Figure A.23.	Visual Assessment Photos of <i>Hwy 17</i> Coordinate 6.251.....	95
Figure A.24.	Visual Assessment Photos of <i>Hwy 17</i> Coordinate 6.346.....	96
Figure A.25.	Visual Assessment Photos of <i>Hwy 17</i> Coordinate 6.441.....	97
Figure A.26.	Visual Assessment Photos of <i>Hwy 17</i> Coordinate 6.561.....	98
Figure A.27.	Visual Assessment Photos of <i>Hwy 17</i> Coordinate 6.656.....	99
Figure A.28.	Visual Assessment Photos of <i>Hwy 17</i> Coordinate 6.751.....	100
Figure A.29.	Visual Assessment Photos of <i>Hwy 17</i> Coordinate 6.846.....	101
Figure A.30.	Visual Assessment Photos of <i>Hwy 17</i> Coordinate 6.941.....	102
Figure A.31.	Visual Assessment Photos of <i>Hwy 17</i> Coordinate 7.061.....	103
Figure A.32.	Visual Assessment Photos of <i>Hwy 17</i> Coordinate 7.156.....	104
Figure A.33.	Visual Assessment Photos of <i>Hwy 17</i> Coordinate 7.251.....	105
Figure A.34.	Visual Assessment Photos of <i>Hwy 17</i> Coordinate 7.346.....	106
Figure A.35.	Visual Assessment Photos of <i>Hwy 17</i> Coordinate 7.441.....	107
Figure A.36.	Visual Assessment Photos of <i>Hwy 17</i> Coordinate 7.561.....	108
Figure A.37.	Visual Assessment Photos of <i>Hwy 17</i> Coordinate 7.656.....	109
Figure A.38.	Visual Assessment Photos of <i>Hwy 17</i> Coordinate 7.751.....	110
Figure A.39.	Visual Assessment Photos of <i>Hwy 17</i> Coordinate 7.846.....	111
Figure A.40.	Visual Assessment Photos of <i>Hwy 17</i> Coordinate 7.880.....	112
Figure A.41.	Visual Assessment Photos of <i>Hwy 35</i> Coordinate 17.868.....	113
Figure A.42.	Visual Assessment Photos of <i>Hwy 35</i> Coordinate 18.678.....	114
Figure A.43.	Visual Assessment Photos of <i>Hwy 35</i> Coordinate 18.868.....	115
Figure A.44.	Visual Assessment Photos of <i>Hwy 35</i> Coordinate 19.678.....	116
Figure A.45.	Visual Assessment Photos of <i>Hwy 35</i> Coordinate 19.868.....	117
Figure A.46.	Visual Assessment Photos of <i>Hwy 35</i> Coordinate 20.678.....	118



## LIST OF TABLES

Table 1.1.	Overview of Distresses Related to Maintenance Activities.....	2
Table 2.1.	Material Quantities From Past Research.....	4
Table 2.2.	Seal Treatment Cost Data of Chen et al. (2002).....	7
Table 3.1.	Gradation Data for <i>Hwy 17</i> Material-Percent Passing.....	14
Table 3.2.	Results of <i>Hwy 17</i> Coring Prior to Test Phases.....	17
Table 3.3.	Viscosity Data of <i>Hwy 17</i> .....	18
Table 3.4.	Results of <i>Hwy 17</i> Coring After Test Phases.....	19
Table 3.5.	Coring Locations for <i>Hwy 35</i> .....	21
Table 3.6.	Radial Distance From Center of <i>FWD</i> Loading.....	25
Table 4.1.	Summary of <i>Hwy 17</i> Test Phases.....	28
Table 4.2.	Summary of <i>Hwy 35</i> Test Phases.....	28
Table 4.3.	<i>Hwy 17</i> Bleeding/Flushing Test Results.....	30
Table 4.4.	<i>Hwy 35</i> Bleeding/Flushing Test Results.....	30
Table 4.5.	Skid Resistance Test Results of <i>Hwy 35</i> .....	31
Table 4.6.	Aggregate Retention Test Results of <i>Hwy 17</i> .....	35
Table 4.7.	<i>Hwy 17</i> Popout Test Results.....	36
Table 4.8.	Aggregate Retention Test Results of <i>Hwy 35</i> Constructed in 2005.....	37
Table 4.9.	Aggregate Retention Test Results of <i>Hwy 35</i> Constructed in 2007.....	37
Table 4.10.	Rutting Test Results of <i>Hwy 17</i> .....	38
Table 4.11.	Automated Rutting Test Results of <i>Hwy 35</i> .....	41
Table 4.12.	<i>IRI</i> Test Results of <i>Hwy 17</i> -Northbound Lane.....	42
Table 4.13.	<i>IRI</i> Test Results of <i>Hwy 17</i> -Southbound Lane.....	43
Table 4.14.	Change in Roughness Test Results for <i>Hwy 17</i> (mm/m).....	44
Table 4.15.	<i>IRI</i> Test Results of <i>Hwy35</i> .....	45
Table 4.16.	Cracking Test Results for Northbound Lane of <i>Hwy 17</i> .....	46
Table 4.17.	Cracking Test Results for Southbound Lane of <i>Hwy 17</i> .....	46
Table 4.18.	Cracking Test Results of <i>Hwy 35</i> .....	47
Table 4.19.	Moisture Content Results of <i>Hwy 17</i> .....	48
Table 4.20.	Temperature Adjustment Parameters After Kim et al. (1995).....	50
Table 4.21.	Adjusted Deflections Under the Center of Loading: Northbound Lane.....	54
Table 4.22.	Adjusted Deflections Under the Center of Loading: Southbound Lane.....	55
Table 4.23.	Effective Structural Capacity Results: Northbound Lane.....	57
Table 4.24.	Effective Structural Capacity Results: Southbound Lane.....	58
Table 4.25.	Average $SN_{eff}$ Values of <i>Hwy 17</i> .....	59
Table 4.26.	Statistical Analysis of $SN_{eff}$ Differences Between Phase 1 and Phase 3.....	59
Table 4.27.	Resilient Modulus Results: Northbound Lane.....	64
Table 4.28.	Resilient Modulus Results: Southbound Lane .....	65

## ACKNOWLEDGEMENTS

The author wishes to thank the Mississippi Department of Transportation (*MDOT*) for funding State Study 202, as well as for funding the complimentary in house research under State Study 203. Mr. Jeff Wages and Mr. Jordan Whittington of the *MDOT* Research Division assisted in planning and testing of *Hwy 17* and *Hwy 35*; their contributions to the success of the work were significant. Mr. Bill Barstis of the *MDOT* Research Division provided valuable guidance to the research and a productive review of the final report and is owed due thanks.

Mr. Jesse Doyle and Mr. Trey Jordan of Mississippi State University (*MSU*) also deserve thanks for their assistance on the project. Both Mr. Doyle and Mr. Jordan assisted in preparation for and conducting of field testing. Their contributions were essential to completion of the project.

The author is especially grateful to the Arkansas Highway and Transportation Department (*AHTD*) for providing the *ROADHOG* computer program and allowing the author to use it in a manner suitable for this research. Mr. Mark Bradley and Ms. Elisha Wright-Kehner of the *AHTD* Planning and Research Division were very helpful and thanks are extended to both of them. Mr. Bradley allowed use of *ROADHOG* and Ms. Wright-Kehner provided multiple *AHTD* research reports and guidance during the research.

The North Carolina Department of Transportation (*NCDOT*) was also very helpful in the project. Dr. Moy Biswas, State Research and Analysis Engineer, provided multiple technical documents for use within the research. The data provided was instrumental to the success of the project and special thanks are due for the support.

# CHAPTER 1-INTRODUCTION

## 1.1 General and Background Information

Construction of the United States Interstate Highway System commenced around 1956. Subsequent efforts focused on development of state highways and low volume roads that has developed one of (if not the) most advanced highway systems in the world. In past years development was of primary concern, while preservation and maintenance was practically non-existent in the context of large scale activities. However, as the US highway system has aged, preservation and maintenance have become more of a priority. To the point, the *Office of Infrastructure* issued a memorandum in 2004 making maintenance activities eligible for federal aid funding. Also in 2004, the *National Center for Pavement Preservation (NCP)* was established. *NCP* serves many functions, with one being to compile technical research related to pavement preservation.

The highway system of Mississippi is fairly developed at present but has only become so in recent years. In the coming years, significant preventative and/or corrective measures will be required to preserve the Mississippi highway system. The *Mississippi Department of Transportation (MDOT)* needs adequate tools to allow placement of the right treatment on the right road at the right time.

In present day the *Mississippi Department of Transportation (MDOT)* and many other DOT's are still posed with questions such as *will a given preservation or maintenance treatment last through the winter* rather than questions such as *is this treatment an efficient use of resources?* With current DOT budgets difficult decisions appear inevitable, but targeted research can: 1) improve the effectiveness of a treatment; 2) improve decisions regarding when and how to apply treatments; and 3) relieve financial pressures that can in turn allow more efficient long term preservation and management practices. Current budgets will often prohibit HMA overlays to be placed on large numbers of low volume roads, so developing engineered seal treatments and corresponding analytical tools, test methods, and resulting performance specifications are extremely important.

According to Kuennen (2006), experience shows that spending \$1 on pavement preservation before the point of rapid and precipitous deterioration can delay or eliminate spending \$6 to \$10 in future rehabilitation or reconstruction. Unfortunately, problems must develop prior to many agencies spending funds from their very limited budgets. A difficulty of pavement maintenance and preservation is to get individuals to give the matter due seriousness and respect. It is a highly complicated matter vital to the future of the nations highway system regardless of past practices or mindsets. Many parameters require improvement, notably optimal timing for treatment application, and performance based material/construction specifications.

Chip seals are a surface treatment that has been common for many years. In essence they are an asphalt emulsion sprayed onto the surface of an existing pavement that is subsequently covered with aggregates. Figure 1.1(a) and Figure 1.1(b) provide photos of the two major steps in a chip seal treatment. Like a chip seal, a scrub seal first sprays asphalt emulsion onto the pavement surface. Unlike a chip seal, a broom is used to "scrub" the emulsion into the pavement before it is covered with aggregate as seen in Figure 1.1(c). Compaction equipment is used with both treatments to roll the aggregate into the emulsion to

provide the adhesion necessary to keep the aggregate in place. The finished product of both chip seals and scrub seals appear similar to a passenger of the roadway; see Figure 1.1(d). The photos in Figure 1.1 were taken during construction of the test sections evaluated herein.

Table 1.1 summarizes parameters common to pavement preservation activities. It shows the major pavement distresses where seal treatments can be effective in preservation.



(a) Chip Seal Emulsion Application-Hwy 17



(b) Covering Emulsion w/ Aggregate-Hwy 17



(c) Scrub Seal Emulsion Application-Hwy 35



(d) Chip or Scrub Seal Completed-Hwy 17

**Figure 1.1. Photos of Chip and Scrub Seal Treatments**

Note that seal treatments in and of themselves have no additional structural capacity but can preserve the existing capacity and thus assist with traffic loading. In addition, they can also restore or improve skid resistance, decrease permeability (air and water) of the pavement, and similar.

**Table 1.1. Overview of Distresses Related to Maintenance Activities**

	<b>Disintegration</b>	<b>Cracking</b>
-Why	-Abrasive traffic action -Stripping due to water	-Temperature change -Traffic loading
• When	• Too little asphalt • Brittle asphalt	• Volume change • Loaded when brittle
○ Distress	○ Pitting ○ Raveling	○ Block cracking ○ Fatigue cracking

The primary purpose of the asphalt binder in the emulsion is to seal (and ideally soften) the surface of the existing pavement while holding the surface aggregate in place. The surface aggregate is to protect the binder and provide adequate skid resistance and macro texture. The overall performance of the seal treatment relies on both components performing their intended functions.

## 1.2 Objectives

The primary objective of *MDOT SS 202* was to evaluate two full scale test sections. They are *Hwy 17* and *Hwy 35*, which contain chip and scrub seal treatments. Specifically, the objectives were to evaluate physical keys to seal treatment performance. They are: 1) maintaining adequate adhesion between asphalt and aggregate to prevent aggregate loss, 2) sustaining acceptable skid resistance, 3) slowing the rate of pavement structural deterioration; 4) minimizing cracking; and 5) maintaining acceptable surface texture while providing acceptable ride quality. Companion work was performed under *State Study No. 203: In House Support to State Study No. 202*. This report fully addresses the objectives mentioned in this paragraph.

A second objective of *MDOT SS 202* was to gather, organize, and interpret a large scale study on *Hwy 84* of chip seals performed in 1989. Both laboratory and field data were available from *MDOT*, consultants, and producers. The information was gathered and used to improve the database of available information. Many of the polymer modified emulsions used on *Hwy 84* are similar to those currently in use. This portion of the research was addressed in Howard and Baumgardner (2009).

## 1.3 Scope

*MDOT SS 202* is the first project in an ongoing research effort in sealing activities. *MDOT SS 211* is a companion laboratory testing effort that encompasses many materials and test methods. Materials obtained from *Hwy 17* are a portion of the materials being evaluated in *SS 211*. The knowledge gained from these projects is intended to be used to improve preservation practices in Mississippi.

A future benchmark in pavement preservation research within Mississippi will likely be to develop specifications based on required material properties that have been correlated to field performance. This will allow materials to be used only if they meet or exceed the properties demonstrated to be critical to field performance. Propriety products necessitate use of performance specifications for optimal efficiency, and these specifications should rely on both laboratory and field data. *SS 202* aims to gain some of the field data needed for this endeavor.

Field tests were conducted on *Hwy 17* and *Hwy 35* at three discrete intervals. The data collected was analyzed for aggregate retention, structural integrity, skid resistance, and overall condition. Comparisons were made between chip and scrub seals, as well as between treatments that had been in place for a period of time and newly constructed seal treatments.

## CHAPTER 2-LITERATURE REVIEW

### 2.1 General Information

A recent national synthesis of practice reported that chip sealing is often viewed in the US as a bulk commodity instead of an engineered and constructed product (Gransberg and James 2005). Historically, thin overlays have been the most common pavement rehabilitation technique. King (2007) reported that effective fog or rejuvenator seals are constructed with performance related specifications. Chip and scrub seals also have the potential to benefit from performance oriented specifications. Information obtained during literature review supports the idea of improving chip seals with performance specifications.

The remainder of this chapter provides information obtained by the author during review of literature as it pertained to the test sections evaluated. Significantly more literature exists than what was included in this report. This project investigated multiple behaviors and as a result literature review was conducted in relation to specific areas that could be useful for analysis and discussion of the test sections evaluated.

### 2.2 Chip Seals

Low to medium cracking, any extent of bleeding, and raveling are appropriate applications for chip seals. Material quantities used in other works are summarized in Table 2.1; this data is not a comprehensive assessment of ranges of material quantities but rather a set of examples of aggregate and emulsion application rates. The primary take away from Table 2.1 is the wide range of both aggregate and binder application rates that can be used in chip seal designs.

**Table 2.1. Material Quantities From Past Research**

Source	Aggregate		Binder			
	Type	Rate (kg/m <sup>2</sup> )	Rate (lb/yd <sup>2</sup> )	Type	Rate (L/m <sup>2</sup> )	Rate (gal/yd <sup>2</sup> )
Udelhofen (2006)	---	11.9	22	---	1.81	0.40
Lee et al. (2006)*	Lightweight	4.9	9	CRS-2	1.18	0.26
Lee et al. (2006)*	Granite	7.6	14	CRS-2	0.91	0.20
Hank and Brown (1949)	Siliceous	10.9	20	AC**	0.68	0.15
Outcalt (2001)	Lightweight	6.5	12	---	1.59	0.35
Outcalt (2001)	Normal Wt.	13.6	25	---	1.59	0.35

\* *Optimum Rates from Research*

\*\* *AC = Asphalt Cement: Note cutback asphalts were also used in the study*

*Specific Pavement Study-3 (SPS-3)* of the *Long Term Pavement Performance (LTPP)* program from Michigan was discussed by Galehouse and O’Doherty (2006). The benefits of multiple treatments (one being emulsion chip seals) in the presence of many factors were studied. Note the *Expert Task Group (ETG)* developed site-specific construction specifications. A notable conclusion was chip seals performed well except for poor pavements in wet/freeze zones, and provided best overall cracking performance (only sections that were evaluated for 14 years were considered). In general, the chip seals

performed longer than expected, and the annualized chip seal cost was \$2,800 per lane mile in 2001. Hildebrand and Dmytrow (2006) reported on the *SPS-3* sections in California that were evaluated under the *LTPP* program. Overall, the five different chip seals performed well; minimal raveling, bleeding, or flushing but reflective cracking was variable.

Delaware County in the state of New York uses chip seals on the pavements within its jurisdiction. Each year, 25% of the roads are chip sealed in July, with the goal being to extend the roads service life by 5 to 6 years (Udelhofen 2006). Outcalt (2001) evaluated three chip seal test sections and a control section and reported all sections to be structurally sound. No bleeding or rutting was observed during testing, and all sections were sealed with rubberized sealant prior to placement of the chip seals.

International knowledge can be a valuable asset in improving chip seal performance. New Zealand practices have been stated to be superior to US practices by Gransberg and James (2005); they are said to be the result of over 30 years of continuous improvement. Chip seal design in New Zealand relies on characterization of macro texture and hardness assessments of the existing surface, and has evolved through, among other parameters, field performance. Gransberg et al. (2005) reports 95% of New Zealand's road network is surfaced with chip seals; an astounding quantity in comparison to the US.

Worldwide there is a push toward performance specifications, but many items are needed to do this effectively (e.g. test methods and property thresholds). New Zealand takes the design approach that the 12 month texture depth is the most accurate performance indication over the chip seals design life (TNZ 2002). New Zealand expects approximately two years more of service (Gransberg et al. 2005) relative to the recently released NCHRP synthesis (Gransberg and James 2005).

### **2.3 Skid Resistance**

Skid resistance devices can be grouped into five general categories: locked wheel, side force, variable slip, fixed slip, and portable pendulum testers (e.g. British Portable Skid Tester defined in *ASTM E 303*). Davis (2001) investigated skid resistance of HMA surface layers (not seal treatments) at the Virginia Smart Road. The author also provided a detailed literature review of skid resistance measurement. Anderson (1986) indicated there could be a day to day fluctuation of pavement skid numbers of approximately 10 to 15 due to extreme changes in weather conditions.

Weissmann and Martino (2009) investigated: 1) Circular Track Meter (*CTM*) of *ASTM E 2157-01* that provides a Mean Profile Depth (*MPD*); and 2) Outflow Meter (*OFM*) of *ASTM E 2380-05* that provides an *Outflow Time*. According to the authors both devices provide pavement texture measurements that have been shown to correlate with skid resistance. A data set of 558 pairs of *MPD* and *Outflow Time* measurements were analyzed.

Previous literature was cited by Weissmann and Martino (2009) that provided a clear relationship between crash rate and macrotexture. The work defined a seal coat threshold with an *MPD* of 0.46 mm (18 mils); failure is below this value. An equivalent *Outflow Time* of 14.5 seconds or greater was also stated as failure. Outcalt (2001) reported K.J. Law skid trailer readings of 55.9 to 62.5 for chip seal test sections.

## 2.4 Field Evaluated Aggregate Retention

Aggregate retention is critical to friction characteristics. NAPA (2007) identified surface characteristics as one of seven areas critical to the *Roadmap* of important challenges for flexible pavements. Aggregate retention testing over a period of months in situ, however, did not appear to be well established in terms of a test method that is widely used and accepted. Coyne (1988) conducted a condition survey where visual estimates of aggregate loss were made over a large area and used for assessment of total aggregate loss. South Dakota adopted an evaluation technique for field performance of seal coats several years ago (Selim and Ezz-Aldin 1990). The technique was purely qualitative and assigned equally weighted numerical values to: 1) chip retention (aggregate loss); 2) skid resistance; 3) uniformity of application; 4) cracking; 5) bleeding. The target use of the method was one year after service. Selim and Ezz-Aldin (1990) modified the method by removing uniformity of application and replacing it with traffic volume.

Howard and Baumgardner (2009) summarized aggregate retention testing on *Hwy 84* in Mississippi where a Plexiglas plate was used to evaluate the same area for aggregate loss over a period of several months. Other methods found, in general, focused only on early aggregate retention or took field specimens to the laboratory for evaluation. Overall, a repeatable and well documented method to evaluate aggregate loss in situ over a period of several months was not found by the author.

Lee and Kim (2008) studied granite aggregates in conjunction with CRS-2 emulsion, for single seal treatments. All samples tested were field samples and tests included: flip over test; *Vialit* test; modified sand circle test; and 3<sup>rd</sup> scale Model Mobile Loading Simulator (MMLS3). Based on all test results, 3 roller coverages were determined to be optimal. The *Vialit* test has also been used for evaluation of field placed seal treatments. This test is being carefully evaluated in ongoing research for the Mississippi DOT by the author and is therefore not discussed in detail in this report.

## 2.5 Seal Treatment Performance

Gransberg (2006) reported on a survey of public US agencies who use chip seals in *NCHRP Synthesis 342*. Ninety-two responses were obtained from the US and abroad. The goal of the synthesis was to correlate individual chip seal performance ratings with construction practices producing those ratings. Temperature specifications were reported for the air and the pavement. In general, pavement temperatures are specified as a maximum to prevent the emulsion from breaking too quickly while the air temperatures are specified as a minimum to allow adhesion between the aggregate and the binder. The higher the air temperature and lower the pavement temperature, the more conservative the specification.

Respondents reporting excellent or good chip seal performance had an average air temperature specification of 15 C (60 F). Specifying minimum ambient air temperature was said to promote success and that chip seal performance increased as specified temperatures increased. Time invested in traffic control was stated to directly correlate with performance of chip seals. Respondents indicating excellent and good performance utilized interim pavement markings and reduced short term speeds. Details varied considerably, but traffic control maintained for as long as possible before opening to full-speed traffic was



recommended. Mississippi rated overall chip seal performance in the mid range of other states who responded to *NCHRP Synthesis 342*.

Temperature problems associated with seal treatments were documented as early as Hank and Brown (1949). Of particular interest are problems associated with air temperature only specifications (i.e. neglecting ground temperature). Note these types of specifications are still common in present day.

Chen et al. (2002) provided data from two *SPS-3* sites in Texas built in 1990 where chip seal, slurry seal, and overlays were used as surface treatments. The objective of the study was to determine the effectiveness of maintenance treatments. One pavement was thicker than the other and carried more traffic. The effectiveness was characterized using *TxDOT* and *LTPP* data, alongside corresponding methods. The *LTPP* method showed the chip seal to be the best performer, and the *TxDOT* method showed the thin overlay to be the best performer (average value of thin overlay was only nine points above chip seal).

Cost data from a statewide Texas survey for 2001 are presented in Table 2.2 and were taken from Chen et al. (2002). A thin overlay cost 2.2 to 2.4 times a chip seal when using corresponding data at the extremes of the Table 2.2 ranges. All factors considered (pavement condition, distress score, ride score, and cost) the chip seal was reported as the most cost-effective alternative. Chen et al. (2002) speculated that for pavements less sound than those investigated that a chip seal would be the treatment the authors would recommend.

**Table 2.2. Seal Treatment Cost Data of Chen et al. (2002)**

<b>Treatments</b>	<b>Cost per lane mile</b>
Thin Overlay (25 mm)	\$17,000 to \$22,000
Slurry Seal	\$8,000 to \$11,000
Chip Seal	\$7,000 to \$10,000
Crack Seal	\$700 to \$1,000

*Note: Data from 2001 in Texas.*

Irfan et al. (2009) synthesized past work related to thin asphalt overlays and their service life. Data from Indiana was then used to further examine thin overlays using deterministic and probabilistic approaches. International roughness index (*IRI*), pavement condition rating (*PCR*), and rut depths were used as performance indicators. The study confirmed past findings that the reported effectiveness of thin HMA overlays is influenced significantly by the performance indicator used, highway functional class, level of traffic, and climate severity in terms of freeze index. In general, thin overlay service life of 7 to 12 years was found in literature and also with the analysis of Irfan et al. (2009). Variations showed the service life as low as 3 years and as high as 24 years.

Lawson and Senadheera (2009) reported findings of past literature, survey questionnaires, and field interviews of the Texas DOT related to bleeding and flushing of chip seals. Contributing factors include aggregate, binder, traffic, environmental, and construction issues. Bleeding and flushing are terms often used interchangeably in academic and operations publications, while the authors state the terms should be differentiated: 1) bleeding refers to rapid onset of live and excess asphalt either during construction or under heavy traffic coupled with extended high temperatures; 2) flushing refers to a slower behavior where asphalt fills voids in the aggregate mat and becomes flush with aggregate but the binder is in solid form.

Aggregate loss results in flushing and/or bleeding and frequently occurs when a chip seal is placed outside the established asphalt season. The use of any asphalt binder outside recommended temperature conditions can lead to aggregate loss, bleeding, and/or flushing. High traffic volumes and heavy vehicles cause flushing and bleeding to appear more quickly.

Temperatures at or above 38 C (100 F) have been observed to turn flushed pavements into bleeding pavements when the humidity is elevated, especially when these conditions persist for several consecutive days. Lawson and Senadheera (2009) present multiple maintenance solutions for bleeding and flushed pavements. All of these solutions, though, come with associated costs and corresponding improvements. The authors concluded that there is no better advice for dealing with bleeding and flushed chip seals than to avoid the problem from the outset. The maintenance thresholds that warrant treatment of a flushed pavement are: 1) slippery surface; 2) low skid resistance; and 3) rutting leading to water accumulation.

Gransberg (2009) compared hot asphalt cement and emulsion chip seal binder performance on ten rural roads over a 3 year period. The primary mechanism of evaluation was the sand circle test (texture depth). Emulsion chip seals lost macrotexture over time more slowly than the hot asphalt cement chip seals. Emulsion chip seals were also shown to be more cost effective for maintaining macrotexture. The data was said to refute the “myth” that chip seals are an art and not a science.

Outcalt (2001) evaluated three chip seals and a control section. *FWD* readings were taken in the spring and then in the summer 3.5 years later. Average readings were shown (similar readings) and were stated to be evidence that the seals were extending pavement life in conjunction with block crack data (only control section experienced block cracking).

## **2.6 Structural Integrity Benefits of Seal Treatments**

Structural deterioration is defined by AASHTO (1993) as any condition that reduces a pavement's load carrying capacity. The only structural attribute of a seal treatment is to preserve the existing structural capacity and as such to delay/eliminate the need for an asphalt overlay (or worse full depth repair). Deflection testing using a Falling Weight Deflectometer (*FWD*) or similar device is the most common method of evaluating structural integrity of in service pavements. Richter (2006) reported that backcalculation of moduli exclusive of frost effects was typically seen to have a coefficient of variation (*cov*) of 5 to 20% for single-point within day testing.

*ROADHOG* is a program developed by the *University of Arkansas (U of A)* for the *Arkansas Highway and Transportation Department (AHTD)* for the purpose of evaluating in-situ subgrade moduli and overlay requirements based on *FWD* measurements. Specific details regarding the program, its functions, and its modifications over time can be found in Elliott et al. (1990); Hall and Elliott (1992); Hall and Tran (2004).

*ROADHOG* is a deflection based and finite element developed procedure. To determine  $M_r$ , a regression algorithm developed using *ILLI-PAVE* is incorporated. The regression equation is valid for pavements with asphalt layers up 40.6 cm (16 in) thick. Many deflection locations were considered during development, but 91.4 cm (36 in) provided the highest correlation coefficient of 4.4 MPa (0.64 ksi). The change in deflection between the center of loading and a distance equal to the pavement thickness was used alongside 4<sup>th</sup>

order polynomial equations for pavement thicknesses of 200, 300, and 600 mm (8, 12, and 24 in) to develop the governing relationships.

The  $M_r$  predicted with *ROADHOG* is intended for the AASHTO (1986) guide (Elliott et al. 1990). Specifically, an  $M_r$  value of 20.7 MPa (3 ksi) was used in the AASHTO Road Test. Testing of soils from the AASHTO Road Test showed 20.7 MPa (3 ksi) was achieved at a deviator stress ( $\sigma_d$ ) of 41.4 kPa (6 psi) and confining pressure ( $\sigma_3$ ) of zero when the soil was 1% above optimum moisture content (*OMC*). The value of  $M_r$  reported by *ROADHOG* is the value at  $\sigma_d$  of 41.4 kPa and  $\sigma_3$  of zero, not the modulus at the deviator stress applied during *FWD* testing (depending on pavement thickness the deviator stress on the subgrade could vary dramatically). The value reported by *ROADHOG* is the breakpoint  $M_r$  (Elliott et al. 1990).

According to Hall and Tran (2004) comparison of *ROADHOG* and Elmod provided reasonable results when the average (50<sup>th</sup> percentile) *ROADHOG* values were used. *AHTD* has used *ROADHOG* statewide since the early 1990's. The *ROADHOG* approach was deemed suitable for the current project with exception of temperature correction procedures.

Many other *FWD* backcalculation programs exist that are based on numerous approaches. Alavi et al. (2008) conducted a national, and to some extent international, synthesis on *FWD* usage. It was stated that the unexpected should be expected. Of primary interest to this work were the data analysis and applications portions of the synthesis.

Ninety percent of state highway agencies were reported to use *FWD* data for pavement layer modulus estimation. Iterative processes were found to be the most common back calculation method. Twelve software programs/back calculation approaches were mentioned specifically in the synthesis; 21% of respondents was the maximum amount found to use any one approach.

A program incorporating *YONAPAVE* algorithms was noted for evaluating effective structural capacity ( $SN_{eff}$ ) that was developed in Israel; a comparison was made to previous empirical *AASHTO* approaches. The synthesis of Alavi et al. (2008) provided examples of using the *FWD* to evaluate paving materials. The synthesis noted that the *FWD* sensor located 0.91 m (36 in) from the load plate more appropriately measured subgrade response. It was also noted that soil moisture was not considered for back-calculation methods, but that it could drastically change soil properties. A final note was that Western Australia used *FWD* data, rutting, roughness, surface texture, and skid resistance as performance indicators for maintenance controls.

Deflection measurements in flexible pavements are most often corrected to a particular loading system and environmental condition. In the pavement engineering community, applicability of deflection correction factors based on 40 kN loads to multiloading deflections has been questioned. Park et al. (2002), though, did not find the *FWD* load level to affect the temperature dependence of deflection correction. The environmental conditions of primary interest are the temperature of the asphalt layer and the moisture content of the subgrade. In general, the temperature of the asphalt layer is a primary consideration while the moisture content of the subgrade is often not considered at all. As noted previously, moisture can drastically change soil properties so in absence of accounting for the moisture conditions at the time of testing, a back calculated  $M_r$  value should be taken as the value at the moisture condition that is often unknown.

Measurement of subgrade moisture content for routine use is often impractical due to its destructive nature which is why typical methods do not consider subgrade moisture

content as an input when calculating  $M_r$  or other overlay requirements even though it is well established that the strength and modulus of many subgrade soils (in particular fine grained soils) is dependent on moisture in laboratory testing. Richter (2006) provides an excellent summary of variables that have been reported to affect laboratory  $M_r$  values of unbound materials.

While moisture effects are detected in laboratory testing for many materials, some studies have indicated relatively minor fluctuations in subgrade moisture do not appreciably affect response in *FWD* testing. Richter (2006) states that in many instances variations in moisture content are not the most important driver of seasonal variations in backcalculated layer moduli for unbound pavement layers. Discussion to this point included: 1) 80% of the subgrade layers evaluated were less strongly correlated with moisture than with one or more stress parameters; 2) some pavement layers observed correlation between mean layer moisture and modulus while others did not; and 3) a high degree of variability in relating change in modulus to change in volumetric moisture content suggests other factors confound the modulus-moisture relationship.

Temperature gradients within a pavement layer can be large and cannot be estimated directly using only a snapshot of surface temperature. An effective value representing the entire layer is needed. AASHTO (1986) provides a method to predict pavement temperature at various depths into the pavement. The inputs are: 1) depth into pavement layer; 2) pavement surface temperature ( $T_{s-FWD}$ ); and 3) average air temperatures for previous five days ( $T_{A-5}$ ). The recommended approach is to find temperature near the top, middle, and bottom of the pavement. The values are averaged. The resulting effective temperature from this method has been labeled  $T_A$  in this report.

The reference temperature of 21.1 C (70 F) has a modulus correction of 1.0 in AASHTO (1986), and the reference temperature for evaluation is almost always between 20.0 and 21.1 C (68 to 70 F) regardless of the method chosen. Below the reference the correction reduces the modulus to 0.22 of its original value at -12.2 C (10 F), and above the reference temperature the correction factor increases almost asymptotically to 90.0 at 65.6 C (150 F). This curve is highly non-linear and should be used rather than data interpolation. The key observation is that higher temperatures are much more critical than lower temperatures.

Deficiencies were reported in the AASHTO (1986) approach in that the effect of differing asphalt layer thickness was not accounted for in determining a deflection correction factor for a specified set of conditions. ASHTO (1993) updated the procedure, but some state highway agencies reported inaccuracies, especially at elevated temperatures. Kim et al. (1995) reported that the AASHTO (1986) approach predicted the mid depth temperature fairly well. The problem, though, was observed when attempting to predict internal temperature for the same day of testing. For example, a given surface temperature and test day had two data points taken (one prior to and one past the peak daily temperature that had noticeably different corrected deflections. For research purposes, this becomes especially significant when comparing test sections via *FWD* testing performed on the same day. An additional problem reported with the AASHTO procedure according to some (e.g. Kim et al. 1995) is accounting for changes in the gradient of temperature with depth. Kim et al. (1995) reported improved data variability when using only the mid depth temperature of AASHTO (1986) rather than the average of the top, middle, and bottom but that the improvement was not to an acceptable level.

The asphalt tested in Kim et al. (1995) and Kim et al. (1995a) was AC-20, which can roughly be translated to *PG 64-22*. This is similar to Mississippi's primary binder grade of *PG 67-22*. The experimental program evaluated asphalt between 64 and 305 mm (2.5 and 12 in) thick, one of the pavements was 3.5 in (89 mm) thick, and the study was conducted during each season of the year. Temperatures during testing ranged between -7.2 to 40.0 C (19 to 104 F) with ample data distributed throughout. All data from Kim et al. (1995) was obtained from the central region of North Carolina.

Kim et al. (1995a) reported that pavements with thicker asphalt layers demonstrated greater temperature dependency; a logical behavior. Variation in deflection due to temperature is minimal for thin asphalt layers, but becomes progressively more important with thickness. Kim et al. (1995) found the heat transfer mechanism was more dominant from the top down (i.e. surface temperature was more critical to gradient than ground temperature). Park and Kim (1997) developed an analytical procedure for temperature correction of flexible pavement surface deflections based on the theory of linear viscoelasticity and time-temperature superposition. The analytical model was used to conclude that the required correction factors for deflections depended primarily on the thermoviscoelastic properties of the mixture type. To use such an approach correctly, state agencies would need to conduct a series of creep tests at different temperatures for typical mixtures, or back calculate creep compliance from backcalculation data.

Shao et al. (1997) extended the work of Kim et al. (1995) related to temperature prediction in asphalt layers. The procedure was based on fundamental principles of heat transfer and used the surface temperature history since yesterday morning, while Kim et al. (1995) was empirically based. The inputs to the approach are: 1) yesterday's maximum air temperature, 2) yesterday's cloud condition, 3) minimum air temperature of today's morning; and 4) surface temperatures measured during *FWD* tests.

Chen et al. (2000) tested 3 sites to evaluate temperature effects on *FWD* measurements: 1) 200 mm (8 in) asphalt layer within a pad constructed for the research; 2) 180 mm (7.1 in) total asphalt of ages varying from 15 to 40 years; and 3) 200 mm (8 in) total asphalt thickness with layers of ages varying from 1957 to 1996. The *FWD* sensors were set up where  $D_1$  was under the center of the load,  $D_2$  was 305 mm (1 ft) from the center of the load,  $D_3$  was 610 mm (2 ft) from the center of the load, and so on. The pavements were instrumented with thermocouples. Chen et al. (2000) noted that Texas DOT does not apply temperature correction to asphalt pavements thinner than 75 mm (3 in), and that they drill holes to measure mid depth temperature when testing.

According to Chen et al. (2000), linear load-deflection relationships may not exist in thinner pavements. The authors used linear deflections for their thicker asphalt layers. Of deflections  $D_1$  to  $D_7$ , only  $D_1$  and  $D_2$  were substantially affected by temperature, with  $D_3$  moderately affected in the newly constructed pad. Cracked locations appeared less affected by temperature. On average, there was 15% difference between cracked and non-cracked sections. Variation among intact pavements was less than 10%. Temperature correction was not found to be site dependent.

Pavements tested by Park et al. (2002) showed that radial distances up to 203 mm (8 in) were affected by temperature in a 115 mm (4.5 in) thick asphalt layer. Eq. 2.1 was proposed to calculate the radial distance requiring temperature correction.

$$D_{eff} = 4.75(t) - 413 \quad (2.1)$$

Where,

$D_{eff}$  = effective radial distance for temperature correction (mm)

$t$  = asphalt layer thickness (mm)

Xu et al. (2002) identified relationships between deflection basin parameters and layer conditions. Of note was the model between the asphalt modulus and deflection basin parameters alongside cracking and stripping as they affect the modulus. Orr and Irwin (2007) used *MODCOMP* for *FWD* backcalculation in the state of New York. Deflections ranged from below 100  $\mu\text{m}$  to in excess of 800  $\mu\text{m}$ .

## CHAPTER 3-EXPERIMENTAL PROGRAM

### 3.1 Experimental Program Overview

The experimental program and corresponding results were broken into four categories. They are: 1) aggregate retention; 2) skid resistance; 3) structural integrity via Falling Weight Deflectometer (*FWD*) testing; and 4) visual and profiler assessments. All five physical characteristics mentioned in the project objectives (Section 1.2) are included. Item 4) of the experimental program addressed cracking, surface texture, and ride quality. Each of these four categories is addressed in separate sections of the experimental program.

The experimental program was performed on two test sections within Mississippi. They are: 1) State Highway 17 (*Hwy 17*) in Carroll County; and 2) State Highway 35 (*Hwy 35*) in Tallahatchie County. Each test section is approximately 9.7 lane kilometers (6 lane miles) long, which represents approximately one typical day of sealing operation. Each test section was evaluated three times and each evaluation is referred to hereafter as a phase. The three test phases of *Hwy 17* occurred on: 1) 1-28-08 (all but *FWD*) and 2-7-08 (*FWD*); 2) 8-14-08; and 3) 1-7-09. The three test phases of *Hwy 35* occurred on: 1) 2-11-08; 2) 8-13-08; and 3) 1-9-09. *MDOT* and *MSU* researchers were present for each phase and actively participated in data collection.

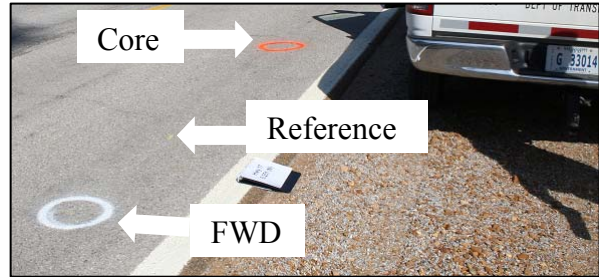
### 3.2 Test Sections

Parameters common to both test sections in all test phases are summarized as follows, while section specific details are presented in the following sub-headings. *ASTM C 33* size 89 limestone is commonly used in Mississippi as a seal aggregate; it was used on both test sections. The source of the aggregate for both chip seals was Hoover, AL. The outer wheel path and lane center were evaluated. Both test sections had 3.05 m (10 ft) lanes. The outer wheel path of both sections was taken at 0.56 m (22 in) from the inside of the white line. Location of testing coordinates was performed using the Distance Measuring Instrument (*DMI*) seen in Figure 3.1(a). They were marked along the shoulder with pavement chalk and/or fluorescent paint. *Hwy 17* was referenced from the Carroll/Holmes county line, while *Hwy 35* was referenced from the Tallahatchie/Panola county line.

The pavement was marked for coring, *FWD* testing, aggregate retention, and visual assessment. An example is shown in Figure 3.1(b). All these parameters were not measured at every location. Figure 3.1(b) is one of the few coordinates where all were measured at the same location. The reference location was determined using vehicle equipped with the *DMI*. The rear hitch of the vehicle was aligned with the county line of reference, so that when the desired distance had been traveled, the research team could use the rear hitch as alignment and mark the reference location with a small mark using pavement chalk. This reference point marked the center of the aggregate retention test, and the center of the area of visual assessment. *FWD* testing was performed 1.22 m (4 ft) behind the reference point to ensure the spike driven for aggregate retention did not affect the test. It was behind the reference since deflection was measured in the direction away from the spike. Coring was performed 3.05 m (10 ft) in front of the reference point to allow the equipment to back into position and not disturb the aggregate retention, visual assessment, or *FWD* test locations.



(a) Distance Measuring Instrument



(b) Marking System for Testing

**Figure 3.1. Location of Testing Coordinates**

### 3.2.1 Hwy 17 Test Section

The test section was constructed on State Highway 17 (*Hwy 17*) in Carroll County Mississippi on November 7, 2007 by *Kimes & Stone Construction Company*; *MDOT* log miles 0.000 to 7.500 were constructed. It was a fairly windy day with clear skies, but much of the test section was overcast from the large trees adjacent to the roadway. Ambient shade temperatures during the majority of construction remained near 7.2 C (45 F). The range of ambient temperatures during test section construction was 5.0 to 14.4 C (41 to 58 F). A supplemental agreement on the project allowed it to be constructed between 1.7 to 29.4 C (35 F to 85 F). The location of *Hwy 17* is estimated to be 30 to 40% shaded at any given time.

The *Hwy 17* emulsion application rate was 1.45 L/m<sup>2</sup> (0.32 gal/yd<sup>2</sup>), and the emulsion was delivered to job site at 60 C (140 F). PASS-CR emulsion was used for the entire project. Samples of PASS-CR were obtained for use in future testing discussed in *MDOT SS 211*. The emulsion was applied in a single coverage. The aggregate used was *ASTM C33* size 89 limestone that had 2.1% moisture at the time of construction. Four samples were taken of the material by DOT personnel, and the gradation properties are shown in Table 3.1. The job was paid according to coverage area so no direct record of aggregate quantity was obtained. The aggregate was rolled into the emulsion with a pneumatic tire roller.

**Table 3.1. Gradation Data for Hwy 17 Material-Percent Passing**

Sieve Size	Specification		Test Results			
	Minimum	Maximum	1	2	3	4
12.5 mm (1/2 in)	100	100	100	100	100	100
9.5 mm (3/8 in)	90	100	90	91	93	92
4.75 mm (No. 4)	20	55	31	41	38	44
2.36 mm (No. 8)	5	30	7	9	8	12
1.18 mm (No. 16)	0	10	1	1	1	2
Fineness Modulus	—	—	6.72	6.58	6.60	6.50

The Hwy 17 test section was laid out as seen in Figure 3.2. As seen, 12 test sections were identified. *MDOT Pavement Management* coordinates were used throughout. The units are in miles and are referenced according to standard *MDOT* procedures. Of the 12 sections, two contain no treatment, six were chip seals, and four were scrub seals.



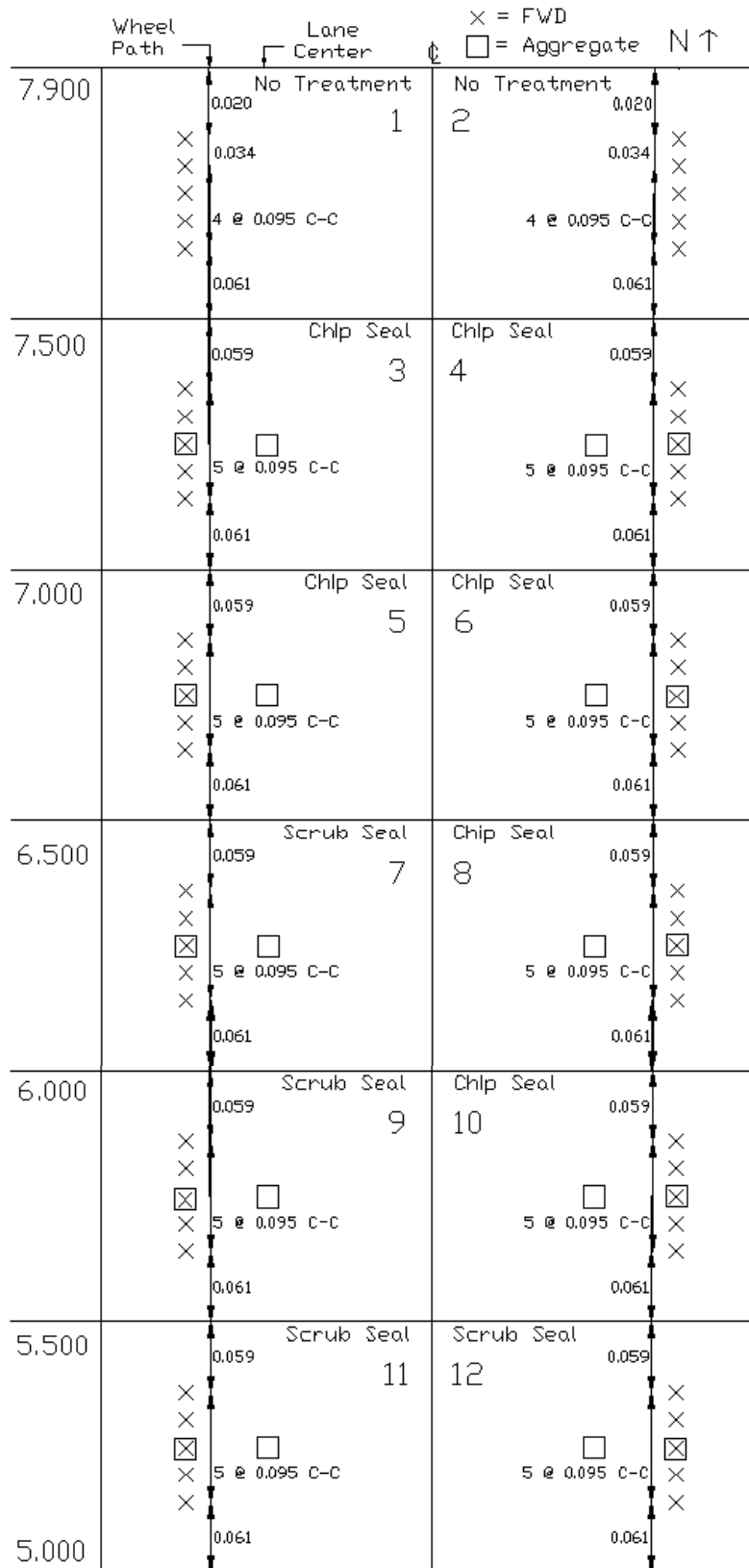


**Figure 3.2. Hwy 17 Test Section Layout**

Determination of the various sections and testing coordinates was performed prior to the research team visiting the site to prevent introduction of bias into the test results.

Traffic was allowed on the test section immediately (even prior to brooming), and it was apparent the emulsion was not set. Aggregate could easily be dislodged. The MSU research team could easily remove aggregate from the pavement as seen in Figure 3.3(a), and vehicles were noticeably stirring up aggregate as seen in Figure 3.3(b). Such early traffic opening could negatively affect the bond between the aggregate and emulsion.



(a) Aggregate Dislodged by Hand



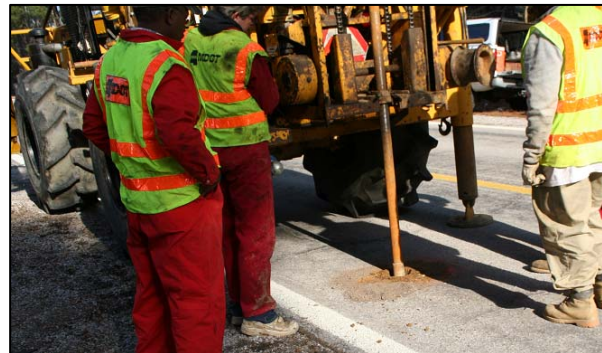
(b) Traffic Prior to Brooming

**Figure 3.3. Hwy 17 Seal Characteristics Immediately After Rolling**

The drill seen in Figure 3.4(a) was used to core the pavement prior to testing. Coring was performed in absence of water as seen in Figure 3.4(b) to simplify determination of subgrade moisture content. Subgrade moisture content can provide valuable data (both qualitative and quantitative) and pavement layer thicknesses were needed for *FWD* backcalculation. The interior of the cored hole was investigated to determine material type and asphalt thickness. The shavings of the asphalt layer were recovered for testing of overall binder properties (seal treatment had been fully applied at the time of coring).



(a) Drilling Equipment Used for Coring



(b) Coring Pavement Without Water

**Figure 3.4. Coring of Pavement for Determination of Thickness and Moisture Content**

Table 3.2 summarizes the pavement properties obtained from coring prior to testing. The asphalt thicknesses varied somewhat between locations. Figure 3.5 contains photos of each core to provide additional physical meaning to the descriptions of Table 3.2. Samples taken from each hole were combined and Atterberg Limit testing performed for the material

indicated as non-cohesive in Table 3.2. The results were a Liquid Limit of 21 and a Plastic Limit of 16.

**Table 3.2. Results of Hwy 17 Coring Prior to Test Phases**

Core	Location <sup>1</sup>	Asphalt - mm (in) <sup>2</sup>	Unbound Layers <sup>3</sup>
1	6.251N	89 (3.5)	≈ 30.5 cm (12 in) sandy gravel over non-cohesive soil
2	5.251N	79 (3.1)	≈ 30.5 cm (12 in) sandy gravel over non-cohesive soil
3	6.751S	84 (3.3)	≈ 30.5 cm (12 in) sandy gravel over non-cohesive soil
4	7.751S	94 (3.7)	≈ 30.5 cm (12 in) sandy pea gravel over non-cohesive soil

1: See Figure 3.2

2: Thickness of HMA layer

3: Core 4 was noticeably different than the other cores

Data obtained from the October 2007 Pavement Management Analysis Sections documents of MDOT are summarized as follows. Original construction of coordinates 0.000 to 7.500 was in January of 1964 and contained 35.56 cm (14 in) of base/subbase and 2.54 cm (1 in) of double bituminous surface treatment. An overlay was placed in October of 1983 that consisted of 5.08 cm (2 in) of asphalt concrete. Pavement management data agrees in general terms with the coring performed; base/subbase slightly thinner from cores and asphalt layer slightly thicker from cores. A condition survey performed on 11/16/05 resulted in: PCR of 61, IRI of 1.87 mm/m (118.5 in/mi), and Rut depth of 3.81 mm (0.15 in).



(a) Core 1 at Coordinate 6.251N



(b) Core 2 at Coordinate 5.251N



(c) Core 3 at Coordinate 6.751S



(d) Core 4 at Coordinate 7.751S

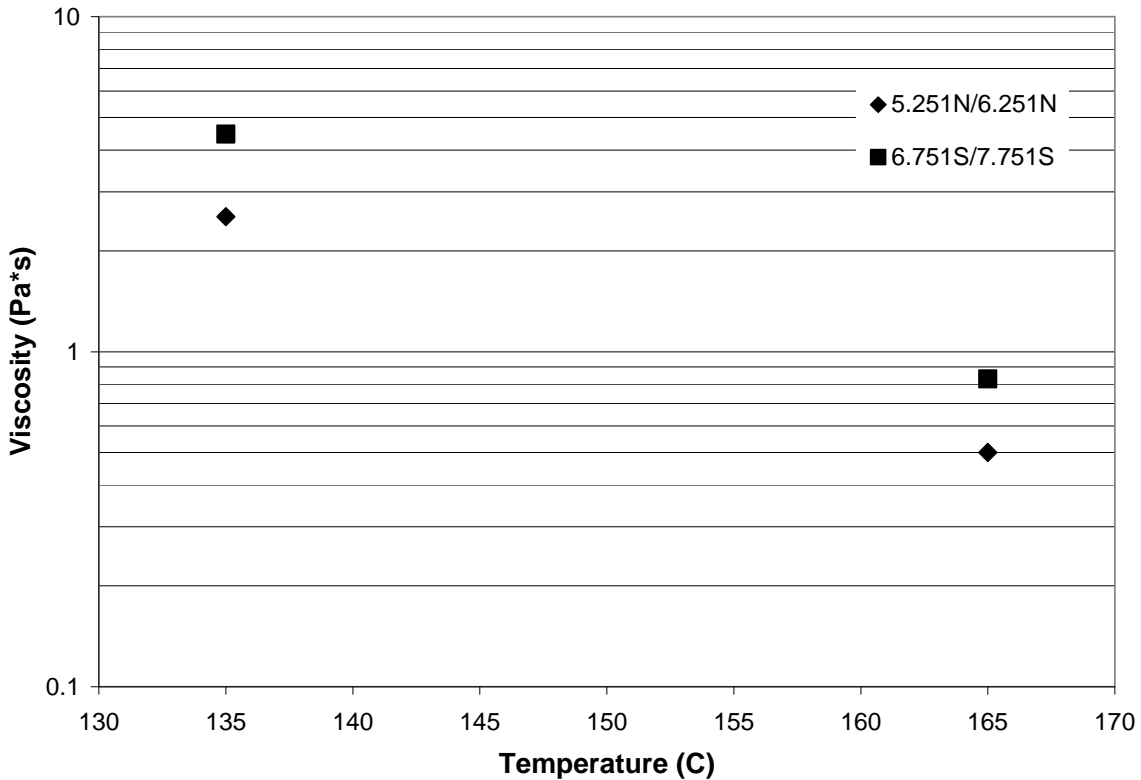
**Figure 3.5. Coring Photos Within Hwy 17 Highlighting Base/Subbase Materials**

Table 3.3 and Figure 3.6 provide viscosity test results of the composite asphalt layer thickness including sealing emulsion. Shavings of coordinates 5.251N and 6.251N were combined, as were shavings from coordinates 6.751S and 7.751S. The binder was extracted

**Table 3.3. Viscosity Data of Hwy 17**

Coordinate(s)	Results at 135 C (Pa*s)		Results at 165 C (Pa*s)	
	Test 1	Test 2	Test 1	Test 2
5.251N/6.251N	2.53, 2.53, 2.53	2.54, 2.54, 2.53	0.45, 0.45, 0.43	0.56, 0.53, 0.56
6.751S/7.751S	4.56, 4.55, 4.56	4.36, 4.38, 4.35	0.80, 0.79, 0.79	0.86, 0.88, 0.86

from the shavings using two 45-minute 15% ethanol and 85% toluene washes, and the binder was recovered with a *Buchi Rotavapor R-114*. This protocol was selected to match complimentary laboratory research under *MDOT SS 211*. A Brookfield Viscometer was used according to *AASHTO T 316-04* with an S27 spindle rotating at 20 rpm.



**Figure 3.6. Average Viscosity Data of Hwy 17**

At the conclusion of testing, additional coring was performed to obtain near surface samples for testing within *SS 211* and to obtain a more accurate depiction of layer thicknesses. Fourteen cores were obtained in the standard fashion (Figure 3.7a) from the northbound lane. Twelve of these cores were taken from the center of the *FWD* test locations so that the actual pavement thickness would be available for portions of the analysis. The two remaining cores were taken 0.001 units (1.6 m) offset from one of the *FWD* cores in the wheel path to obtain the remaining material needed for near surface testing of *SS 211* and to

provide thickness repeatability measurements. The results of coring are provided in Table 3.4. Note that five of the twelve locations had stripped significantly (Figure 3.7b) and that the core at coordinate 7.251 had a crack through the core.



(a) Coring of FWD Test Location



(b) Example of Stripped Core

**Figure 3.7. Coring of Hwy 17 After Test Phases**

**Table 3.4. Results of Hwy 17 Coring After Test Phases**

Coordinate	Seal Type	Thickness (mm)	Thickness (in)	Stripping
5.061	Scrub	86	3.4	No
5.156	Scrub	94	3.7	Yes
5.251	Scrub	84	3.3	No
5.346	Scrub	91	3.6	Yes
5.751	Chip	91	3.6	No
6.251	Chip	94	3.7	No
6.751	Chip	91	3.6	Yes
7.251	Chip	84	3.3	Yes
7.656	None	81	3.2	No
7.751	None	79	3.1	No
7.846	None	91	3.6	Yes
7.880	None	119	4.7	No
7.881	None	119	4.7	No
7.879	None	119	4.7	No

Note: Coordinate 7.251 had a crack through the core.

### 3.2.2 Hwy 35 Test Section

The sealing activities were performed at two different times; March 25, 2005 and November 5, 2007. The March 2005 increment used application rates of 1.36 L/m<sup>2</sup> (0.30 gal/yd<sup>2</sup>) for the emulsion and 7.6 kg/m<sup>2</sup> (14 lb/yd<sup>2</sup>) for the ASTM C33 size 89 limestone aggregate for the majority of placement. The emulsion was applied in two passes of 0.68 L/m<sup>2</sup> (0.15 gal/yd<sup>2</sup>) each. Aggregate was rolled into the emulsion with a pneumatic tire roller. Very brief periods differed from the standard approaches in one of the following ways: 1) 1.45 L/m<sup>2</sup> (0.32 gal/yd<sup>2</sup>) of emulsion; 2) 0.45/0.90 kg/m<sup>2</sup> (0.1/0.2 gal/yd<sup>2</sup>) PASS-CR coverages of emulsion; and/or 3) aggregate application rate of 8.7 kg/m<sup>2</sup> (16 lb/yd<sup>2</sup>).

Temperatures at the beginning of construction were 11.7 C (53 F) [ambient], 11.7 C (53 F) [pavement in the sun], and 8.9 C (48 F) [pavement in the shade]. The maximum pavement temperature during construction was measured to be 32.2 C (90 F) in the sun.

The November 2007 sealing activities on *Hwy 35* consisted of the following. The target emulsion and aggregate application rates were 1.45 L/m<sup>2</sup> (0.32 gal/yd<sup>2</sup>) and 7.6 kg/m<sup>2</sup> (14 lb/yd<sup>2</sup>), respectively. The aggregate was *ASTM C 33* size 89 limestone. Construction plans consisted of one shot of emulsion followed immediately by aggregate placement and rolling.

The entire *Hwy 35* test section was scrub seal with PASS-CR emulsion. Figure 3.8 shows a plan view of the test section numbered according to *MDOT Pavement Management* coordinates. The actual coordinates where the sections begin and end are shown (drive ways and similar caused slight modification of the planned section lengths of 1.6 km (1 mile). There are 6 test sections as shown in the upper right hand corners. Sections 3 and 4 were built in 2005, while the sections on either side are the sections constructed in 2007.

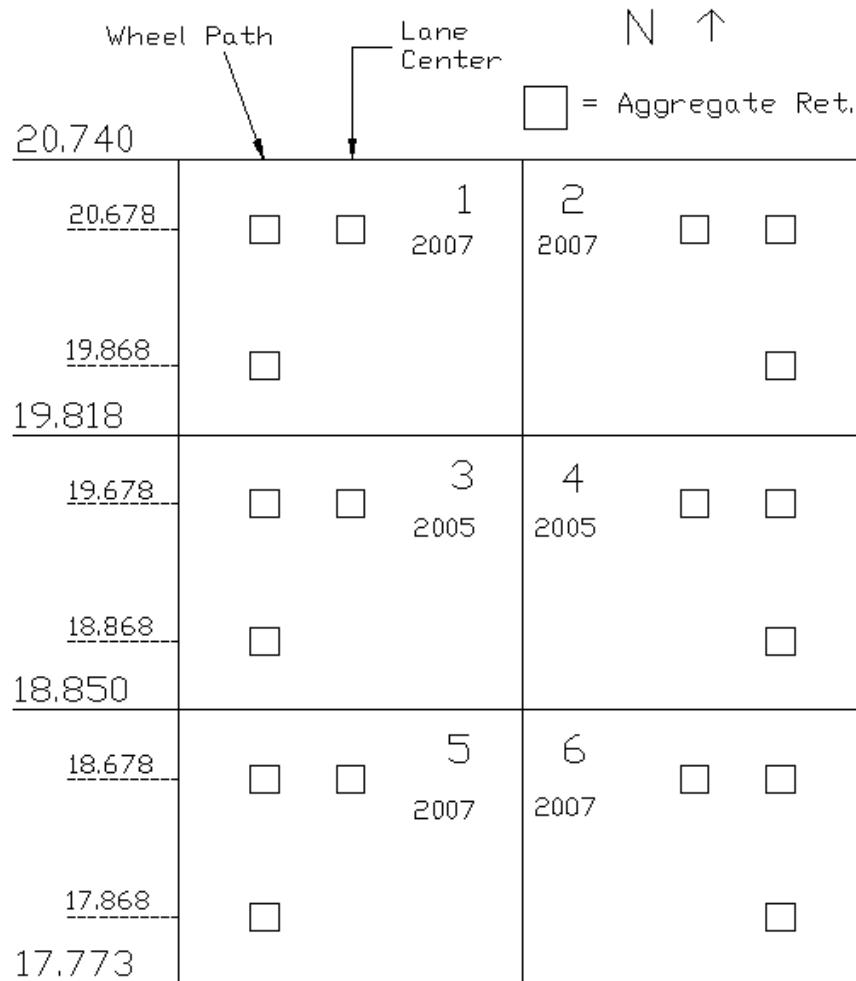


**Figure 3.8. Hwy 35 Test Section Layout**

Coring was performed in sections 3 and 4 prior to the 2005 scrub seal construction. Table 3.5 summarizes the locations of the cores. Figure 3.9 provides photos of the cores and estimates of layer thickness.

**Table 3.5. Coring Locations for Hwy 35**

Core	Lane	Location	Coordinate*
1	Southbound	Center	19.625
2	Northbound	Inside Wheelpath	19.615
3	Northbound	Center	19.125
4	Southbound	Inside Wheelpath	19.115

\* MDOT Pavement Management Coordinate



(a) Hwy 35 Core 1



(b) Hwy 35 Core 2



(c) Hwy 35 Core 3



(d) Hwy 35 Core 4

**Figure 3.9. Coring Photos of Hwy 35**

Data obtained from the October 2007 Pavement Management Analysis Sections documents of MDOT are summarized as follows. Original construction of coordinates 12.481 to 19.273 was in January of 1959 and contained 38.10 cm of base/subbase and 2.54 cm of double bituminous surface treatment. An overlay was placed in January of 1983 that

consisted of 5.08 cm (2 in) of asphalt concrete. A condition survey performed on 11/16/05 resulted in: *PCR* of 77, *IRI* of 1.30 mm/m (82.37 in/mi), and Rut depth of 6.1 mm (0.24 in). Original construction of coordinates 19.273 to 23.465 was in January of 1965 and contained 35.6 cm (14 in) of base/subbase and 2.54 cm (1 in) of double bituminous surface treatment. An overlay was placed in December of 1983 that consisted of 5.08 cm (2 in) of asphalt concrete. A condition survey performed on 11/16/05 resulted in: *PCR* of 63, *IRI* of 1.76 mm/m (111.5 in/mi), and Rut depth of 3.3 mm (0.13 in). Figure 3.10 provides photos taken by MDOT at discrete intervals prior to sealing activities.



(a) Two Months Prior to 2005 Seal

(b) Ten Months Prior to 2007 Seal

**Figure 3.10. Photos of Hwy 35 Prior to Sealing Activities**

### 3.3 Aggregate Retention

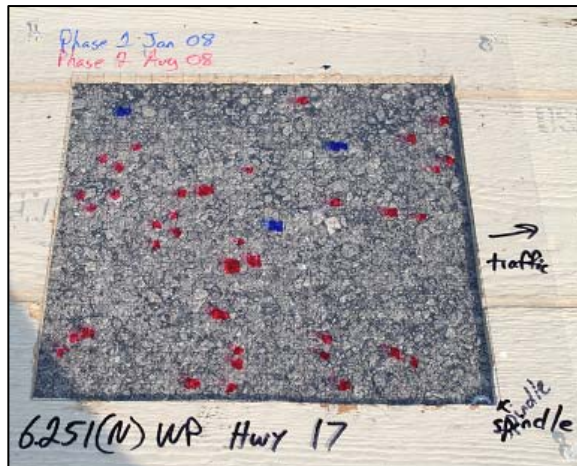
A metal spindle was driven into the pavement to mark the corner of the area to be evaluated for aggregate retention. This allowed the same 930 cm<sup>2</sup> (1 ft<sup>2</sup>) area to be evaluated in each test phase. Conceptually, aggregate retention testing was performed in the manner shown in Figure 3.11, with a photo taken of each location during each test phase. A wooden template with a square hole with side dimensions of 30.5 cm (1 ft) was used. Initially, US issued currencies (pennies) were used to mark the locations (Phase 1 shown in Figure 3.11a). This was the standard *MDOT* approach, but after consideration by *MDOT* and *MSU* researchers an alternate approach was used. The size of the penny, 2.85 cm<sup>2</sup> (0.442 in<sup>2</sup>), and the time consuming process of identifying previous phase aggregate loss were the primary factors in employing a different approach. The approach adopted was a slight modification of that used some two decades ago on *US 84* as described in (Howard and Baumgardner 2009); the following paragraphs detail the approach used.

A piece of clear Plexiglas was placed over the hole and a transparency with a printed grid with horizontal and vertical spacing of 1.27 cm (0.5 in), or 256 squares, was subsequently placed onto the Plexiglas (the same transparency was used between phases). Some testing did not make use of the Plexiglas or the wooden board, but at least one of these items was present for all testing. The areas where aggregate was lost in a given phase were colored onto the transparency with a permanent marker; a different color was used for each test phase on the same transparency. The operator colored 1/4, 1/2, 3/4, or the entire square.





(a) Original Method (Phase 1)



(b) Final Method (Phases 2 and 3)

**Figure 3.11. Aggregate Retention Testing**

To accommodate the use of pennies in Phase 1, the photos taken were used during Phase 2 to re-locate the areas, mark them with the color indicated for Phase 1, and proceed with aggregate retention testing. A single operator was used for Phases 2 and 3, while a different operator was used in Phase 1.

Aggregate loss was visually estimated by looking through the transparency film and noted by marking the areas of missing aggregate with colored markers. The entire area that was judged to be aggregate loss was colored onto the transparency film suspended just above the pavement surface. Aggregate particles on the order of the No 8 sieve and larger left imprints in the surface texture in locations where aggregate had been removed by traffic action. These imprints were often manifested by small amounts of binder film being visible in the indentation left from the missing particle. At other locations within the testing area

there was no binder film visible however an indentation or space between adjacent aggregate particles where a particle had been positioned was discernable. Both of these categories of observation were judged to be evidence of aggregate particle loss and were marked on the transparency film. Aggregate particles smaller than approximately 2.36 mm (No 8 sieve) were too small for their absence to be reliably discerned and were ignored in the aggregate retention test.

In some instances large areas (on the order of 12.7 mm (0.5 in)) were observed with no large aggregate particles. They were characterized by a smooth surface texture and only small to very fine particles on the surface. These areas were noticed in Phase 3 testing and had not been observed in previous testing phases. These areas were considered to be evidence of extensive aggregate loss and were colored on the transparency film as aggregate loss.

Bleeding and/or flushing of binder film on the surface were observed in several test locations. Few individual aggregate particles could be discerned and the surface was primarily black in color and often tacky in texture. In test locations where this was observed the aggregate retention test was not considered meaningful. The observation of bleeding and/or surface flushing was noted and the aggregate retention test was not conducted.

### 3.4 Skid Resistance

Skid testing was performed on *Hwy 35* as per ASTM E 274-97. The test employs a locked wheel skid device pulled behind a truck. All testing was performed at 65 km/h (40 mph) and a ribbed tire was used making the test data SN(65)R. The test was conducted three times within each section. Skid testing was not performed at the same time as the test phases due to scheduling and other *MDOT* commitments for the equipment. *K.J. Law Engineers, Inc* manufactured the skid trailer model T1290, and Figure 3.12 is a photo of the device.



*Figure 3.12. Locked Wheel Skid Trailer*

### 3.5 Structural Deterioration

The Falling Weight Deflectometer (*FWD*) used during testing was a *Dynatest® Model 8000*. Figure 3.13 contains photos of the device. The *FWD* works by dropping weights a known distance onto a cushioned load plate resting on the pavement to produce a desired impulse into the pavement. The force applied to the pavement is measured with a load cell and the stress is calculated using the known dimensions of the load plate.



(a) FWD Photo 1 of 2



(b) FWD Photo 2 of 2

**Figure 3.13. Falling Weight Deflectometer Used for Testing**

Deflections are measured at discrete intervals from the center of the load plate to provide a measure of pavement response. Table 3.6 provides the distances from the center of the load plate where deflections were measured. As seen, the sensors were evenly spaced at 305 mm (12 in). Three load levels between 31 and 58 kN (7 to 13 kip) were applied at each location during each test phase. The FWD was not re-aligned at a given section between load levels.

**Table 3.6. Radial Distance From Center for FWD Loading**

Sensor	$D_1$	$D_2$	$D_3$	$D_4$	$D_5$	$D_6$	$D_7$
mm	0	305	610	915	1220	1525	1830
in	0	12	24	36	48	60	72

### 3.6 Manual Rut Measurements

Manual rut measurements were performed with a metal rut bar as shown in Figure 3.14. A rigid bar with lateral distance markers was leveled and a caliper was used to measure



**Figure 3.14. Manual Rut Measurements**

to the pavement surface at twelve locations across the lane width. Some of the measurements were used for cross slope calculations and the remaining measurements were used to determine the rut depth profile of the lane. These measurements were performed only on *Hwy 35* to provide a baseline measurement for comparison to profiler data, as well as for general information regarding the test sections. Manual rut measurements were not performed on *Hwy 17* due to logistical and traffic control constraints.

Figure 3.15 provides a schematic of the rut measurement process. The method is not highly accurate, especially on a textured surface such as a chip/scrub seal. To be effective, rutting should commence as shown in Figure 3.15. The points labeled 1 to 5 (or some combination thereof) are used to develop the slope of the section and subtracted from the relative depth measured from the top of the rigid bar; the maximum value would be taken as the rut depth.

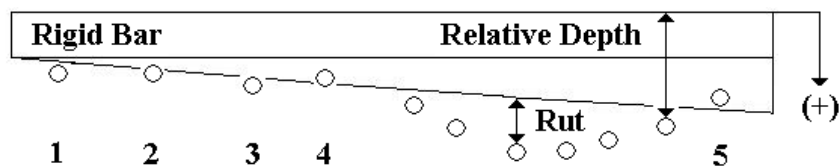


**Figure 3.15. Schematic of Relative Depth and Rut Measurements**

### 3.7 Automated Distress Measurements

A *Pathway Services Inc.* profiler was used to collect distress data under *Mississippi State Study 173* that was used in this project. A *PathRunner XP* model *LG-23* was used to collect the data. Data was collected in three phases. The data collection vehicle collects the necessary automated road survey data in one pass at normal highway speeds. The vehicle is equipped with cameras, lasers, accelerometers, distance measuring interfaces, global positioning system features, and electronic controls. Data collected for this project were: 1) rut depths (*Rut*), 2) International Roughness Index (*IRI*), 3) Fatigue cracking ( $C_F$ ) 4) longitudinal cracking ( $C_L$ ); 5) Transverse cracking ( $C_T$ ); and 6) Block cracking ( $C_B$ ). Photos of the *PathRunner XP* can be seen in Figure 3.16.



**Figure 3.16. Automated Data Collection Vehicle Used for Roadway Profiles**

### 3.8 Visual Assessments

Visual assessments were performed on each test section in each test phase. The author led the assessments and was provided input from the remaining *MDOT* and *MSU* researchers present during testing. Bleeding/flushing, popouts, and microcracks of the seals were of primary interest while transverse cracking, longitudinal cracking and anomalies were also noted. Parameters of interest were given a rating of: *None* (0), *Very Low* (1), *Low* (2), *Medium* (3), *High* (4), and *Very High* (5). The assessments were made over a few meter distance on either side of the test coordinate in the corresponding lane. They should not be considered sophisticated, or highly accurate. They were intended to provide an estimate of behavior of the seals within two minutes. A photo was also taken of each test coordinate during each test phase.

## CHAPTER 4-TEST RESULTS AND DATA ANALYSIS

### 4.1 General Field Testing Results

Table 4.1 provides general information regarding the *Hwy 17* test phases, while Table 4.2 provides general information regarding the *Hwy 35* test phases. An initial attempt to obtain field data from *Hwy 35* occurred on January 25, 2008. Freezing rain forced testing to be postponed after minimal data had been collected. The data was discarded and the entire test phase performed on February 11, 2008.

**Table 4.1. Summary of *Hwy 17* Test Phases**

Phase	Date	Weather	Temperature-C (F)			
			Ambient		Pavement	
			Begin	End	Begin	End
1	1/28/08 <sup>1</sup>	Clear with slight breeze	7.8 (46)	---	6.1 (43)	---
2	8/14/08	Sunny	22.7 (73)	36.1 (97)	25.0 (77)	43.9 (111)
3	1/7/09	Sunny	4.4 (40)	14.4 (58)	8.3 (47)	12.8 (55)

1: FWD Testing Performed on 2/7/08.

**Table 4.2. Summary of *Hwy 35* Test Phases**

Phase	Date	Weather	Temperature-C (F)			
			Ambient		Pavement	
			Begin	End	Begin	End
1	2/11/08	Sunny with wind	12.2 (54)	21.1 (70)	17.2 (63)	22.2 (72)
2	8/13/08	Overcast with slight breeze	22.7 (73)	30.0 (86)	23.3 (74)	37.8 (100)
3	1/9/09	Sunny with wind	11.7 (53)	23.9 (75)	11.1 (52)	19.4 (67)

The remainder of this chapter provides test data and analysis for each behavior investigated. They are separated by type of behavior and further separated by test section. Appendix A contains numerous photographs taken during testing. The windshield surveys (Section A.1) and visual assessment photos taken at every test location in every test phase (Section A.2) provide qualitative assessments of the pavements and the reader is encouraged to review the photos prior to and during the remainder of this chapter.

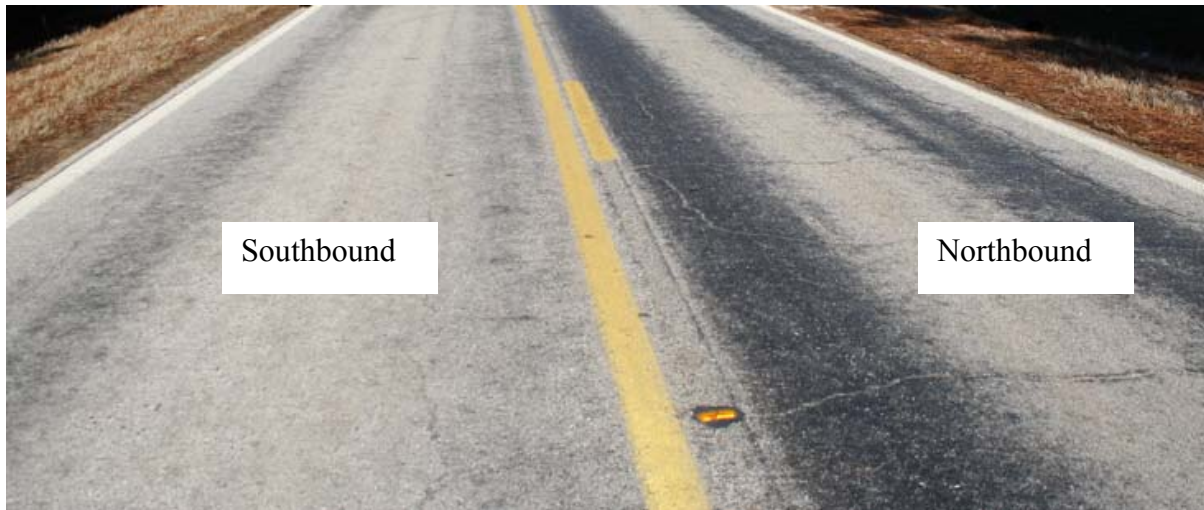
It is important to note the *Hwy 17* test section was analyzed in many cases as a northbound lane and a southbound lane. The test section was not planned in this manner, rather conditions observed during testing and occurrences during analysis warranted separation of the lanes. The primary observation that led the author to feel it prudent to perform separate analysis was the bleeding/flushing data discussed in the next section.

### 4.2 Bleeding/Flushing Test Results

#### 4.2.1 *Hwy 17* Bleeding/Flushing Test Results

Drastic differences were observed in the northbound and southbound lanes of *Hwy 17*. The northbound lane contained significantly more bleeding/flushing than did the southbound lane (Figure 4.1). Traffic patterns observed during testing provide evidence into

this behavior. Empty log trucks were frequently traveling southbound, were loaded, and traveled loaded on the northbound lane of the test section. No quantitative data was obtained



(a) *Relative Bleeding/Flushing Photo 1 of 2*



(b) *Relative Bleeding/Flushing Photo 2 of 2*

**Figure 4.1. Relative Differences in Hwy 17 Wheel Path Aggregate Coverage (Jan 2009)**

(e.g. weigh in motion data) but the trend of the northbound lane experiencing more bleeding/flushing while also experiencing heavier truck traffic agrees with the findings of the literature, survey questionnaires, and interviews of the Texas DOT performed by Lawson and Senadheera (2009) that is discussed more completely in Chapter 2. This observation should also be correlated to the initial temperature when constructing the northbound lane of Hwy

17, which was 5.0 C (41 F). Lawson and Senadheera (2009) also reported aggregate loss leading to flushing and/or bleeding frequently occurred with a chip seal placed outside the established asphalt season.

To investigate relative bleeding/flushing effects between chip and scrub seals, a small sample *t-test* was performed assuming equal variances. The null hypothesis ( $H_o$ ) was  $(\mu_1 - \mu_2) = 0$ . Two alternative hypotheses ( $H_a$ ) were compared to  $H_o$ : 1) upper tailed test where  $H_a: (\mu_1 - \mu_2) > 0$  and test statistic ( $t_a$ ) for the conditions considered was 1.71; and 2) two tailed test where  $H_a: (\mu_1 - \mu_2) \neq 0$  and test statistic ( $t_{a2}$ ) for the conditions considered was 2.07. Chip seal data was represented by  $\mu_1$  and scrub seal data was represented by  $\mu_2$ . Separate calculations were performed on the northbound and southbound lanes for each test phase using a level of significance of 5% ( $\alpha = 0.05$ ), and the results can be seen in Table 4.3.

**Table 4.3. Hwy 17 Bleeding/Flushing Test Results**

Direction	Ph	Age <sup>1</sup>	<i>t</i>	Upper Tail	Two Tail	Chip Seal			Scrub Seal		
						<i>n</i>	$\bar{x}$	<i>s</i>	<i>n</i>	$\bar{x}$	<i>s</i>
North	1	2.70	6.13	Reject	Reject	20	2.8	1.01	5	0.0	0.00
	2	9.24	3.19	Reject	Reject	20	4.2	0.99	5	2.6	0.89
	3	14.01	2.93	Reject	Reject	20	4.0	1.21	5	2.2	1.30
South	1	2.70	0.42	Accept	Accept	10	0.9	0.74	15	0.7	1.10
	2	9.24	2.23	Reject	Reject	10	2.0	1.56	15	0.9	0.99
	3	14.01	2.80	Reject	Reject	10	2.2	1.55	15	0.9	0.83

1: Age of seal expressed in months (1 month taken as 30.4 days).

The data in Table 4.3 shows that the bleeding/flushing was greater in the chip seal than in the scrub seal. The only instance where a statistically significant difference could not be detected was in the southbound lane of Phase 1. In all cases where  $H_o$  was rejected, the *t* statistic was larger than the critical value by a noticeable margin indicating the data to be fairly reliable even when considering that the data was collected in an approximate fashion (See Section 3.8).

#### 4.2.2 Hwy 35 Bleeding/Flushing Test Results

Drastic differences were not observed in the northbound and southbound lanes of Hwy 35. Refer to Section A.1 for windshield survey photos. With only scrub seal test sections statistical analysis of bleeding/flushing data was not meaningful. The key observation was that bleeding/flushing was not significant on Hwy 35. The data is provided in Table 4.4.

**Table 4.4. Hwy 35 Bleeding/Flushing Test Results**

Ph	Built (3/25/05)			Built (11/5/07)			All Data		
	<i>n</i>	$\bar{x}$	<i>s</i>	<i>n</i>	$\bar{x}$	<i>s</i>	<i>n</i>	$\bar{x}$	<i>s</i>
1	4	1.5	1.00	8	0.5	0.76	12	0.8	0.94
2	4	1.0	1.15	8	1.5	0.93	12	1.3	0.98
3	4	0.8	0.96	8	1.4	1.06	12	1.2	1.03



### 4.3 Skid Resistance Test Results

Table 4.5 summarizes all *Hwy 35* skid testing. As seen, average *Skid Number (SN)* values were generally above 40 and below 55. Each run in Table 4.5 is the average of six or more determinations of *SN*. Figure 4.2 plots the average values shown in Table 4.5 for each test section. The sections constructed in March of 2005 (3 and 4) have time overlap with the sections constructed in November of 2007 (1, 2, 5, and 6). As seen in Figure 4.2, the data from the 2007 construction at 9.74 months aligns on the order of the data from the 2005 construction at 11.88 months.

**Table 4.5. Skid Resistance Test Results of *Hwy 35***

Months Since Construction <sup>1</sup>	Avg Test Temp (C [F])	Date	Section <sup>2</sup>					
			1 (SN)	2 (SN)	3 (SN)	4 (SN)	5 (SN)	6 (SN)
6.09	23.3 [74]	5/8/08	51.6	52.0	---	---	53.2	53.0
			50.4	52.9			51.5	51.7
			50.0	52.1			51.2	50.8
			<b>50.7</b>	<b>52.3</b>			<b>52.0</b>	<b>51.8</b>
9.74	28.3 [83]	8/27/08	46.6	47.7	---	---	51.2	49.1
			42.0	45.9			46.5	44.6
			43.5	44.1			44.4	44.3
			<b>44.0</b>	<b>45.9</b>			<b>47.4</b>	<b>46.0</b>
15.26	17.8 [64]	2/11/09	51.7	52.8	---	---	49.9	49.8
			48.8	49.8			49.8	49.8
			48.1	48.4			49.7	47.9
			<b>49.5</b>	<b>50.3</b>			<b>49.8</b>	<b>49.2</b>
11.88	10.0 [50]	3/21/06	---	---	47.5	48.1	---	---
					45.3	46.0		
					43.8	44.5		
					<b>45.5</b>	<b>46.2</b>		
37.47	23.3 [74]	5/8/08	---	---	42.9	46.3	---	---
					44.1	46.8		
					41.2	45.7		
					<b>42.7</b>	<b>46.3</b>		
41.12	28.3 [83]	8/27/08	---	---	40.8	42.0	---	---
					36.7	39.4		
					34.3	38.4		
					<b>37.3</b>	<b>39.9</b>		
46.64	17.8 [64]	2/11/09	---	---	43.7	46.5	---	---
					43.4	46.7		
					41.9	45.2		
					<b>43.0</b>	<b>46.1</b>		

1: A month was defined as 30.4 days.

2: Data not in bold are individual test runs while values in bold are the average of the test runs.

The data from the 2007 construction at 9.74 months was taken on the same day as that for the 2005 construction at 41.12 months (note the groups of sections were built 31.41 months apart), which is noteworthy since all this data falls below the trend of the remaining data. The temperature measured by the skid testing equipment is shown in Table 4.5 and shows the temperature on this day of testing was higher than for any other test interval. The temperature could have lowered the readings by livening the binder and thus allowing more flexibility of the cover aggregates, though this is purely speculation since skid data is not adjusted for temperature and no quantifiable data is available to support the statement.

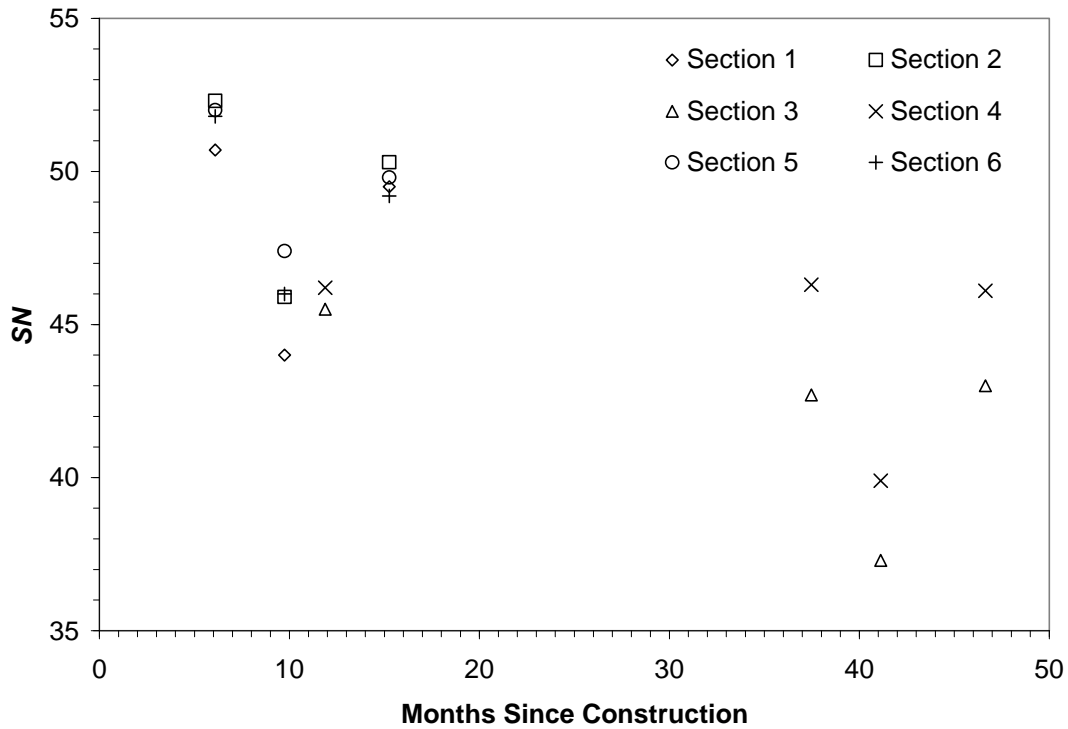


**Figure 4.2. Skid Data of Individual Test Sections**

Figure 4.3 plots the average values of all skid data collected. The data is identical to Figure 4.2 with the exception that all data was plotted as one series. The trend line of Figure 4.3 could be used to estimate the time to achieve a given threshold of SN. The large amount of scatter in the data coupled with the relatively small number of measurements makes this merely a crude estimate, but it has value when applied in the context of a rough approximation.

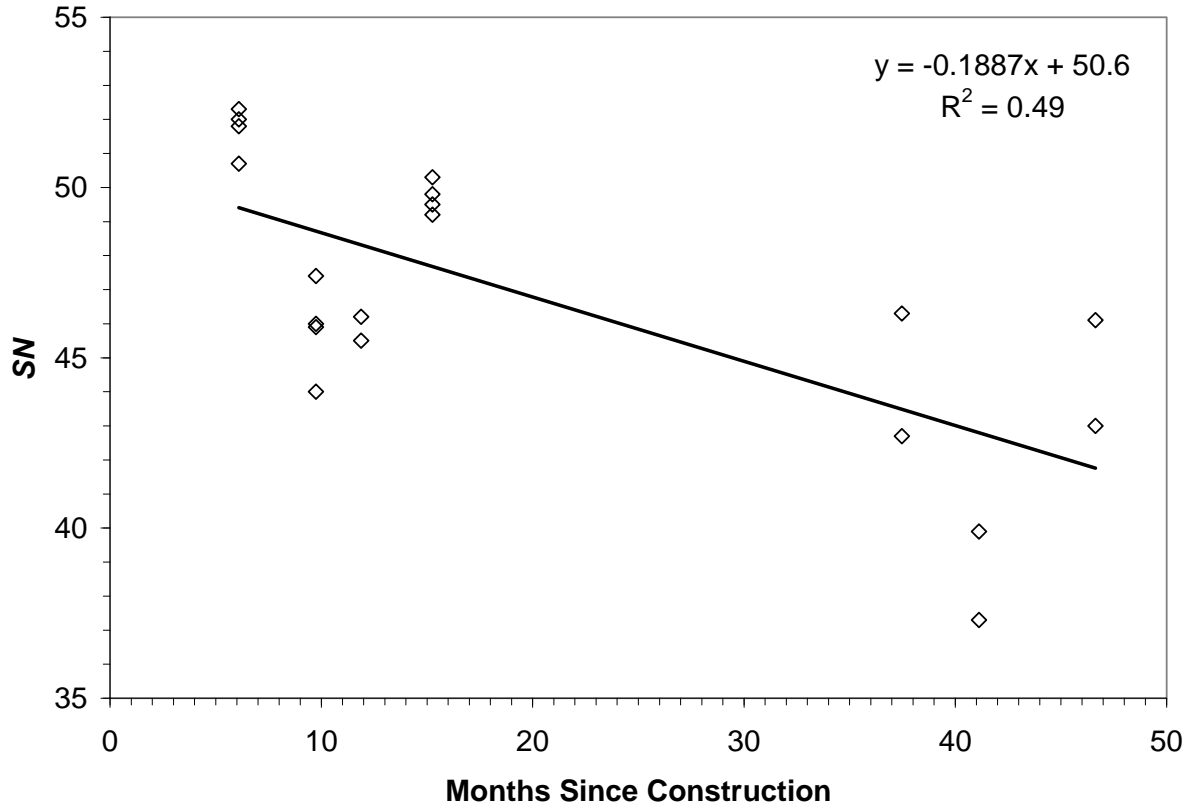


*Figure 4.3. Skid Data Used to Develop Trend Line for Hwy 35 Scrub Seal*

#### 4.4 Aggregate Retention Test Results

Aggregate retention became more subjective as testing progressed, especially on *Hwy 17*. Areas where aggregate had been dislodged became much harder to determine. There were many of areas of smooth bituminous material on *Hwy 17*. These areas are difficult to identify as aggregate loss in that bleeding/flushing could be the mechanism. In either case bituminous material is exposed, but the research team attempted to isolate the behaviors in the research. Popouts were investigated during the visual assessments and the results were presented in this chapter.

##### 4.4.1 *Hwy 17* Aggregate Retention Test Results

Figure 4.4 visually compares the aggregate retention performance of the chip and scrub sealed test sections. Visually, the scrub seal sections out performed the chip seal sections. However, the amount of this performance to be attributed to aggregate retention cannot be quantified due to the bleeding/flushing experienced in this lane.

Table 4.6 provides all aggregate retention data collected on *Hwy 17* during all phases as well as the total aggregate loss during testing. The data reported for each individual phase was the aggregate lost since the previous phase, not the aggregate lost to that point in testing. The total aggregate loss was the sum of the individual phases. The excessive bleeding/flushing (B/F) that occurred in the northbound lane wheel path lessened the ability

for effective evaluation. The average total aggregate loss of the two chip seal sections was 2.89%, while the average total aggregate loss of the four scrub seal sections was 3.45%. The slightly higher loss of aggregate from the scrub seal sections, though, should be considered in the context that all four scrub seal sections were able to be evaluated while only two of the six chip seal sections were able to be evaluated.



(a) Scrub Seal Cores



(b) Chip Seal Cores



(c) All Cores

**Figure 4.4. Photos of Cores Taken From Northbound Hwy 17**

A paired  $t$ -test was performed for total aggregate loss on the six sections of Table 4.6 that did not experience bleeding/flushing problems. The null hypothesis ( $H_o$ ) was  $(\mu_1 - \mu_2) = 0$ . Two alternative hypotheses ( $H_a$ ) were compared to  $H_o$ : 1) upper tailed test where  $H_a: (\mu_1 - \mu_2) > 0$  and critical value ( $t_{\alpha}$ ) for the conditions considered was 2.02; and 2) two tailed test where  $H_a: (\mu_1 - \mu_2) \neq 0$  and critical value ( $t_{\alpha/2}$ ) for the conditions considered was 2.57. Lane center ( $LC$ ) data was represented by  $\mu_1$  and wheel path ( $WP$ ) data was represented by  $\mu_2$ . A level of significance of 5% ( $\alpha = 0.05$ ). The test statistic ( $t$ ) was computed to be 1.68, which does not warrant rejection of  $H_o$  for either condition indicating there is no statistically significant evidence that the aggregate loss in the center of the lane is different from that in the wheel path for the six test sections that did not experience excessive bleeding/flushing. All but one of the six pairs had aggregate loss higher in the lane center than the wheel path, but the data set was relatively small (especially after removal of four test sections).

**Table 4.6. Aggregate Retention Test Results of Hwy 17**

Location	Lane	Type	Months Since Construction	Coordinate	Aggregate Loss (%)			
					2.70	9.24	14.01	14.01
				Ph 1	Ph 2	Ph 3	Total	
<i>WP</i>	NB	Chip	7.251	7.251	1.09	B/F	B/F	B/F
		Chip	6.751	6.751	0.00	B/F	B/F	B/F
		Chip	6.251	6.251	0.30	2.00	0.39	2.69
		Chip	5.751	5.751	0.00	B/F	B/F	B/F
		Scrub	5.251	5.251	0.69	1.09	0.43	2.21
	SB	Chip	7.251	7.251	0.61	2.13	0.35	3.08
		Chip	6.751	6.751	0.82	B/F	B/F	B/F
		Scrub	6.251	6.251	0.26	4.30	0.30	4.86
		Scrub	5.751	5.751	0.48	4.17	0.22	4.86
		Scrub	5.251	5.251	0.00	0.82	1.09	1.91
<i>LC</i>	NB	Chip	7.251	7.251	0.35	3.95	0.48	4.77
		Chip	6.751	6.751	0.39	3.95	1.00	5.34
		Chip	6.251	6.251	0.56	3.91	0.87	5.34
		Chip	5.751	5.751	0.56	2.86	1.35	4.77
		Scrub	5.251	5.251	0.61	7.20	1.35	9.16
	SB	Chip	7.251	7.251	0.43	2.95	0.35	3.73
		Chip	6.751	6.751	0.78	4.60	0.56	5.95
		Scrub	6.251	6.251	0.35	3.39	1.56	5.30
		Scrub	5.751	5.751	0.35	2.65	0.74	3.73
		Scrub	5.251	5.251	0.00	3.47	0.35	3.82

In that no statistically significant difference were found between the wheel path and lane center, all Table 4.6 data was combined for chip seals and scrub seals. The variances were too different to perform an equal variance (i.e. pooled) *t*-test. The small number of samples (8 for each seal type) made removal of data points to reduce the variance somewhat undesirable. A frequency histogram (Figure 4.5) was thus felt most appropriate for

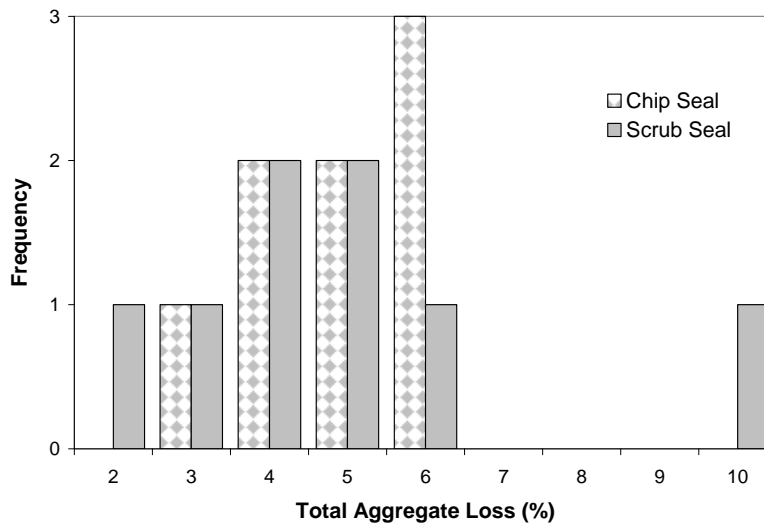


**Figure 4.5. Comparison of Chip and Scrub Seal Aggregate Loss on Hwy 17**

comparison of the chip and scrub seal sections total aggregate loss. The horizontal axis should be interpreted as the maximum aggregate loss in a given category (e.g. 6 would represent aggregate loss of 5.01 to 6.00%). The plot shows no major differences between the chip and scrub seals though the scrub seal is more variable. Both the highest and lowest aggregate losses occurred on a scrub seal. The only difference in performance would be two of the chip seal sections in the 6% category, the scrub seal in the 2% category, and the scrub seal in the 10% category. Otherwise, the histogram is identical between sections. Overall, the chip seal performance would be slightly favored over the scrub seal based on Figure 4.5.

Table 4.6 data is comparable to that found on US 84 (Howard and Baumgardner 2009; Howard et al. 2009) where 11 months after construction less than 5% aggregate loss had been experienced with exception of one data point. If one were to exclude the four sections where excessive bleeding occurred prior to Ph 2 and sum the aggregate losses of Ph 1 and Ph 2 only two sections had exceeded 5% aggregate loss within approximately 9 months. Five sections had exceeded 5% aggregate loss approximately 14 months into the life of the seal treatments (four of them had only exceeded the 5% threshold by a relatively small margin).

To investigate popouts from visual observation between chip and scrub seals, a small sample *t*-test was performed assuming equal variances. The null hypothesis ( $H_o$ ) was  $(\mu_1 - \mu_2) = 0$ . Two alternative hypotheses ( $H_a$ ) were compared to  $H_o$ : 1) upper tailed test where  $H_a: (\mu_1 - \mu_2) > 0$  and test statistic ( $t_a$ ) for the conditions considered was 1.71; and 2) two tailed test where  $H_a: (\mu_1 - \mu_2) \neq 0$  and test statistic ( $t_{a2}$ ) for the conditions considered was 2.07. Chip seal data was represented by  $\mu_1$  and scrub seal data was represented by  $\mu_2$ . Separate calculations were performed on the northbound and southbound lanes for each test phase using a level of significance of 5% ( $\alpha = 0.05$ ), and the results can be seen in Table 4.7. With exception of one case,  $H_o$  was not rejected indicating no statistically significant evidence exists the mean level of popouts was different between chip and scrub seal sections.

**Table 4.7. Hwy 17 Popout Test Results**

Direction	Ph	Age <sup>1</sup>	<i>t</i>	Upper Tail	Two Tail	Chip Seal			Scrub Seal		
						<i>n</i>	$\bar{x}$	<i>s</i>	<i>n</i>	$\bar{x}$	<i>s</i>
North	1	2.70	2.05	Reject	Accept	20	1.9	0.97	5	1.0	0.00
	2	9.24	-0.57	Accept	Accept	20	0.8	0.52	5	1.0	1.22
	3	14.01	1.06	Accept	Accept	20	1.6	1.15	5	1.0	0.00
South	1	2.70	-0.72	Accept	Accept	10	1.3	0.82	15	1.6	1.12
	2	9.24	-1.49	Accept	Accept	10	0.8	0.79	15	1.2	0.56
	3	14.01	0.00	Accept	Accept	10	0.6	0.70	15	0.6	0.74

*1: Age of seal expressed in months (1 month taken as 30.4 days).*

#### 4.4.2 Hwy 35 Aggregate Retention Test Results

Tables 4.8 and 4.9 contain all test results of the Hwy 35 test sections constructed in 2005 and 2007, respectively. The tables provide the aggregate loss measured during each individual phase and then the total for all phases. Note that since no measure of aggregate retention was obtained for the 2005 constructed sections soon after placement, the values shown should not necessarily be considered total aggregate loss, rather aggregate loss over a 10.92 month period beginning 34.63 months after construction. The heat in Mississippi can

reach levels that cause the bituminous material to become somewhat plastic and with time remove the shape that would be present from a newly dislodged aggregate particle, which was a primary item the aggregate retention operators were looking for.

**Table 4.8. Aggregate Retention Test Results of Hwy 35 Constructed in 2005**

	Months Since Construction		Aggregate Loss (%)			
			34.63	40.69	45.55	45.55
Location	Lane	Coordinate	Ph 1	Ph 2	Ph 3	Total
WP	NB	18.868	1.04	2.99	2.13	6.16
WP	NB	19.678	0.48	1.43	0.61	2.52
WP	SB	19.678	0.30	0.82	1.39	2.52
WP	SB	18.868	0.22	0.35	0.56	1.13
LC	NB	19.678	0.26	1.95	1.09	3.30
LC	SB	19.678	0.43	1.26	1.26	2.95

**Table 4.9. Aggregate Retention Test Results of Hwy 35 Constructed in 2007**

	Months Since Construction		Aggregate Loss (%)			
			3.22	9.28	14.14	14.14
Location	Lane	Coordinate	Ph 1	Ph 2	Ph 3	Total
WP	NB	17.868	0.22	1.87	2.04	4.12
WP	NB	18.678	0.35	0.61	2.99	3.95
WP	NB	19.868	0.35	2.00	0.48	2.82
WP	NB	20.678	0.52	1.43	0.39	2.34
WP	SB	20.678	0.39	0.74	0.78	1.91
WP	SB	19.868	0.56	1.04	0.35	1.95
WP	SB	18.678	0.09	1.61	1.82	3.52
WP	SB	17.868	0.48	0.82	3.43	4.73
LC	NB	18.678	0.35	2.17	2.86	5.38
LC	NB	20.678	0.35	1.61	1.52	3.47
LC	SB	20.678	0.48	1.13	2.17	3.78
LC	SB	18.678	0.69	2.21	9.81	12.72

A paired *t*-test was performed for total aggregate loss on the six sections of Tables 4.8 and 4.9 where a wheel path and lane center measurement were available. The null hypothesis ( $H_o$ ) was  $(\mu_1 - \mu_2) = 0$ . Two alternative hypotheses ( $H_a$ ) were compared to  $H_o$ : 1) upper tailed test where  $H_a: (\mu_1 - \mu_2) > 0$  and critical value ( $t_{\alpha}$ ) for the conditions considered was 2.02; and 2) two tailed test where  $H_a: (\mu_1 - \mu_2) \neq 0$  and critical value ( $t_{\alpha/2}$ ) for the conditions considered was 2.57. Lane center (LC) data was represented by  $\mu_1$  and wheel path (WP) data was represented by  $\mu_2$ . A level of significance of 5% ( $\alpha = 0.05$ ). The test statistic (*t*) was computed to be 1.82, which does not warrant rejection of  $H_o$  for either condition indicating there is no statistically significant evidence that the aggregate loss in the center of the lane is different from that in the wheel path on Hwy 35.

Note the 18.678 southbound (SB) coordinate is noticeably different than the other data though there is no other reason to question its validity. Provided it is removed from the data, the test statistic is 4.51 which warrants rejection of  $H_o$  in favor of either an upper tail ( $t_{\alpha}$  of 2.13) or lower tail ( $t_{\alpha/2}$  of 2.78). Rejection of  $H_o$  would provide statistically significant

evidence that more aggregate loss occurred in the lane center than in the wheel path. The data set is limited and there isn't a strong case for omission of the 18.678 southbound (SB) coordinate from the analysis, though the author would slightly favor this analysis in favor of the one where all data was considered.

A pooled variance *t*-test was conducted in a similar manner as described previously comparing all data from the 2005 construction to the 2007 construction. The result was there was no statistical evidence the mean values were different between the 2005 and 2007 scrub seals. The analysis was also conducted without the 18.678 SB coordinate with the same result. With only scrub seal test sections; pop out data from *Hwy 35* provided little physical meaning and was not used in analysis.

## 4.5 Rutting Test Results

Rutting data was collected with an automated van for *Hwy 17* and *Hwy 35* and also using a manual method for *Hwy 35*. Specific details were provided in Chapter 3. With the automated van, rut depths are measured by using three lasers: one in the outer wheel path, one in the inner wheel path, and one in the center of the lane. The maximum rut value is recorded as the rut depth. The outer wheel path was measured using the manual method.

### 4.5.1 *Hwy 17* Rutting Test Results

Table 4.10 contains rutting test results of *Hwy 17*. Rut depths were not significant. Rut depths ranged from 1.8 to 5.3 mm (0.07 to 0.21 in). All six northbound test sections had higher rut depths than their southbound counterparts, indicating a heavier traffic pattern. Performance indicators noted elsewhere support this behavior.

**Table 4.10. Rutting Test Results of *Hwy 17***

Months Since Construction		-0.66		3.68		15.89	
		Rut (in)	Rut (mm)	Rut (in)	Rut (mm)	Rut (in)	Rut (mm)
Section	Direction						
1	South	---	---	0.15	3.8	0.14	3.6
2	North	---	---	0.19	4.8	0.20	5.1
3	South	---	---	0.08	2.0	0.09	2.3
4	North	0.14	3.6	0.12	3.0	0.18	4.6
5	South	---	---	0.09	2.3	0.09	2.3
6	North	0.17	4.3	0.14	3.6	0.21	5.3
7	South	---	---	0.07	1.8	0.07	1.8
8	North	0.12	3.0	0.12	3.0	0.14	3.6
9	South	---	---	0.07	1.8	0.06	1.5
10	North	0.12	3.0	0.18	4.6	0.16	4.1
11	South	---	---	0.08	2.0	0.10	2.5
12	North	0.21	5.3	0.07	1.8	0.18	4.6



### 4.5.2 Hwy 35 Rutting Test Results

Manual rut measurements were taken on Hwy 35 using a rigid bar as described in Section 3.6. The accuracy of measurement for small magnitudes is not high (especially with seal treatments); rather the method is intended to measure pavement profiles where the rutting is more pronounced (e.g. Figure 3.15). In absence of a defined rut profile the data is valuable in the qualitative sense that substantial rutting has not occurred.

Figures 4.6 through 4.8 provide the relative depths measured during testing. As seen, they do not produce a noticeable depression in the wheel path which makes calculation of rut depths unproductive. The magnitude of rut depths calculated would be within the noise of the method used to make the measurements and would thus be of little value. Qualitatively, the data shows little to no rutting occurring within the test sections.

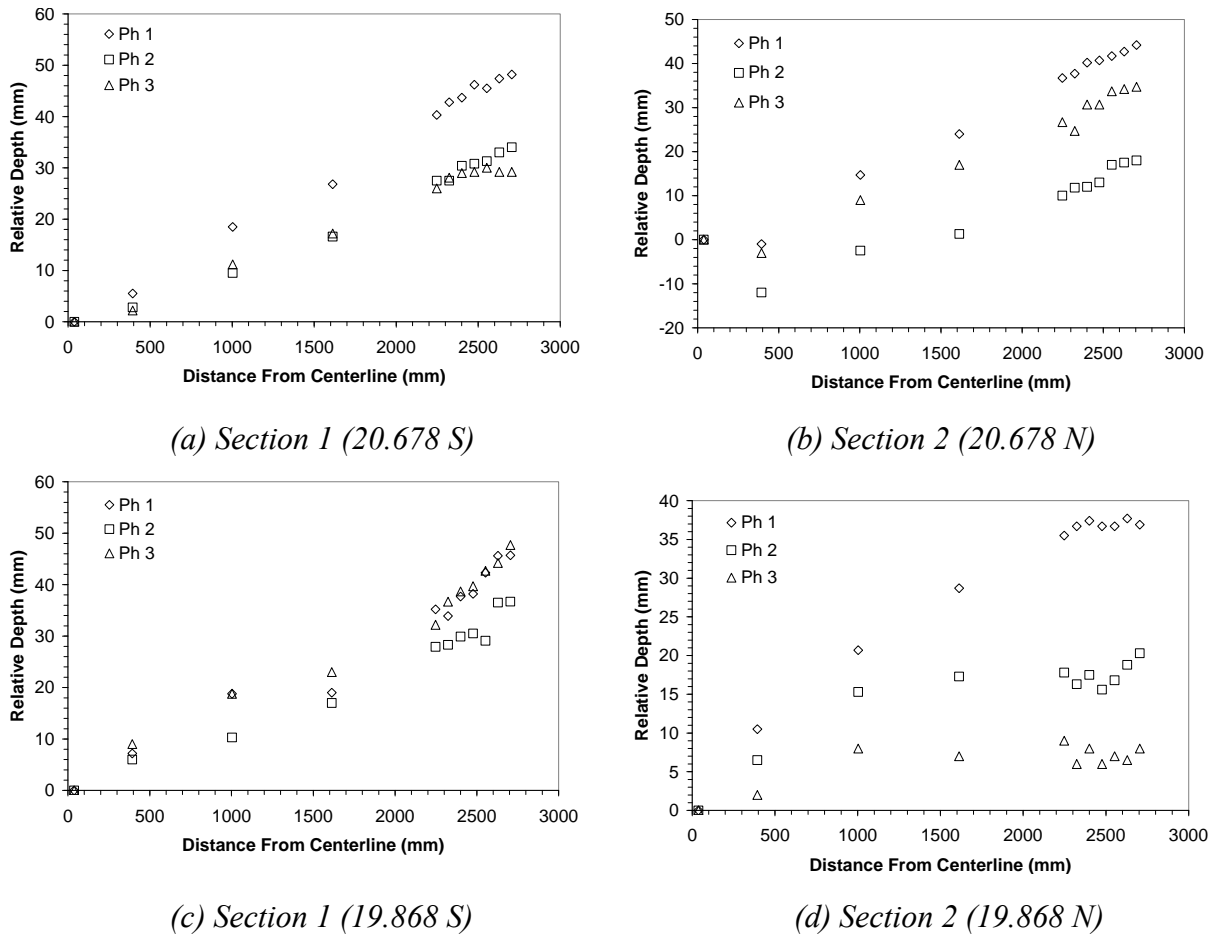


**Figure 4.6. Relative Depth Profiles of Hwy 35 Sections 1 and 2**

When the relative depths were measured, the research team did not take extreme measures to level the rigid bar; rather a bubble level was placed in the center of the bar and as long as the bubble was within the indicated marks on the level measurement proceeded. Over the width of the lane the bubble being within the marks yet near the centerline mark would be expected to give a slightly different slope than the bubble being within the mark yet

near the shoulder mark. Also, the transverse alignment of the bar was performed visually. As seen in Figures 4.6 through 4.8, the relative depths vary somewhat between test phases (largely due to the aforementioned parameters). The measured rut depths were of interest, though, which could still be measured with adequate precision had the general shape of Figure 3.15 been observed.

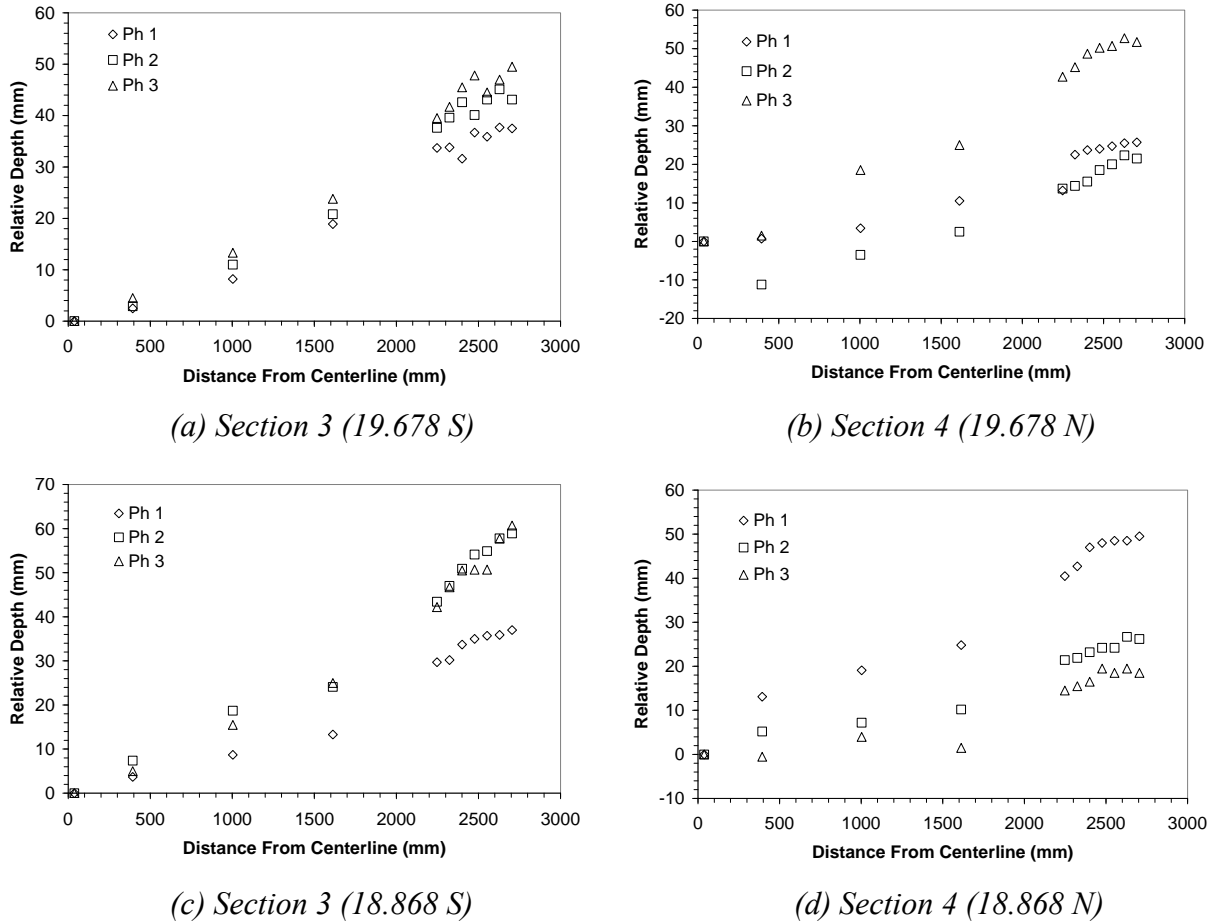
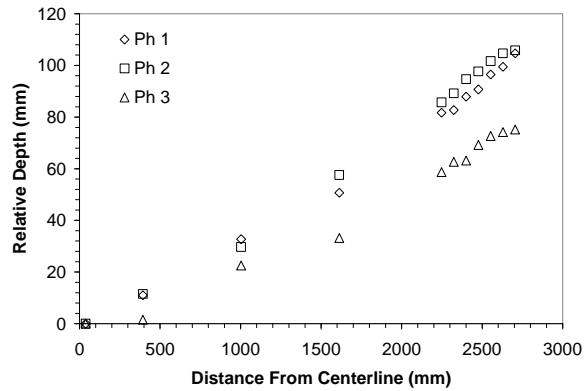
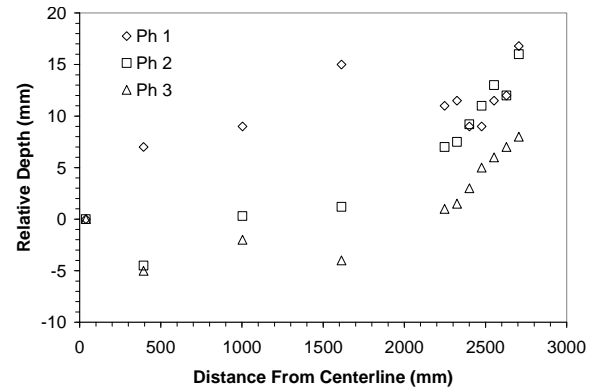


**Figure 4.7. Relative Depth Profiles of Hwy 35 Sections 3 and 4**

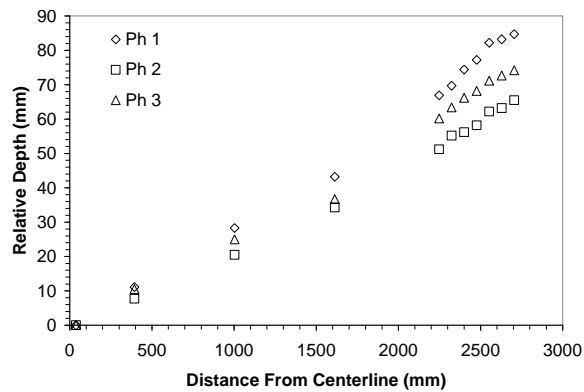
Table 4.11 contains automated rutting test results of Hwy 35. Rut depths were not significant. Rut depths ranged from 1.3 to 5.8 mm (0.05 to 0.23 in). No meaningful trends were observed other than rutting was not problematic according to the automated measurements.



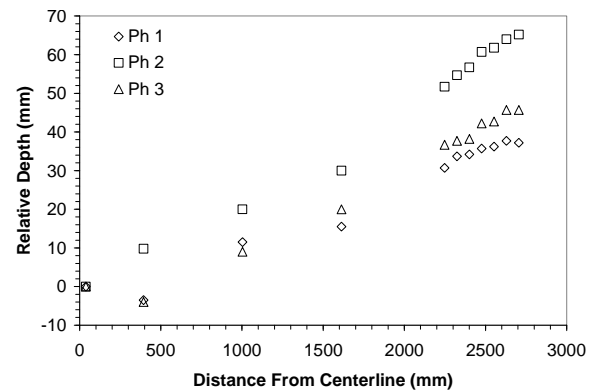
(a) Section 5 (18.678 S)



(b) Section 6 (18.678 N)



(c) Section 5 (17.868 S)



(d) Section 6 (17.868 N)

**Figure 4.8. Relative Depth Profiles of Hwy 35 Sections 5 and 6**

**Table 4.11. Automated Rutting Test Results of Hwy 35**

Section	Direction	Months Since Construction	Rut (in)	Rut (mm)
1	South	-0.63	---	---
		3.75	0.05	1.3
		15.95	0.07	1.8
2	North	-0.63	0.11	2.8
		3.75	0.09	2.3
		15.95	0.11	2.8
3	South	30.79	---	---
		35.16	0.21	5.3
		47.37	0.23	5.8
4	North	30.79	0.19	4.8
		35.16	0.15	3.8
		47.37	0.21	5.3
5	South	-0.63	---	---
		3.75	0.15	3.8
		15.95	0.21	5.3
6	North	-0.63	0.23	5.8
		3.75	0.15	3.8
		15.95	0.19	4.8

## 4.6 Roughness Test Results

Roughness was characterized using the *International Roughness Index (IRI)*. In essence, the *IRI* is the cumulative vertical movement divided by the distance traveled. The higher the *IRI*, the rougher the pavement. The automated van recorded data at intervals on the order of 0.15 m (6 in), which was used for computation. Data was collected in both the inner and outer wheel path (WP).

### 4.6.1 Hwy 17 Roughness Test Results

Tables 4.12 and 4.13 contain the *IRI* test results of *Hwy 17*. Distress data was not obtained during the summer of 2008. No consistent trends with time were observed. Five of the twelve test sections were tested three times; inner and outer WP for a total of ten conditions of three data points each. All five of these were treated sections in the northbound lane. The *IRI* decreased between -0.66 months and 3.68 months and then increased to above the -0.66 month value at 15.89 months in five of the ten cases. One case continually became smoother, three cases were roughest at 3.68 months and one case was smoother at 3.68 months and 15.89 months relative to -0.66 months yet rougher at 15.89 months than 3.68 months.

Trends of roughness were more consistent in the southbound lane, though only two data points were available for each section. Nine of the twelve possible data points (six sections with inner and outer wheel paths) were rougher at 15.89 months than at 3.68 months, two were smoother, and one did not change between the test intervals. The southbound lane was not tested for distress prior to sealing; standard *MDOT* protocol obtains northbound data.

**Table 4.12. *IRI* Test Results of *Hwy 17*-Northbound Lane**

Section	Months <sup>1</sup>	<i>IRI</i> (mm/m)			<i>IRI</i> (in/mi)		
		Inner WP	Outer WP	Avg	Inner WP	Outer WP	Avg
2	-0.66	---	---	---	---	---	---
	3.68	1.70	2.32	2.01	107.7	147.0	127.4
	15.89	1.65	2.41	2.03	104.6	152.7	128.6
4	-0.66	1.66	2.04	1.85	105.2	129.3	117.2
	3.68	1.52	1.95	1.73	96.3	123.6	109.6
	15.89	1.79	2.13	1.96	113.4	135.0	124.2
6	-0.66	1.56	1.87	1.72	98.9	118.5	109.0
	3.68	1.45	1.68	1.57	91.9	106.5	99.5
	15.89	1.70	1.90	1.80	107.7	120.4	114.1
8	-0.66	1.57	1.60	1.58	99.5	101.4	100.1
	3.68	1.50	1.74	1.62	95.1	110.3	102.7
	15.89	1.44	1.67	1.55	91.3	105.8	98.2
10	-0.66	1.32	1.72	1.52	83.6	109.0	96.3
	3.68	1.67	2.01	1.84	105.8	127.4	116.6
	15.89	1.37	1.68	1.52	86.8	106.5	96.3
12	-0.66	1.97	2.41	2.19	124.8	152.7	138.8
	3.68	1.66	2.27	1.97	105.2	143.8	124.8
	15.89	1.91	2.47	2.19	121.0	156.5	138.8

1: Months Since Construction.

**Table 4.13. IRI Test Results of Hwy 17-Southbound Lane**

Section	Months <sup>1</sup>	IRI (mm/m)			IRI (in/mi)		
		Inner WP	Outer WP	Avg	Inner WP	Outer WP	Avg
1	-0.66	---	---	---	---	---	---
	3.68	1.28	1.14	1.21	81.1	72.2	76.7
	15.89	1.37	1.34	1.36	86.8	84.9	86.2
3	-0.66	---	---	---	---	---	---
	3.68	1.66	1.57	1.62	105.2	99.5	102.7
	15.89	1.66	1.64	1.65	105.2	103.9	104.6
5	-0.66	---	---	---	---	---	---
	3.68	1.42	1.31	1.36	90.0	83.0	86.2
	15.89	1.44	1.38	1.41	91.3	87.5	89.4
7	-0.66	---	---	---	---	---	---
	3.68	1.47	1.38	1.42	93.2	87.5	90.0
	15.89	1.44	1.40	1.42	91.3	88.7	90.0
9	-0.66	---	---	---	---	---	---
	3.68	1.49	1.40	1.44	94.4	88.7	91.3
	15.89	1.47	1.44	1.46	93.2	91.3	92.5
11	-0.66	---	---	---	---	---	---
	3.68	1.65	1.79	1.72	104.6	113.4	109.0
	15.89	1.72	1.95	1.84	109.0	123.6	116.6

1: Months Since Construction.

The IRI ranged from 1.32 to 1.97 and from 1.60 to 2.47 in the inner and outer wheel paths of the northbound lane of Hwy 17, respectively. The IRI ranged from 1.28 to 1.72 and from 1.14 to 1.95 in the inner and outer wheel paths of the southbound lane of Hwy 17, respectively. A paired *t*-test was performed individually for IRI between the inner and outer wheel paths of each lane. The null hypothesis ( $H_o$ ) was  $(\mu_1 - \mu_2) = 0$ . The alternative hypotheses were one tailed. A level of significance of 5% ( $\alpha = 0.05$ ) was used. For the northbound lane the test statistic (*t*) was 8.60 and the critical value ( $t_\alpha$ ) was 1.75. Statistical evidence was found that the outer wheel path was rougher than the inner wheel path of the northbound lane of Hwy 17. For the southbound lane, the absolute value of the test statistic was 0.89 and the critical value ( $t_\alpha$ ) was 1.80. No statistical evidence that the roughness of the inner and outer wheel paths were different was found for the southbound lane of Hwy 17.

Comparison of IRI between no treatment, chip seals, and scrub seals provided only qualitative information. The lack of complete pre-seal data, lack of data in the summer of 2008, and the differences in the northbound and southbound lanes (especially in terms of bleeding/flushing) made quantitative comparisons unproductive beyond basic computations. The change in roughness for all combinations of seal type, lane, and test interval was deemed the most suitable analysis technique. The results are shown in Table 4.14, which were developed using the data in Tables 4.12 and 4.13.

As seen in Table 4.14 nine of the eleven possible data sets were generated using the two distress surveys taken after sealing. Of these nine data sets, the three sets where both lanes were analyzed together are believed to be the most reliable and provide no compelling argument that the pavement roughness was affected positively or negatively by the seal treatments. The chip seal had a lower average roughness, but it also had much higher variability. The scrub seal and no treatment were very similar in terms of average value and variability. The only noticeable difference between 3.68 and 15.89 months after sealing

construction was the chip seal sections where the pavement was significantly smoother. As seen further into Table 4.14, these sections were all in the northbound lane where it was shown earlier in this report that substantial bleeding/flushing occurred, which could have resulted in some sections becoming noticeably smoother. Section 10 (coordinate 5.751 of Table 4.6 is within this section) could not be evaluated for aggregate retention due to excessive bleeding/flushing, which is where the substantial smoother values were measured by the automated van (e.g. -0.33 minimum value shown in Table 4.14). If the *IRI* values from Section 10 were removed from the calculations, the average value for this condition would increase from 0.03 to 0.10, which would align it with the average values of the scrub seal and no treatment of 0.09 and 0.08, respectively.

The data from the northbound lane between -0.66 months (pre-seal treatment construction) to 15.89 months supports the statement in the previous paragraph that neither seal treatment seemed to affect the *IRI*. The chip seal average was 0.04 mm/m rougher and the scrub seal average was 0.00 mm/m rougher. Note that this data set should not be considered conclusive relative to roughness effects of seal treatments; the data set did not show apparent differences in average values or variability between chip seals, scrub seals, and no seal treatment.

**Table 4.14. Change in Roughness Test Results for Hwy 17 (mm/m)**

Seal	Lane	Duration <sup>1</sup>	Avg	St.Dev	Max	Min	n
Chip	Both	15.89 to 3.68	0.03	0.20	0.27	-0.33	12
Scrub	Both	15.89 to 3.68	0.09	0.10	0.25	-0.03	8
None	Both	15.89 to 3.68	0.08	0.10	0.20	-0.05	4
Chip	South	15.89 to 3.68	0.04	0.04	0.07	0.00	4
Scrub	South	15.89 to 3.68	0.04	0.07	0.16	-0.03	6
None	South	15.89 to 3.68	0.15	0.08	0.20	0.09	2
Chip	North	15.89 to 3.68	0.02	0.25	0.27	-0.33	8
Scrub	North	15.89 to 3.68	0.23	0.04	0.25	0.20	2
None	North	15.89 to 3.68	0.02	0.10	0.09	-0.05	2
Chip	North	15.89 to -0.66	0.04	0.09	0.14	-0.13	8
Scrub	North	15.89 to -0.66	0.00	0.08	0.06	-0.06	2

*1: Values computed by taking the difference in roughness between the months since construction indicated. Positive values indicate a rougher pavement and negative values indicate a smoother pavement.*

#### 4.6.2 Hwy 35 Roughness Test Results

Table 4.15 contains the *IRI* test results of Hwy 35. A paired *t*-test was performed for *IRI* between the inner and outer wheel paths of the entire Hwy 35 test section. The null hypothesis ( $H_0$ ) was  $(\mu_1 - \mu_2) = 0$ . The alternative hypothesis was one tailed. A level of significance of 5% ( $\alpha = 0.05$ ) was used. The test statistic (*t*) was 2.62 and the critical value ( $t_\alpha$ ) was 1.76. Statistical evidence was found that the outer wheel path was rougher than the inner wheel path of Hwy 35. The sections constructed in 2005 did not appear to be increasing in roughness with time at a different rate than those constructed in 2007. Note the variability within the range of change in *IRI* was fairly high. It is noteworthy that both 2005 constructed test sections became rougher with time in all cases whereas the 2007 constructed sections sometimes became rougher with time and other times became smoother with time according to the data.

**Table 4.15. IRI Test Results of Hwy35**

Section	Months <sup>1</sup>	IRI (mm/m)			IRI (in/mi)		
		Inner WP	Outer WP	Avg	Inner WP	Outer WP	Avg
1	-0.63	---	---	---	---	---	---
	3.75	1.54	1.84	1.69	97.6	116.6	107.1
	15.95	1.51	1.92	1.71	95.7	121.7	108.4
2	-0.63	1.74	1.65	1.69	110.3	104.6	107.1
	3.75	1.61	1.67	1.64	102.0	105.8	103.9
	15.95	1.64	1.72	1.68	103.9	109.0	106.5
3	30.79	---	---	---	---	---	---
	35.16	1.48	1.71	1.59	93.8	108.4	100.8
	47.37	1.53	1.80	1.66	97.0	114.1	105.2
4	30.79	1.56	1.51	1.54	98.9	95.7	97.6
	35.16	1.60	1.48	1.54	101.4	93.8	97.6
	47.37	1.60	1.56	1.58	101.4	98.9	100.1
5	-0.63	---	---	---	---	---	---
	3.75	1.22	1.66	1.44	77.3	105.2	91.3
	15.95	1.20	1.61	1.41	76.0	102.0	89.4
6	-0.63	1.11	1.10	1.11	70.3	69.7	70.3
	3.75	1.13	1.17	1.15	71.6	74.1	72.9
	15.95	1.17	1.21	1.19	74.1	76.7	75.4

1: Months Since Construction.

## 4.7 Cracking Test Results

Crack data was used for qualitative purposes. A full survey was not available prior to sealing, which limited quantitative uses. Of primary interest in terms of cracking was the overall condition of the pavement. The following sections provide all crack data from Hwy 17 and Hwy 35.

### 4.7.1 Hwy 17 Cracking Test Results

Tables 4.16 and 4.17 contain cracking test results for the northbound and southbound lanes of Hwy 17, respectively. The data collected prior to construction in the northbound lane showed the section had significant cracking prior to placement of the seal treatment. Block cracking was so prevalent that it was not recorded when the data was reduced since for practical purposes the entire northbound lane was block cracked. Longitudinal and transverse cracking had essentially all progressed into block cracking. Some of the cracking could be identified as fatigue cracking, which was quantified and included in Table 4.16.

Each Hwy 17 test section had approximately 2,450 m<sup>2</sup> (26,400 ft<sup>2</sup>) of surface area. Section 12 experienced the highest level of fatigue cracking, with approximately 17% of its total area cracked prior to sealing. Block cracking for the northbound lane was near 100% of its surface area. Varying levels of longitudinal and transverse cracking were observed from profile testing. With one exception, both block and fatigue cracking could be observed reflecting through the seal more at 15.89 months after construction than at 3.68 months after construction. Overall, Hwy 17 was found to be a heavily cracked pavement with varying type and amount of cracks from section to section.

**Table 4.16. Cracking Test Results for Northbound Lane of Hwy 17**

Section ---	Months <sup>1</sup> ---	Fatigue (m <sup>2</sup> )	Block (m <sup>2</sup> )	Long. (m)	Long. (Qty.)	Trans. (m)	Trans. (Qty.)
2	-0.66	---	---	---	---	---	---
	3.68	103	3	46	23	265	128
	15.89	336	15	36	12	199	126
4	-0.66	15	---	---	---	---	---
	3.68	7	6	148	69	841	362
	15.89	62	246	113	25	652	267
6	-0.66	107	---	---	---	---	---
	3.68	0	0	188	96	669	310
	15.89	11	500	111	23	487	196
8	-0.66	55	---	---	---	---	---
	3.68	0	0	250	110	799	322
	15.89	19	469	96	25	488	214
10	-0.66	15	---	---	---	---	---
	3.68	0	0	332	123	757	303
	15.89	12	298	147	43	538	227
12	-0.66	417	---	---	---	---	---
	3.68	1	0	359	160	1178	472
	15.89	71	275	310	74	512	259

1: Months Since Construction.

**Table 4.17. Cracking Test Results for Southbound Lane of Hwy 17**

Section ---	Months <sup>1</sup> ---	Fatigue (m <sup>2</sup> )	Block (m <sup>2</sup> )	Long. (m)	Long. (Qty.)	Trans. (m)	Trans. (Qty.)
1	-0.66	---	---	---	---	---	---
	3.68	83	15	84	30	320	191
	15.89	106	42	69	29	250	157
3	-0.66	---	---	---	---	---	---
	3.68	55	160	416	103	593	274
	15.89	46	319	155	39	490	219
5	-0.66	---	---	---	---	---	---
	3.68	46	243	316	108	524	253
	15.89	54	625	65	28	351	160
7	-0.66	---	---	---	---	---	---
	3.68	24	59	285	69	510	240
	15.89	94	194	98	22	421	195
9	-0.66	---	---	---	---	---	---
	3.68	8	158	118	23	362	185
	15.89	10	107	103	23	310	146
11	-0.66	---	---	---	---	---	---
	3.68	27	102	159	44	492	241
	15.89	109	427	70	20	320	157

1: Months Since Construction.



Micro cracking was investigated by way of visual assessment. Mean values for test phases 1, 2, and 3 were 0.84, 0.00, and 0.16. All values are low and of no major significance, but note no micro cracking was observed during phase 2 (August of 2008). It is likely that the bituminous portion of the seal material was heated to a semi-plastic state and closed the few microcracks observed during phase 1.

#### 4.7.2 Hwy 35 Cracking Test Results

Table 4.18 contains cracking test results for Hwy 35. The survey in 2007 (-0.63 months) showed section 2 was heavily cracked prior to sealing. There was so much block cracking that it was not measured; near 100% of the section was block cracked. The operator also noted difficulty identifying cracks in section 4 for the 2007 survey (30.79 months). In general, block and fatigue cracking increased between 35.16 and 47.37 months.

**Table 4.18. Cracking Test Results of Hwy 35**

Section	Months <sup>1</sup>	Fatigue (m <sup>2</sup> )	Block (m <sup>2</sup> )	Long. (m)	Long. (Qty.)	Trans. (m)	Trans. (Qty.)
1	-0.63	---	---	---	---	---	---
	3.75	5	55	59	18	544	236
	15.95	168	699	195	45	691	319
2	-0.63	484	---	---	---	---	---
	3.75	3	43	95	20	847	266
	15.95	579	931	81	18	363	220
3	30.79	---	---	---	---	---	---
	35.16	0	0	148	31	414	169
	47.37	0	203	244	46	542	207
4	30.79	29	98	---	---	122	51
	35.16	25	425	90	20	467	174
	47.37	7	534	264	50	347	130
5	-0.63	---	---	---	---	---	---
	3.75	0	0	6	1	73	26
	15.95	137	21	133	28	168	90
6	-0.63	500	13	151	38	132	115
	3.75	2	12	74	16	131	51
	15.95	205	0	122	23	141	73

1: Months Since Construction.

Micro cracking was investigated by way of visual assessment. Mean values for test phases 1, 2, and 3 were 0.75, 0.67, and 0.25. All values are low and of no major significance. Note that there was no major reduction in observed micro cracking during phase 2 (August of 2008) as occurred with Hwy 17. Hwy 35 did not experience significant bleeding/flushing problems (indicated free bituminous material) which is likely the reason all the cracks were not closed in phase 2.

## 4.8 Structural Integrity Analysis and Test Results

*FWD* data taken during three discrete test intervals was used for evaluation of structural integrity. To do so, a method was developed by assembling components of methods developed by other researchers. The method and discussion pertaining to development can be found in Section 4.8.1. The data collected and corresponding analysis is presented in Section 4.8.2.

### 4.8.1 *FWD* Backcalculation and Structural Integrity Assessment

Based on review of literature, the *FWD* data was analyzed with a method developed by combining key elements from procedures employed by Arkansas, North Carolina, and Texas DOT's. The resulting procedure is tailored to Mississippi materials, and was specifically selected based on properties of *Hwy 17*. Note that some empirical data is contained in the procedures so English and SI units are used; one should carefully note the units of each step. The remainder of Section 4.8.1 describes the methods used to account for environmental conditions and to calculate structural integrity based on *FWD* measurements.

#### 4.8.1.1 Moisture Content During *FWD* Testing

Table 4.19 provides moisture content results during *FWD* testing. This data was not used directly in calculations. Section 2.6 provides discussion of moisture conditions of unbound materials pertaining to *FWD* testing. The moisture content during phase 1 was noticeably higher than that from phase 2 or 3 though with the method used the data from each phase becomes less reliable. Note the values presented should be considered approximate moisture contents due to their spatial orientation in the test section and the manner in which they were obtained. In general, the moisture in the summer of 2008 appeared lower than in the winter of 2008 as expected.

**Table 4.19. Moisture Content Results of *Hwy 17***

Phase	Date	Coordinate	Average Moisture Content (%)
1*	1/28/08	5.251N	15.8
		6.251N	21.3
		6.751S	15.6
		7.751S	17.4
		<b>Average</b>	<b>17.5</b>
2	8/14/08	5.251N	13.4
		6.251N	10.9
		6.751S	12.3
		7.751S	12.1
		<b>Average</b>	<b>12.2</b>
3	1/7/09	5.251N	12.3
		6.251N	11.1
		6.751S	11.1
		7.751S	12.5
		<b>Average</b>	<b>11.8</b>

\* *FWD* testing occurred on 2/7/08 due to equipment difficulties; 1 rainfall between.

#### 4.8.1.2 Temperature Prediction for use With *FWD* Measurements

Two temperature correction methods were selected for the research: 1) Kim et al. (1995); and 2) *AASHTO* procedure. The approach of Kim et al. (1995) was selected since a similar binder grade and the same pavement thickness were included in both studies (See Section 2.6 for additional information). The *AASHTO* procedure was selected since it is familiar to many pavement engineers and at present is the nationally accepted method. Applicable data from the *AASHTO* (1986) procedure is re-produced in Figure 4.9 for depths near the top, near the middle, and at the bottom of *Hwy 17*.

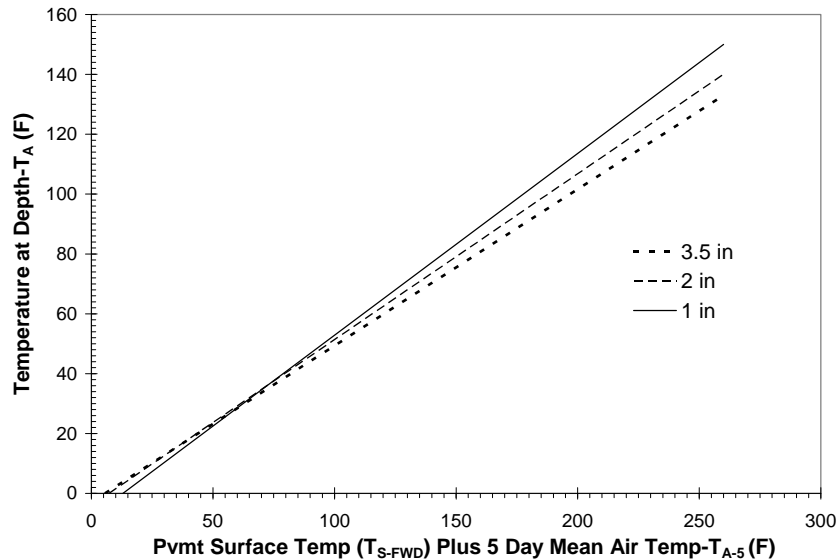


**Figure 4.9. *AASHTO* (1986) Temperature Predictions for Depths of Interest**

The work of Shao et al. (1997) is perhaps more theoretically appropriate than Kim et al. (1995), but the empirical nature of Kim et al. (1995) was ultimately selected in favor of Shao et al. (1997) for two reasons. First, all key parameters of *Hwy 17* were accounted for in the testing program of Kim et al. (1995), drastically increasing the appeal of the empirical study. Second, Shao et al. (1997) recommended evaluation of the model for use in other states. The model was stated to provide more general applicability than empirical models (e.g. Kim et al. 1995) when calibrated with local temperature measurements. This study, though, was not to calibrate temperature models, rather to evaluate performance of chip and scrub seals.

*ROADHOG's* temperature prediction procedure was not believed by the author to be optimal for the current needs. The procedure contained in the program is detailed in Elliott et al. (1990). In general, the elastic modulus used was for typical Arkansas materials near 21 C (70 F), and adjustment curves were based on linear elastic analysis. The typical Arkansas mixture did not merit the modification, rather the temperature adjustment procedure.

Temperature prediction according to Kim et al. (1995) is performed as follows. A depth of 37.5 mm (1.5 in) is selected as the reference location since it was found to be optimal in the study. Selection of this location as a reference made gradient overlap more precise within the pavement, and it minimized the effect of radiation and sunlight on the

surface temperature. Regression analysis was performed below 37.5 mm (1.5 in), which made selection of an average reference temperature at this location at a particular hour of the day necessary. Table 4.20 summarizes the regression coefficients determined, as well as reference temperatures at 37.5 mm (1.5 in) into the pavement. A reasonable surface temperature corresponding to the 37.5 mm (1.5 in) reference temperature was also provided in Table 4.20. A shift factor (ratio of measured to reference surface temperature) is used to adjust to field conditions.

**Table 4.20. Temperature Adjustment Parameters After Kim et al. (1995)**

<b>Time of Day</b>	<b>A</b>	<b>B</b>	<b>Reference 1.5 in (37.5 mm) Temp (<math>T_{R-1.5}</math>)-F (C)</b>	<b>Reference Surface Temp (<math>T_{RS}</math>)-F (C)</b>
8:00	53.79	0.0530	55 (12.8)	55 (12.8)
9:00	58.84	0.0213	60 (15.6)	60 (15.6)
10:00	64.79	-0.0344	70 (21.1)	70 (21.1)
11:00	76.83	-0.0914	75 (23.9)	79 (26.1)
12:00	83.75	-0.1433	80 (26.7)	86 (30.0)
13:00	88.61	-0.1246	85 (29.4)	95 (35.0)
14:00	83.42	-0.1173	90 (32.2)	85 (29.4)
15:00	89.27	-0.1151	85 (29.4)	85 (29.4)
16:00	83.65	-0.0926	80 (26.7)	80 (26.7)
17:00	78.20	-0.0768	75 (23.9)	76 (24.4)

Eq. 4.1 contains all input parameters needed to calculate the pavement mid-depth temperature ( $T$ ) according to Kim et al. (1995).

$$T = \left[ \frac{T_{s-FWD}}{T_{RS}} \right] A \left( \frac{t}{2} \right)^B \quad (4.1)$$

Where,

$T$  = asphalt layer mid depth temperature (F)

$T_{s-FWD}$  = surface temperature measured at time of *FWD* testing (F)

$T_{RS}$  = reference surface temperature shown in Table 4.22

$A$  = regression coefficient shown in Table 4.22

$t$  = pavement thickness (in)

$B$  = regression coefficient shown in Table 4.22

#### 4.8.1.3 *FWD* Deflection Adjustments to Reference Temperature

Once the temperature of the asphalt layer has been predicted according to Section 4.8.1.2, selected measured deflections must be adjusted to account for the effects of temperature. The reference temperature to which selected deflections were adjusted was 20 C (68 F). To select which deflections to adjust for temperature, information from literature review (See Section 2.6) was used as follows. The value of  $D_{eff}$  (See Section 2.6) for *Hwy 17* was well below  $D_2$  at 305 mm (12 in) and as a result only the center deflection ( $D_1$ ) was

corrected for temperature. All other deflections were sufficiently far from the load for the relatively thin pavement to not warrant temperature correction.

Two methods were used for adjustment of deflections for temperature: 1) Kim et al. (1995); and 2) AASHTO (1993) procedure. AASHTO (1993) adjusts non destructive deflection under the center of loading only. The inputs are total asphalt thickness and asphalt mix (i.e. effective internal) temperature at the time of testing. The correction of deflection under the center of loading ranges from 0.40 to 1.35 and is referred to as  $C_A$  in this report.

The AASHTO (1993) correction curves linearly (or very near linearly) relate correction factor to temperature. Kim et al. (1995) found the expression shown in Eq. (4.2) to be more appropriate for wheel path testing. For the 3.5 in (89 mm) thick (on average) pavement of *Hwy 17*, the two approaches are plotted in Figure 4.10 for the same predicted effective asphalt temperature ( $T$  or  $T_A$ ). Refer to Section 4.8.1.2 for effective temperature calculations.

$$C = 10^{3.67 (10^{-4}) (t^{1.4635}) (68-T)} \quad (4.2)$$

Where,

$t$  = asphalt layer thickness (in)

$T$  = asphalt layer mid-depth temperature (F)

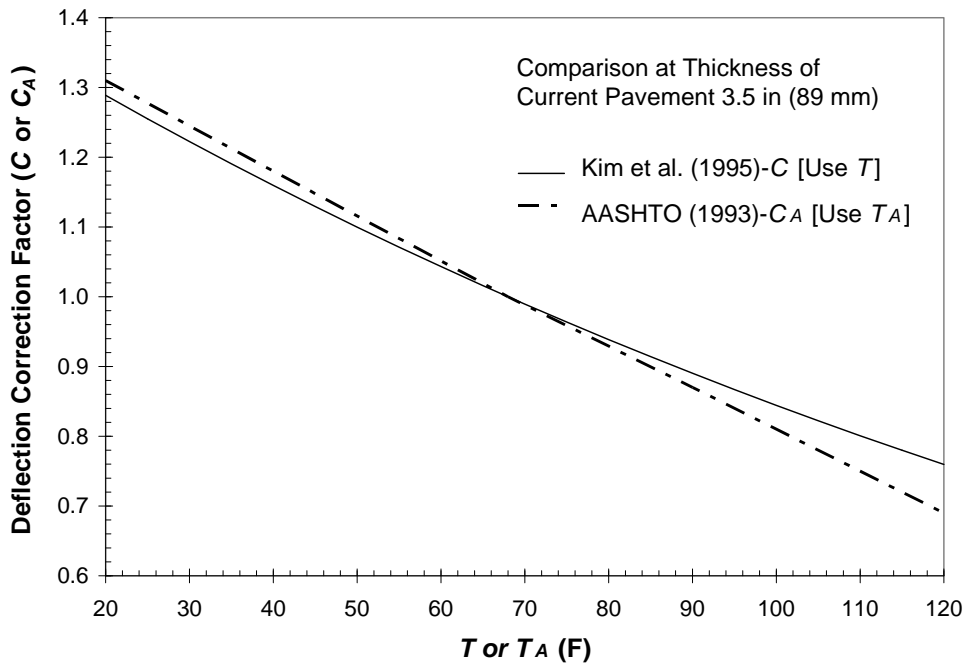


**Figure 4.10. Comparison of Deflection Correction Factors**

As the pavement thickness increases, the approach of Kim et al. (1995) and that of AASHTO (1993) vary much more drastically. At higher temperatures the two curves vary much more than at lower temperatures. Near the reference temperature the two approaches give practically the same result for the same effective asphalt temperature.

The *FWD* deflection adjustment procedure in the wheel path is seen in Eq. 4.3. The correction factor depends on which method is used ( $C$  or  $C_A$ ); AASHTO (1993) or Kim et al. (1995). It also depends on which method is used for temperature adjustment ( $T_A$  or  $T$ ).

$$D_{1-68-i} = C_i (D_{T_i})(40/P) \quad (4.3)$$

Where,

$D_{1-68-i}$  = adjusted deflection to reference temperature of 20 C (68 F) with method ( $i$ )

$C_i$  = correction factor represented in Figure 4.13 with method ( $i$ );  $C$  or  $C_A$

$D_{T_i}$  = deflection at temperature  $T_i$  (F)

$P$  = applied *FWD* load (kN)

The two methods employed are labeled: 1) Kim et al. (1995)- $D_{1-68-TC}$  and 2) AASHTO- $D_{1-68-TA}C_A$ . Both methods are applied to the center deflection under a 40 kN (9,000 lb) load. Park et al. (2002) showed load level did not affect temperature dependence, so the approaches were applied to all load levels. All deflections were linearly adjusted to 40 kN (9,000 lb) using the ratio of 40 kN to the applied *FWD* load.

#### 4.8.1.4 Structural Integrity Calculations

All structural integrity calculations were performed using *ROADHOG* with data adjusted as previously discussed. To determine the effective structural capacity of the existing in-situ pavement ( $SN_{eff}$ ), the corrected deflection at the center of loading and at a distance equal to the pavement thickness are used by *ROADHOG*.  $M_r$  is determined from the deflection 91.4 cm (36 in) from the center of loading.  $SN_{eff}$  and  $M_r$  are independently calculated.  $M_r$  is calculated using Eq. 4.4, and  $SN_{eff}$  is calculated using Eq. 4.5. Note English units are used since the equations are empirically derived, and the values from *ROADHOG* will not exactly equal Eq. 4.4 and 4.5 due to rounding.

$$M_r = 25.0346 - 5.2454 D_4 + 0.2864 D_4^2 \quad (4.4)$$

$$SN_{eff} = 0.3206((D_1 - D_T)/10)^{-0.42} (T_p)^{0.8175} \quad (4.5)$$

Where,

$M_r$  = resilient modulus (ksi)

$D_4$  = deflection 0.91 m (36 in) from the center of loading (mils)

$SN_{eff}$  = effective structural capacity of existing in-situ pavement

$D_1$  = corrected deflection under the center of loading (mils)

$D_T$  = deflection at a distance from load center equal to the pavement thickness (mils)

$T_p$  = pavement thickness considering asphalt, base, and subbase (in)

To perform the overlay design calculations, a standard set of parameters was used. The *MDOT Roadway Design* division currently uses a modified version of the 1972 edition of the AASHTO design guide, which does not include reliability components. These

parameters are used within *ROADHOG*, so AASHTO (1993) was used for typical values. The standard deviation ( $S_o$ ) was taken as 0.45, reliability ( $R$ ) at 95%, and the allowable change in serviceability as 4.2 to 2.0, or 2.2. The initial serviceability of 4.2 was the original recommendation from the AASHTO Road Test, and the terminal serviceability of 2.0 is recommended in AASHTO (1993) for low volume roadways.

Traffic was obtained from *MDOT* for *Hwy 17*. This allowed the overlay design estimates to be realistic for the roadway. The estimated traffic count over a five year period beginning in 2007 and ending in 2012 was 132,000 ESALS for one lane. Projections near the end of this duration were an ADT of 990 with 14% trucks.

The overlay asphalt was assumed to have a modulus of 3.1 GPa (450 ksi) at 20 C (68 F), which results in a layer coefficient ( $a_1$ ) of 0.44. *ROADHOG* calculates the capacity that would be required if the existing pavement had no structural capacity in the same way as stated in the AASHTO Guide, and it is referred to as  $SN_{new}$ . Eq. 4.6 is used for calculation of the overlay thickness.

$$H_{OL} = \left[ \frac{SN_{New} - SN_{eff}}{a_1} \right] \quad (4.6)$$

Where,

$H_{OL}$  = required overlay thickness

$a_1$  = layer coefficient of asphalt used for overlay

## 4.8.2 FWD Test Results and Data Analysis

The *FWD* data collected in this study and used for analysis was separated into four categories: 1) corrected deflection under the center of loading using the two temperature correction methods ( $D_{1-68-TC}$  and  $D_{1-68-TACA}$ ); 2) resilient modulus ( $M_r$ ); 3) effective in-situ structural capacity using deflections corrected by the two aforementioned methods ( $SN_{eff-TC}$  and  $SN_{eff-TACA}$ ); and 4) new structural capacity ( $SN_{New}$ ) requirements as affected by the seal treatments. Each of these behaviors is discussed in the remainder of this section.

### 4.8.2.1 Analysis of FWD Corrected Deflections

*FWD* data collected under the center of loading was corrected for temperature using two methods and is interpreted in this section. This section focused on the relative deflection prediction of the two temperature correction methods and provided the centerline deflection data for reference that was used for additional calculations. Centerline deflection is critical to prediction of  $SN_{eff}$ . Tables 4.21 and 4.22 contain all adjusted deflections under the center of loading obtained using a pavement thickness of 89 mm (3.5 in). The values from a given test phase were averaged after being corrected for applied stress and temperature.

Figure 4.11 compares the corrected deflections obtained by the Kim et al. (1995) and the AASHTO procedure ( $D_{1-68-TC}$  and  $D_{1-68-TACA}$ , respectively). Observation of Tables 4.21 and 4.22 revealed Kim et. al. (1995) resulted in higher corrected deflections. In general, the deflection was 5 to 20  $\mu$ m higher with Kim et al. (1995) than with the AASHTO procedure as seen in Figure 4.11. The corrected deflections varied by slight amounts depending on the

thickness used (average value of 89 m (3.5 in) or thickness after coring test locations) for temperature calculations. These variations were on the order of 1 to 2  $\mu\text{m}$  and were considered irrelevant; values shown in Figure 4.11 are for 89 mm (3.5 in) thickness.

**Table 4.21. Adjusted Deflections Under the Center of Loading: Northbound Lane**

Section	Phase Coordinate	$D_{I-68-TC}$			$D_{I-68-TACA}$		
		1 $\mu\text{m}$	2 $\mu\text{m}$	3 $\mu\text{m}$	1 $\mu\text{m}$	2 $\mu\text{m}$	3 $\mu\text{m}$
2	7.880	508	427	549	494	408	527
None	7.846	344	368	572	334	348	550
	7.751	633	486	718	619	470	697
	7.656	622	461	701	609	449	680
	7.561	874	776	---	859	750	---
4	7.441	394	245	371	380	234	355
Chip	7.346	582	400	467	567	383	450
	7.251	296	210	320	289	201	310
	7.156	230	154	227	225	148	219
	7.061	467	425	502	457	406	493
6	6.941	294	213	287	288	206	283
Chip	6.846	361	167	332	355	162	326
	6.751	441	338	467	428	321	452
	6.656	288	200	299	279	190	291
	6.561	426	285	531	416	269	515
8	6.441	330	312	365	321	295	355
Chip	6.346	256	137	347	250	129	338
	6.251	455	328	464	446	313	455
	6.156	352	226	331	344	214	322
	6.061	687	456	599	668	437	585
10	5.941	418	350	442	405	343	428
Chip	5.846	343	229	359	330	224	347
	5.751	373	284	380	359	277	366
	5.656	714	328	640	691	321	615
	5.561	417	326	408	402	317	393
12	5.441	548	407	535	536	398	522
Scrub	5.346	422	411	474	412	402	465
	5.251	629	460	636	614	452	615
	5.156	355	228	352	342	223	337
	5.061	308	246	381	297	241	365

Note: 25.4  $\mu\text{m}$  is equivalent to 1 mil.



**Table 4.22. Adjusted Deflections Under the Center of Loading: Southbound Lane**

Section	Phase Coordinate	<i>D</i> <sub>I-68-TC</sub>			<i>D</i> <sub>I-68-TACA</sub>		
		1	2	3	1	2	3
		μm	μm	μm	μm	μm	μm
1	7.880	468	437	542	453	413	526
None	7.846	404	374	485	392	352	467
	7.751	471	523	734	462	493	702
	7.656	428	390	533	417	368	509
	7.561	324	280	423	314	263	411
	3	7.441	443	260	425	430	245
Chip	7.346	341	213	307	329	200	294
	7.251	319	276	266	308	260	255
	7.156	282	154	245	272	146	236
	7.061	358	252	304	348	238	294
	5	6.941	347	232	294	336	219
Chip	6.846	257	146	306	249	138	295
	6.751	318	216	300	306	204	287
	6.656	255	171	271	248	167	266
	6.561	263	156	238	255	151	232
	7	6.441	311	191	346	301	186
Scrub	6.346	294	161	233	285	156	231
	6.251	423	234	402	412	228	395
	6.156	378	196	379	368	191	374
	6.061	580	352	566	564	345	553
	9	5.941	453	226	436	440	220
Scrub	5.846	242	160	192	234	156	190
	5.751	380	195	290	369	190	286
	5.656	524	345	456	514	349	451
	5.561	363	213	320	353	212	314
	11	5.441	343	275	343	389	279
Scrub	5.346	722	507	620	715	513	615
	5.251	376	337	461	368	343	455
	5.156	410	211	356	400	214	357
	5.061	205	112	161	202	113	162

Note: 25.4 μm is equivalent to 1 mil.

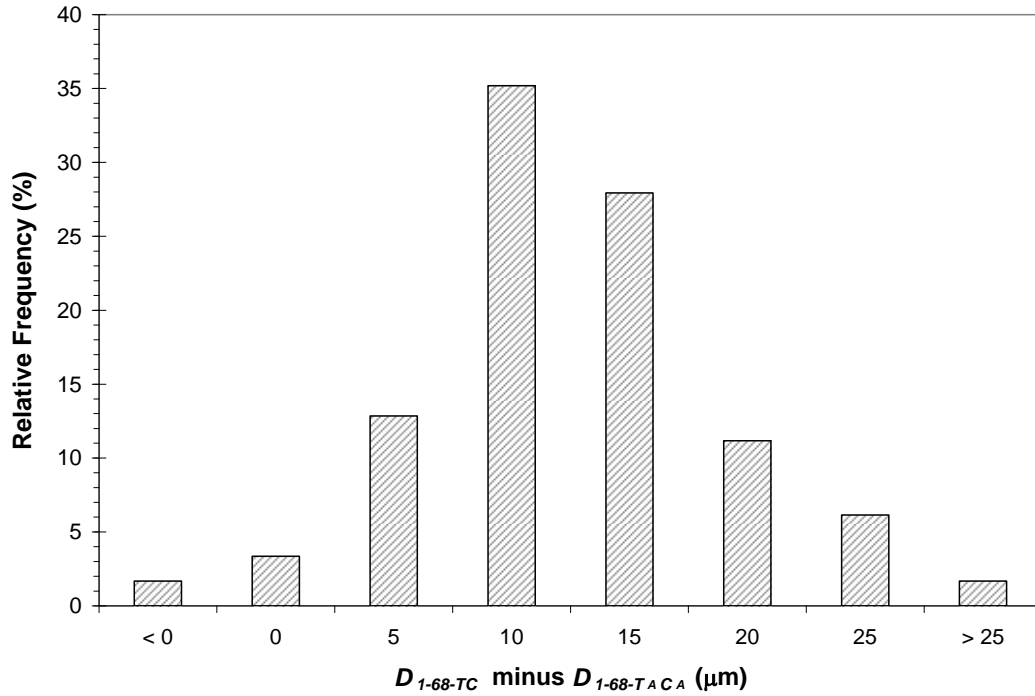


**Figure 4.11. Comparison of  $D_{1-68-TC}$  and  $D_{1-68-TACA}$**

#### 4.8.2.2 Analysis of $SN_{eff}$ Data

For a two layer pavement such as *Hwy 17*, the structural capacity is represented in general terms when following the AASHTO (1993) procedure and setting all drainage parameters to unity by Eq. 4.7.

$$SN = a_1(D_1) + a_2(D_2)m_2 \quad (4.7)$$

Where,

$SN$  = structural number of pavement

$a_1$  = layer coefficient of asphalt layer

$a_2$  = layer coefficient of base layer

$D_1$  = thickness of asphalt layer (in)

$D_2$  = thickness of base layer (in)

$m_2$  = drainage coefficient (taken as 1.0 for this analysis)

The  $SN$  for *Hwy 17* is on the order of 2.8 according to Eq. 4.7 using average properties obtained from coring and layer coefficients of 0.44 and 0.10 for the asphalt and base layers, respectively.  $SN_{eff}$  is intended to measure the effective capacity of the pavement in situ and represents only these pavement layers (asphalt and base in the case of *Hwy 17*).

Tables 4.23 and 4.24 contain all  $SN_{eff}$  values obtained using an asphalt thickness of 89 mm (3.5 in) and a pavement thickness of 406 mm (16 in). An immediate observation from the data in Tables 4.25 and 4.26 is that the effective structural capacity increased between

phase 1 and phase 2 for all but a few test coordinates in both the northbound and southbound lanes. Without a contributing mechanism (e.g. lower moisture), structural capacity of pavements does not increase with time; many sections experienced a noticeable increase in structural capacity according to the phase 2 data which was a point of attention.

**Table 4.23. Effective Structural Capacity Results: Northbound Lane**

Section	Phase Coordinate	$SN_{eff-TC}$			$SN_{eff-TACA}$		
		1	2	3	1	2	3
2	7.880	3.26	3.69	3.08	3.34	3.88	3.20
None	7.846	4.89	3.60	2.91	5.22	3.78	3.01
	7.751	2.68	3.17	2.51	2.73	3.26	2.56
	7.656	2.89	3.38	2.59	2.94	3.47	2.65
	7.561	2.27	2.39	---	2.29	2.45	---
4	7.441	3.67	4.91	3.69	3.80	5.18	3.84
Chip	7.346	2.94	3.85	3.37	3.01	4.04	3.50
	7.251	4.32	5.31	3.94	4.43	5.66	4.07
	7.156	5.50	6.22	4.64	5.68	6.52	4.83
	7.061	3.63	3.65	3.22	3.72	3.85	3.26
6	6.941	5.24	5.96	4.50	5.43	6.31	4.59
Chip	6.846	3.61	5.28	3.92	3.66	5.45	3.98
	6.751	3.77	4.85	3.28	3.92	5.33	3.37
	6.656	4.16	5.06	4.03	4.30	5.39	4.12
	6.561	3.63	4.25	3.13	3.72	4.50	3.22
8	6.441	4.74	4.89	4.01	4.98	5.36	4.14
Chip	6.346	4.80	6.04	4.00	4.92	6.41	4.11
	6.251	3.32	3.99	3.15	3.38	4.19	3.19
	6.156	4.33	5.13	4.31	4.45	5.57	4.48
	6.061	3.12	4.03	3.23	3.22	4.30	3.31
10	5.941	3.74	4.16	3.49	3.88	4.28	3.60
Chip	5.846	4.05	4.95	3.69	4.22	5.06	3.82
	5.751	3.72	4.12	3.52	3.86	4.21	3.64
	5.656	3.02	4.50	2.95	3.13	4.64	3.05
	5.561	3.49	3.97	3.37	3.61	4.07	3.49
12	5.441	3.10	3.58	3.03	3.16	3.65	3.09
Scrub	5.346	3.49	3.39	3.10	3.57	3.45	3.15
	5.251	2.84	3.40	2.68	2.89	3.46	2.75
	5.156	4.09	5.26	3.83	4.28	5.42	4.00
	5.061	4.10	4.45	3.25	4.26	4.54	3.36

Investigation of this behavior after data collection focused on: 1) measured temperatures during testing; 2) measured deflections; 3) method of temperature correction; 4) expected structural capacity based on layer thicknesses; and 5) moisture. Temperatures measured during testing via a hand held thermometer (Table 4.1) agreed with the values measured by the *FWD*. The *FWD* was calibrated after testing according to *MDOT* personnel. Both temperature correction methods independently calculated the same trends with values

on the order of each other. Phase 2 occurred during the summer while phases 1 and 3 were during winter. Moisture differences would explain many of the observed behaviors (Table 4.19), while temperature differences were not believed to be the culprit with two independent temperature correction methods providing similar answers. As calculated previously, the  $SN$  value of the pavement based on typical layer coefficients and average thicknesses would be less than backcalculated values. Based on all factors that could be investigated by the author, phase 2 data should be considered under different conditions than phase 1 or 3. As such, use of phase 2 data was limited to qualitative statements between the chip seal, scrub seal, and no treatment sections during phase 2; the data was not used for discussion between phases. The data from phases 1 and 3 was collected approximately 11 months apart and was used for the majority of the analysis and comparison of test sections.

**Table 4.24. Effective Structural Capacity Results: Southbound Lane**

Section	Phase Coordinate	$SN_{eff-TC}$			$SN_{eff-TACA}$		
		1	2	3	1	2	3
1	7.880	3.35	3.47	3.00	3.45	3.68	3.08
None	7.846	3.41	3.55	3.05	3.51	3.75	3.15
	7.751	3.97	2.97	2.45	4.09	3.11	2.53
	7.656	3.50	3.55	3.02	3.58	3.75	3.14
	7.561	3.91	4.03	3.45	4.04	4.25	3.54
	3	7.441	3.26	4.26	3.00	3.35	4.51
Chip	7.346	3.97	4.89	4.15	4.10	5.20	4.34
	7.251	4.16	4.20	4.35	4.33	4.45	4.53
	7.156	4.75	7.21	4.81	5.00	8.15	5.04
	7.061	4.34	5.18	4.42	4.48	5.67	4.59
	5	6.941	4.05	4.64	4.29	4.19	4.93
Chip	6.846	4.44	5.67	3.99	4.58	6.08	4.12
	6.751	4.60	6.46	4.41	4.86	7.37	4.64
	6.656	4.38	5.48	3.95	4.51	5.66	4.01
	6.561	4.86	7.45	4.87	5.04	8.03	5.02
	7	6.441	4.40	5.23	3.67	4.58	5.42
Scrub	6.346	4.50	6.12	4.99	4.70	6.41	5.01
	6.251	3.62	5.54	3.54	3.72	5.73	3.59
	6.156	3.93	5.06	3.71	4.04	5.21	3.74
	6.061	3.38	4.64	3.10	3.50	4.79	3.16
	9	5.941	3.48	4.71	3.51	3.59	4.85
Scrub	5.846	5.33	8.19	5.33	5.62	8.69	5.42
	5.751	3.73	6.08	4.26	3.85	6.36	4.32
	5.656	3.70	5.11	3.67	3.80	4.99	3.70
	5.561	4.03	5.70	3.97	4.16	5.70	4.04
	11	5.441	3.91	4.72	3.88	3.97	4.64
Scrub	5.346	3.02	3.98	3.13	3.05	3.91	3.16
	5.251	3.87	4.01	3.24	3.97	3.94	3.28
	5.156	3.97	6.57	4.11	4.08	6.41	4.09
	5.061	5.76	11.24	6.21	5.87	10.88	6.12

Table 4.25 provides average  $SN_{eff}$  values for both  $TC$  and  $T_A C_A$  conditions for all phases calculated with an 89 mm (3.5) in thick asphalt layer. As seen, the sections with no seal treatment appeared to deteriorate from phase 1 to phase 3 (not considering phase 2 for previously mentioned reasons) more than the sections that had been sealed. This was especially true in the less damaged southbound lane. This behavior is investigated further in the following paragraph.

**Table 4.25. Average  $SN_{eff}$  Values of Hwy 17**

Lane	Type	Seal	Phase 1	2	3
			$SN_{eff}$	$SN_{eff}$	$SN_{eff}$
North	$TC$	None	3.20	3.25	2.77
		Chip	3.94	4.76	3.67
		Scrub	3.52	4.02	3.18
	$T_A C_A$	None	3.30	3.37	2.86
		Chip	4.07	5.02	3.78
		Scrub	3.63	4.10	3.27
South	$TC$	None	3.63	3.51	2.99
		Chip	4.28	5.54	4.22
		Scrub	4.04	5.79	4.02
	$T_A C_A$	None	3.73	3.71	3.09
		Chip	4.44	6.01	4.38
		Scrub	4.17	5.86	4.06

Table 4.26 summarizes statistical comparison testing where unequal variances are considered along with unequal sample sizes. The data analyzed was the algebraic difference in  $SN_{eff}$  values between phase 1 and phase 3 for each individual coordinate; note that phase 1 values were typically higher than phase 3 values. In the northbound lane, the variability in the data prevented statistically significant differences from being detected between the coordinates with no treatment and the sealed sections (chip or scrub) even though the mean

**Table 4.26. Statistical Analysis of  $SN_{eff}$  Differences Between Phase 1 and Phase 3**

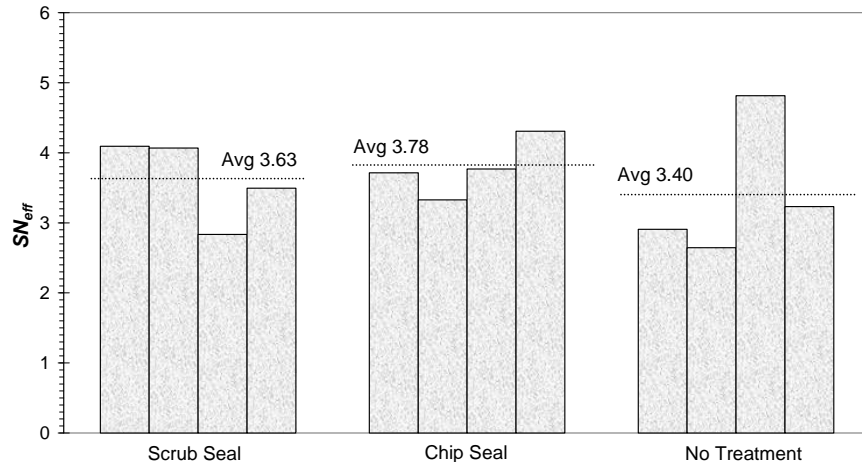
Lane	Type	$\mu_1 (\bar{x}, s^2)$	$\mu_2 (\bar{x}, s^2)$	$H_a$	$t$	$t_a (t_{\alpha/2})$	Result
North	$TC$	None (0.66, 0.78)	Chip (0.27, 0.13)	$\mu_1 - \mu_2 > 0$	0.87	2.35	Accept
	$TC$	None (0.66, 0.78)	Scrub (0.35, 0.09)	$\mu_1 - \mu_2 > 0$	0.67	2.13	Accept
	$T_A C_A$	None (0.70, 1.01)	Chip (0.29, 0.15)	$\mu_1 - \mu_2 > 0$	0.82	2.35	Accept
	$T_A C_A$	None (0.70, 1.01)	Scrub (0.36, 0.11)	$\mu_1 - \mu_2 > 0$	0.65	2.13	Accept
	$TC$	Chip (0.27, 0.13)	Scrub (0.35, 0.09)	$\mu_1 - \mu_2 \neq 0$	-0.49	(2.36)	Accept
	$T_A C_A$	Chip (0.29, 0.15)	Scrub (0.36, 0.11)	$\mu_1 - \mu_2 \neq 0$	-0.45	(2.36)	Accept
South	$TC$	None (0.63, 0.25)	Chip (0.06, 0.07)	$\mu_1 - \mu_2 > 0$	2.43	2.02	Reject
	$TC$	None (0.63, 0.25)	Scrub (0.02, 0.13)	$\mu_1 - \mu_2 > 0$	2.54	2.02	Reject
	$T_A C_A$	None (0.65, 0.06)	Chip (0.06, 0.08)	$\mu_1 - \mu_2 > 0$	2.37	2.02	Reject
	$T_A C_A$	None (0.65, 0.06)	Scrub (0.11, 0.12)	$\mu_1 - \mu_2 > 0$	2.18	2.02	Reject
	$TC$	Chip (0.06, 0.07)	Scrub (0.02, 0.13)	$\mu_1 - \mu_2 \neq 0$	0.29	(2.07)	Accept
	$T_A C_A$	Chip (0.06, 0.08)	Scrub (0.02, 0.13)	$\mu_1 - \mu_2 \neq 0$	-0.38	(2.07)	Accept

Note:  $H_0$  was that  $\mu_1 - \mu_2 = 0$ .

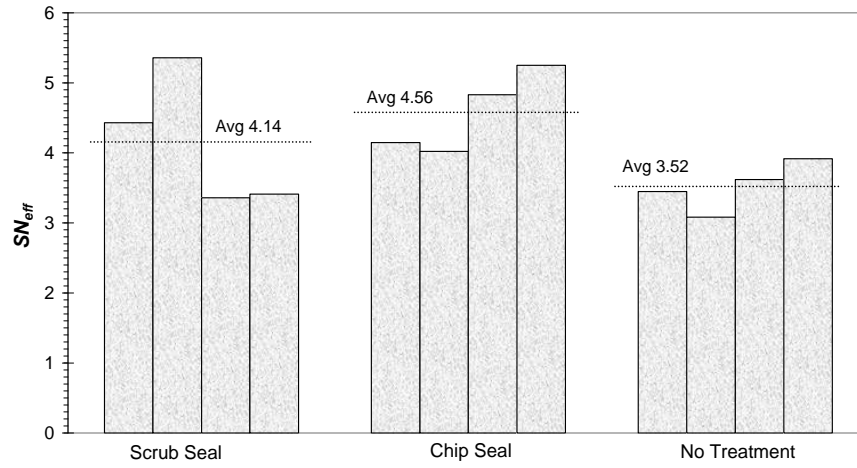
decrease in  $SN_{eff}$  was much higher for the coordinates with no treatment than for either of the sealed sections. In the southbound lane, both seals out performed no seal treatment to a level where statistically significant differences were detected. There were no apparent differences between the chip and scrub seal sections. Statistical analysis provided evidence that the southbound lane seal treatments were more effective at maintaining structural integrity than northbound lane seal treatments. The evidence should not be considered conclusive, but it does show the effects of a seal being damaged as was the northbound lane seal.

Figures 4.12 and 4.13 show  $SN_{eff}$  values for the twelve test coordinates that were cored at the conclusion of *FWD* testing. Calculations for these twelve coordinates pertaining to Figures 4.12 and 4.13 used measured asphalt thicknesses. Total pavement thicknesses were adjusted based on the asphalt thickness. The average asphalt thickness of 89 mm (3.5 in) and total pavement thickness of 406 mm (16 in) were used as a reference. For example, a cored asphalt thickness of 86 mm (3.4 in) used a pavement thickness of 404 mm (15.9 in) and a cored asphalt thickness of 94 mm (3.7 in) used a pavement thickness of 412 mm (16.2 in). The data in Figures 4.12 and 4.13 further support the superior performance of the sealed sections.

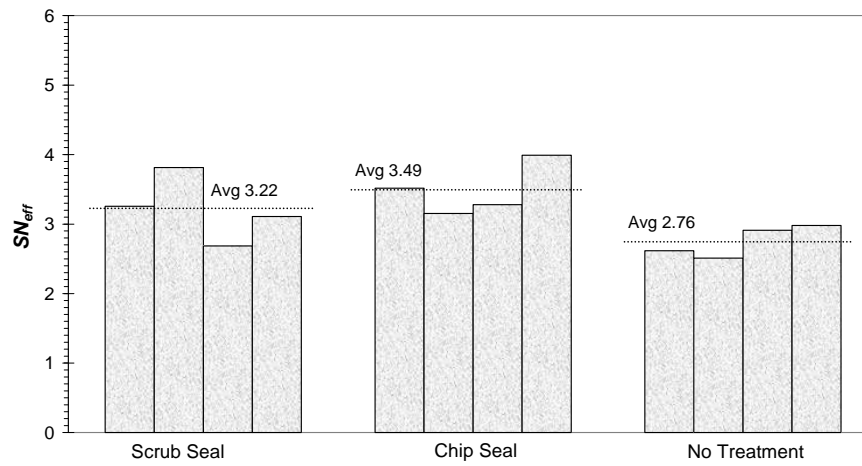
Figure 4.14 compares the  $SN_{eff}$  values for the two different approaches (*TC* and *T<sub>A</sub>C<sub>A</sub>*). The *TC* approach generally calculated between 0.1 to 0.3 less units of structural capacity relative to the AASHTO approach (*T<sub>A</sub>C<sub>A</sub>*). Based on the estimated structural capacity of a pavement during design with the average layer thicknesses of the test section, lower  $SN_{eff}$  values appear to be more reasonable. The *TC* approach would be slightly favored by the author for the conditions encountered.



(a) Phase 1 (Feb 08)

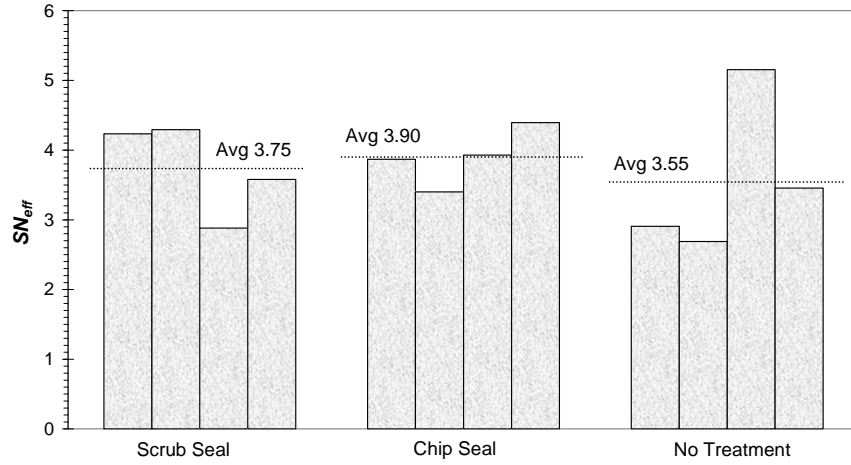


(b) Phase 2 (Aug 08)

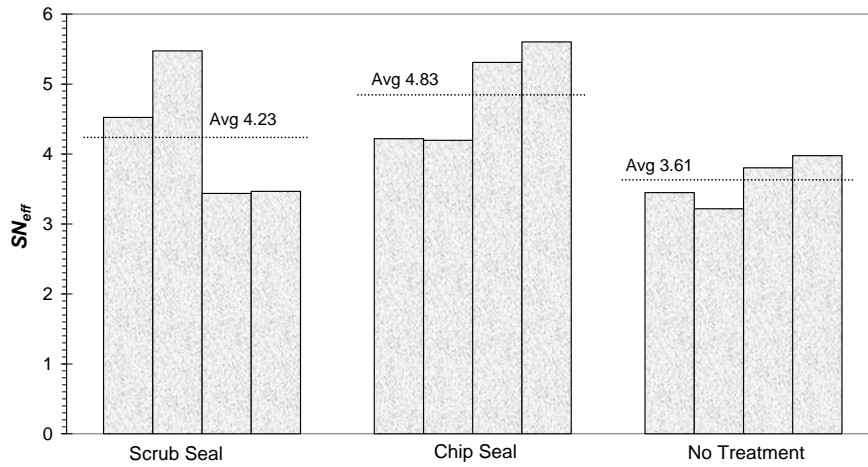


(c) Phase 3 (Jan 09)

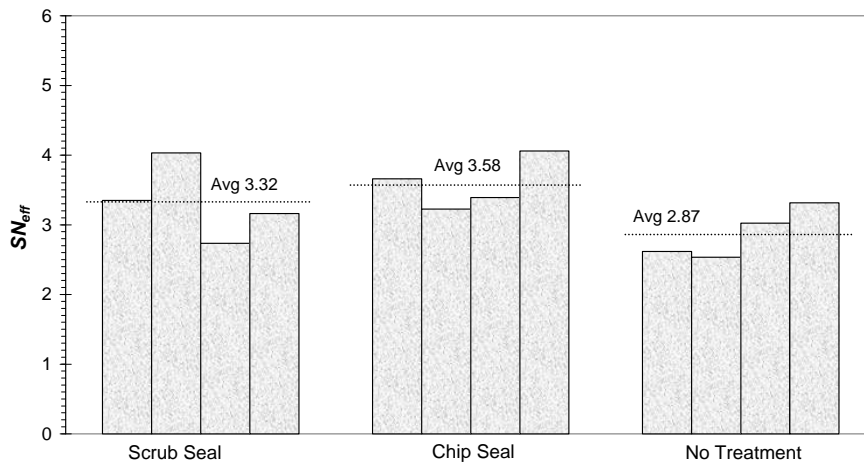
**Figure 4.12.  $SN_{eff-TC}$  Results for Cored Test Sections**



(a) Phase 1 (Feb 08)



(b) Phase 2 (Aug 08)



(c) Phase 3 (Jan 09)

**Figure 4.13.  $SN_{eff-TACA}$  Results for Cored Test Sections**



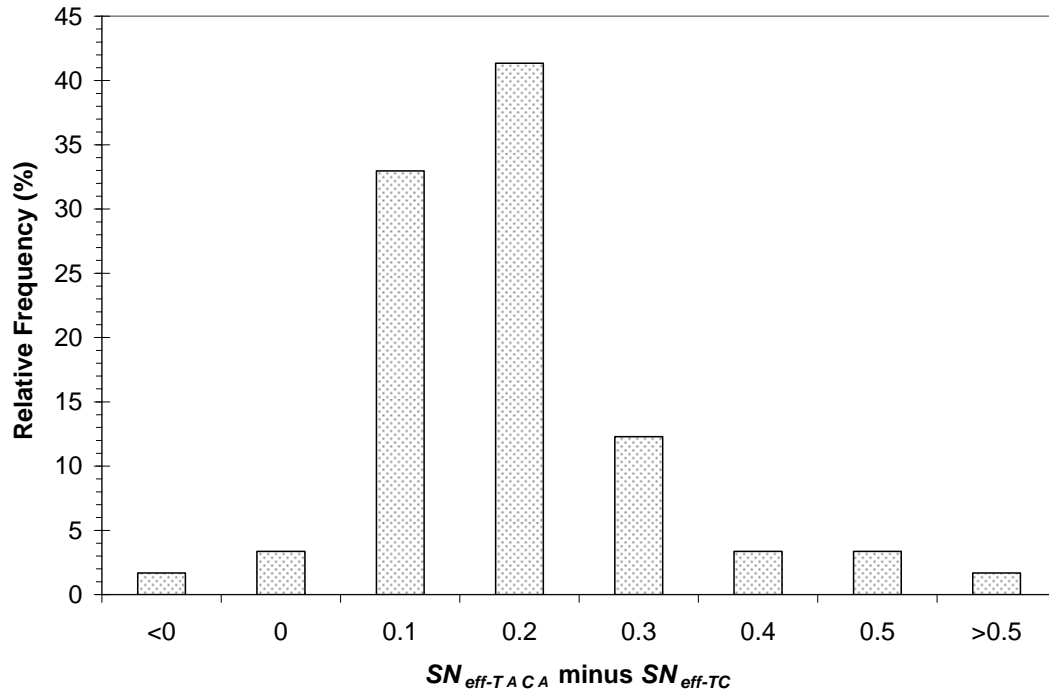


**Figure 4.14. Comparison of Effective Structural Capacity Calculation Methods**

#### **4.8.2.3 Analysis of Backcalculated $M_r$ Values**

Tables 4.27 and 4.28 provide average back calculated  $M_r$  values. Note the  $M_r$  values calculated are independent of asphalt thickness so providing the data using cored thicknesses was redundant.  $M_r$  values were used primarily to calculate the new structural capacity discussed in the following section.

**Table 4.27. Resilient Modulus Results: Northbound Lane**

Section	Phase Coordinate	$M_r$			$M_r$		
		1 psi	2 psi	3 psi	1 MPa	2 MPa	3 MPa
2	7.880	6582	8743	6539	45.38	60.27	45.08
None	7.846	7500	11528	7502	51.71	79.47	51.72
	7.751	9784	12484	10297	67.45	86.06	70.99
	7.656	5802	9039	7142	40.00	62.31	49.24
	7.561	14584	15968	---	100.54	110.08	---
4	7.441	8200	11884	9762	56.53	81.93	67.30
Chip	7.346	4958	9043	8247	34.18	62.34	56.85
	7.251	13711	14097	12842	94.52	97.18	88.53
	7.156	10929	15689	13713	75.34	108.16	94.54
	7.061	7032	8941	7238	48.48	61.64	49.90
6	6.941	6455	10737	8345	44.50	74.02	57.53
Chip	6.846	11701	16947	12354	80.67	116.83	85.17
	6.751	3482	4787	5218	24.00	33.00	35.97
	6.656	14881	15422	14753	102.59	106.32	101.71
	6.561	7986	13209	7966	55.06	91.06	54.92
8	6.441	4295	7071	6892	29.61	48.75	47.51
Chip	6.346	11614	17236	9043	80.07	118.82	62.34
	6.251	9470	11532	10192	65.29	79.50	70.26
	6.156	9010	12360	10192	62.11	85.21	70.26
	6.061	1377	3664	2826	9.49	25.26	19.48
10	5.941	7032	10089	8941	48.48	69.55	61.64
Chip	5.846	10844	12968	10736	74.76	89.40	74.01
	5.751	9010	12845	10519	62.11	88.55	72.52
	5.656	1125	6983	2655	7.76	48.14	18.30
	5.561	8128	9561	8941	56.03	65.91	61.64
12	5.441	8056	12113	10402	55.54	83.51	71.71
Scrub	5.346	7775	10737	10513	53.60	74.02	72.48
	5.251	6838	10039	9140	47.14	69.21	63.01
	5.156	6089	9972	8542	41.98	68.75	58.89
	5.061	11965	13717	12595	82.49	94.56	86.83

**Table 4.28. Resilient Modulus Results: Southbound Lane**

Section	Phase Coordinate	$M_r$			$M_r$		
		1 psi	2 psi	3 psi	1 MPa	2 MPa	3 MPa
1 None	7.880	7569	9762	8637	52.18	67.30	59.54
	7.846	10272	12719	11184	70.82	87.68	77.10
	7.751	9315	12476	9656	64.22	86.01	66.57
	7.656	8786	12352	8442	60.57	85.15	58.20
	7.561	14095	16383	11995	97.17	112.94	82.69
3 Chip	7.441	7777	12962	11759	53.61	89.36	81.07
	7.346	7709	12239	8737	53.15	84.38	60.23
	7.251	10429	12723	12601	71.90	87.71	86.87
	7.156	7100	13212	9343	48.95	91.08	64.41
	7.061	7232	11079	9343	49.86	76.38	64.41
5 Chip	6.941	8635	13086	10295	59.53	90.21	70.97
	6.846	11876	18252	11645	81.87	125.83	80.28
	6.751	5675	9043	7871	39.12	62.34	54.26
	6.656	12960	15697	14097	89.35	108.22	97.18
	6.561	10761	14359	11415	74.19	98.99	78.70
7 Scrub	6.441	8492	14898	11532	58.54	102.71	79.50
	6.346	9626	15829	12117	66.36	109.13	83.53
	6.251	8562	11415	10081	59.03	78.70	69.50
	6.156	8785	15160	9243	60.56	104.51	63.72
	6.061	2091	5229	3897	14.42	36.05	26.87
9 Scrub	5.941	8128	13713	8159	56.03	94.54	56.25
	5.846	9013	11299	12595	62.14	77.90	86.83
	5.751	9547	13589	12595	65.82	93.68	86.83
	5.656	2713	5975	5292	18.70	41.19	36.48
	5.561	7501	12117	10960	51.71	83.53	75.56
11 Scrub	5.441	8128	12476	10624	56.03	86.01	73.24
	5.346	1370	2915	3002	9.44	20.10	20.70
	5.251	7845	10089	8643	54.08	69.55	59.58
	5.156	5011	10413	8152	34.55	71.79	56.20
	5.061	11965	15284	14359	82.49	105.37	98.99

**4.8.2.4 Analysis of  $SN_{New}$  Data**

The delay of an overlay is an additional measure to investigate preservation treatment quality. The new structural capacity required ( $SN_{New}$ ) for the backcalculated  $M_r$  is the required pavement capacity if only the subgrade were in place. Typical  $SN_{New}$  values were calculated between 2.0 to 3.5, with extreme fluctuations of  $M_r$  causing extremes of 1.8 and 4.9. Occasional, yet unrepeated, data showed the need for an overlay. For example, coordinate 6.061 in the southbound lane showed a needed overlay on the order of 25.4 mm (1 in) for phase 1, but the next two phases did not support the need for overlay. These cases are believed to be anomalies. With the traffic data provided by *MDOT*, overlay requirements were practically non-existent and could not differentiate between the test sections.

## CHAPTER 5-SUMMARY CONCLUSIONS AND RECOMMENDATIONS

### 5.1 Summary

The research conducted provides guidance to assist *MDOT* with chip and scrub seals. The information gained from *SS 202* is to be used in *SS 211*, though significant portions of the information can be used in a stand alone fashion. The effectiveness of seal treatments was a key consideration for *SS 202*. Field testing was the primary component of the research; three field tests were conducted on each pavement. The pavements evaluated in this study were *Hwy 17* in Carroll County and *Hwy 35* in Tallahatchie County. Both sections used *PASS-CR* emulsion and 89 limestone from Hover, AL.

*Hwy 17* contained on the order of 30.5 cm (12 in) of base and 8.9 cm (3.5 in) of asphalt. Significant stripping had occurred in many areas. The emulsion application rate for *Hwy 17* was 1.45 L/m<sup>2</sup> (0.32 gal/yd<sup>2</sup>); there was no set aggregate application rate. The test contained twelve sections; two with no treatment, six chip seals, and four scrub seals. Ambient temperatures during the majority of *Hwy 17* construction were near 7.2 C (45 F) and ranged from 5.0 to 14.4 C (41 to 58 F).

The emulsion application rate of *Hwy 35* was 1.36 to 1.45 L/m<sup>2</sup> (0.30 to 0.32 gal/yd<sup>2</sup>) and the aggregate application rate was 7.6 kg/m<sup>2</sup> (14 lb/yd<sup>2</sup>). Six test sections were present, all were scrub seals, two of the seals were placed in 2005, and four of the seals were placed in 2007. For the 2007 sealing, temperatures were 8.9 to 32.2 C (48 to 90 F).

Testing consisted of aggregate retention, skid resistance, *FWD*, rutting, roughness, cracking, and visual assessments. Analysis consisted of data interpretation focusing on trends and statistical analysis using existing methods with exception of *FWD* data. *FWD* data was analyzed with a method developed for this research that combined key elements from the methods of Arkansas, North Carolina, and Texas.

### 5.2 Conclusions

- It is a distinct possibility that *Hwy 17* was cracked too excessively for a seal treatment to be effective. The pavement was significantly cracked prior to application of the treatment with varying types and quantities of cracks. Low to medium cracking is more appropriate for chip and scrub seals. Review of literature indicated that chip seal performance on poor pavements in terms of cracking might not be optimal relative to other methods.
- Temperature control and opening the seal to traffic were less stringent than the best practice findings of *NCHRP Synthesis 342*. Traffic was allowed immediately onto *Hwy 17* after the seal was placed; aggregate could easily be dislodged during this period. Temperatures were cool during placement. Based on literature review, aggregate loss was said to occur more frequently when a chip seal was placed outside the established season. Also, high traffic volumes and heavy vehicles were stated to lead to bleeding/flushing in some cases. The *Hwy 17* northbound lane experienced bleeding/flushing that was significantly higher than the southbound lane. Loaded log trucks were observed heading northbound while the pavement was being tested.

Essentially, the northbound lane of *Hwy 17* provides supporting evidence for all the aforementioned statements.

- Statistics showed bleeding/flushing was greater in the chip seal than in the scrub seal for *Hwy 17*. Bleeding/flushing was not an issue on *Hwy 35*.
- The aggregate retention approach used in this research is superior to the previous *MDOT* method but flaws remain in the approach. An in-situ aggregate retention test method for evaluating a small area over time that is widely used and accepted was not found and is needed.
- Visually the scrub seal sections out performed the chip seal sections on *Hwy 17* in terms of aggregate retention. Aggregate loss values in the lane center were, in general, higher than in the wheel path, but there was no statistically significant evidence to support the observation. There were no statistically significant differences in popouts between chip and scrub seals. The chip seal aggregate retention results were slightly favored over scrub seal results, but the data was far from conclusive.
- No statistically significant differences were detected between aggregate loss in the lane center and wheel path when all *Hwy 35* data was used, but removal of one data point allowed statistically significant differences to be detected where aggregate loss was higher in the lane center. It is borderline whether the aggregate loss was greater in the lane center.
- Rut depths were not significant on *Hwy 17* or *Hwy 35*, but rut depths were greater in the northbound lane of *Hwy 17* indicating heavier traffic heading northbound.
- The outer wheel path of *Hwy 17* and *Hwy 35* was rougher than the inner wheel path but there was no statistical difference in the northbound and southbound lanes based on *IRI* data. There was no compelling evidence that roughness was affected positively or negatively by the seal treatments relative to the sections with no seal treatment.
- *FWD* use for evaluation of seal treatments in past work does not appear as well conceptualized as that used on *Hwy 17*.
- The procedure of Kim et al. (1995) resulted in 5 to 20  $\mu\text{m}$  higher corrected deflections than the AASHTO procedure, which translated to 0.1 to 0.3 less units of structural capacity. The approach of Kim et al. (1995) would be slightly favored over the AASHTO procedure based on its performance on *Hwy 17*.
- $SN_{eff}$  values of *Hwy 17* were generally higher in phase 1 than phase 3 indicating a deteriorating pavement. Variability prevented statistical differences from being detected in the northbound lane even though the mean decrease in  $SN_{eff}$  was much larger for no treatment sections than for sealed sections. In the southbound lane both seal treatments out performed the sections with no treatment and the differences were statistically significant. There was no apparent difference in performance between the chip and scrub seal, only between sealed and non-sealed pavement where sealed pavement was the superior performer.
- Statistical analysis provided evidence that the southbound lane seal treatments were more effective at maintaining structural integrity than the northbound lane seal treatments. The damage to the northbound lane seal could have affected its performance in terms of maintaining structural integrity. The test coordinates cored after testing also supported superior performance of sealed sections.

- An overlay was not found to be needed for added structural capacity at the time of the analysis.
- Based on the performance during testing, scrub seals would be favored over chip seals. Specific statements related to the difference in performance could be as a result of a superior technique, or they could be related to project specific parameters. For example, the emulsion application rate could have been the cause of the superior scrub seal performance. With the data available, the only statement that can be made is that for the conditions encountered scrub seals out performed chip seals.

### 5.3 Recommendations

- Some at *MDOT* have indicated the emulsion application rate may be too high and that the lower end of the acceptable range may warrant investigation. It is recommended to conduct research related to emulsion application rates where a variety of aged pavements are included in the test protocol. Many other parameters could, and perhaps should, be included but evaluation of the emulsion application rate in conjunction with aged pavement is not commonplace and would be useful.
- Some pavement engineers feel that testing recovered binder is not sufficient to evaluate properties of the surface, rather that a mixture test is necessary. *SS 211* is currently conducting near surface mixture tests where emulsion has been applied to field aged specimens. A variety of other tests are being conducted as part of *SS 211* related to emulsion performance when used in seal treatments. It is recommended to await the results of *SS 211*, incorporate the results of *SS 202*, and use the data to plan additional field test sections based on the results obtained.
- The test sections investigated in this report provided valuable data but due to unforeseen events in the early stages of this project they did not incorporate a carefully crafted experimental design. A second field test is thus recommended. Selection of pavements should be performed well ahead of sealing activities by performing a full site investigation, interpreting the results, and ensuring the pavements provide the desired factor and level combinations deemed of interest from the research performed in *SS 202* and *SS 211*. Anticipated parameters to include are: seal treatment type, emulsion application rate, pavement condition, and traffic. Note that upon completion of *SS 211* other parameters may be of higher priority.

## CHAPTER 6-REFERENCES

AASHTO (1986). *AASHTO Guide for Design of Pavement Structures*. American Association of State Highway and Transportation Officials, Washington, D.C.

AASHTO (1993). *AASHTO Guide for Design of Pavement Structures*. American Association of State Highway and Transportation Officials, Washington, D.C.

Alavi, S., LeCates, J.F., and Tavares, M.P. (2008). *Falling Weight Deflectometer Usage*. NCHRP Synthesis 381, National Cooperative Highway Research Program, Washington, D.C.

Anderson, D.A., Meyer, W.E, and Rosenberger, J.L. (1986). "Development of a Procedure for Correcting Skid Resistance Measurements to a Standard End of Season Value," *Transportation Research Record: Journal of the Transportation Research Board*, 1084, 40-48.

Chen, D-H., Lin, D-F., and Bilyeu, J. (2002). "Determination of the Effectiveness of Preventative Maintenance Treatments," *International Journal of Pavement Engineering*, 3(2), 71-83.

Chen, D-H., Bilyeu, J., Lin, H-H., and Murphy, M. (2000). "Temperature Correction on Falling Weight Deflectometer Measurements," *Transportation Research Record: Journal of the Transportation Research Board*, 1716, 30-39.

Coyne, L.D. (1988). "Evaluation of Polymer Modified Chip Seal Coats," *Proceedings of the Association of Asphalt Paving Technologists*, 57, 545-575.

Davis, R.M. (2001). *Comparison of Surface Characteristics of Hot-Mix Asphalt Pavement Surfaces at the Virginia Smart Road*. MS Thesis, Virginia Polytechnic Institute, Blacksburg, VA.

Elliott, R.P., Hall, K.D., Morrison, N.T., and Kong, K.S. (1990). *The Development of ROADHOG-A Flexible Pavement Overlay Design Procedure*. Final Report FHWA/AR-91-003, pp. 178.

Galehouse, L., and O'Doherty, J. (2006). "Anticipation is Sweet," *Pavement Preservation Compendium II*, FHWA Publication FHWA-IF-06-049, pp. 29-32.

Gransberg, D.D. (2009). "Comparing Hot Asphalt Cement and Emulsion Chip Seal Binder Performance Using Macrotecture Measurements, Qualitative Ratings, and Economic Analysis," *Transportation Research Board 88<sup>th</sup> Annual Meeting, Washington, D.C.*, 09-0411.

Gransberg, D.D. (2006). "Correlating Chip Seal Performance and Construction Methods," *Transportation Research Record: Journal of the Transportation Research Board*, 1958, 54-58.

Gransberg, D.D., and James, D.M.B. (2005). *Chip Seal Best Practices*. NCHRP Synthesis of Highway Practice, No 342, Transportation Research Board of the National Academics, Washington, D.C.

Gransberg, D.D., Pidwerbesky, B., and James, D.M.B. (2005). "Analysis of New Zealand Chip Seal Design and Construction Practices," *Transportation Research Circular: Papers from the First National Conference on Pavement Preservation*, No E-C078, 3-15.

Hall, K.D., and Elliott, R.P. (1992). "ROADHOG – A Flexible Pavement Overlay Design Procedure," *Transportation Research Record: Journal of the Transportation Research Board*, 1374, 9-18.

Hall, K.D., and Tran, N.H. (2004). *Improvements to the ROADHOG Overlay Design Program*. Final Report TRC-0209, Arkansas Highway and Transportation Department.

Hank, R.J., and Brown, M. (1949). "Aggregate Retention Studies of Seal Coats," *Proceedings of the Association of Asphalt Paving Technologists*, Vol 18, pp. 261-277.

Hildebrand, G., and Dmytrow, S. (2006). "Looking at Long-Term Results," *Pavement Preservation Compendium II*, FHWA Publication FHWA-IF-06-049, pp. 76-77.

Howard, I.L., and Baumgardner, G. (2009). *US Highway 84 Chip Seal Field Trials and Laboratory Test Results*. Final Report FHWA/MS-DOT-RD-09-202-VI, Mississippi Department of Transportation, pp. 22.

Howard, I.L., Hemsley, J.M., Baumgardner, G.L., and Jordan, W.S. (2009). "Chip and Scrub Seal Binder Evaluation By Frosted Marble Aggregate Retention Test," *Transportation Research Board 88<sup>th</sup> Annual Meeting*, Washington, D.C., Jan 11-15, Paper 09-1662.

Irfan, M., Khurshid, M.B., and Labi, S. (2009). "Service Life of Thin HMA Overlay Using Different Performance Indicators," *Transportation Research Board 88<sup>th</sup> Annual Meeting*, Washington, D.C., 09-2359.

Kim, Y.R., Hibbs, B.O., Lee, Y-C, and Inge, E.H. (1995). *Asphalt Paving Material Properties Affected by Temperature*. Final Report FHWA/NC/95-001, North Carolina Department of Transportation, pp. 178.

Kim, Y.R., Hibbs, B.O., and Lee, Y-C. (1995a). "Temperature Correction of Deflections and Backcalculated Asphalt Concrete Moduli," *Transportation Research Record: Journal of the Transportation Research Board*, 1473, 55-62.

King, H.W. (2007). "Study Shows Reliable Fog, Rejuvenator Seals Underutilized by State DOT's," *Pavement Preservation Journal*, 1(2), 10-12.



- Kuennen, T. (2006). "Pavement Preservation: Techniques for Making Roads Last," *Pavement Preservation Compendium II*, FHWA Publication FHWA-IF-06-049, pp. 12-14.
- Lawson, W.D., and Senadheera, S. (2009). "Chip Seal Maintenance: Solutions for Bleeding and Flushed Pavement Surfaces," *Transportation Research Board 88<sup>th</sup> Annual Meeting*, Paper 09-0659.
- Lee, J. and Kim, Y.R. (2008). "Optimizing the Rolling Protocol for Chip Seals," *Transportation Research Board 87<sup>th</sup> Annual Meeting*, Paper 08-2554.
- NAPA. (2007). *National Asphalt Roadmap: A Commitment to the Future*. National Asphalt Pavement Association Special Report 194, Lanham, MD, pp. 23.
- Orr, D.P., and Irwin, L.H. (2007). *Seasonal Variations of In Situ Materials Properties in New York State*. Final Report RF 55657-01-14, Cornell University, Ithaca, NY, pp. 260.
- Outcalt, W. (2001). *SHRP Chip Seal*. Report CDOT-DTD-R-2001-20, Colorado Department of Transportation, Denver, CO.
- Park, S.W., and Kim, Y.R. (1997). "Temperature Correction of Backcalculated Moduli and Deflections Using Linear Viscoelasticity and Time-Temperature Superposition," *Transportation Research Record: Journal of the Transportation Research Board*, 1570, 108-117.
- Park, H.M., Kim, Y.R., and Park, S. (2002). "Temperature Correction of Multiload-Level Falling Weight Deflectometer Deflections," *Transportation Research Record: Journal of the Transportation Research Board*, No 1806, 3-8.
- Richter, C.A. (2006). *Seasonal Variations in the Moduli of Unbound Pavement Layers*. Final Report FHWA-HRT-04-079, pp. 283.
- Selim, A.A., Ezz-Aldin, M.A. (1990). "Chip Seals, Friction Courses, and Asphalt Pavement Rutting," *Transportation Research Record: Journal of the Transportation Research Board*, 1259, 53-62.
- Shao, L., Park, S.W., and Kim, Y.R. (1997). "Simplified Procedure for Prediction of Asphalt Pavement Subsurface Temperatures Based on Heat Transfer Theories," *Transportation Research Record: Journal of the Transportation Research Board*, 1568, 114-123.
- TNZ. (2002). *Notes for the Specification for Bituminous Reseals*. Transit New Zealand, TNZ P17, Wellington.
- Udelhofen, G. (2006). "It's a Matter of Economics," *Pavement Preservation Compendium II*, FHWA Publication FHWA-IF-06-049, pp. 5-7.

Weissmann, J., and Martino, M.M. (2009). "Evaluation of Seal Coat Performance Using Macro-Texture Measurements," *Transportation Research Board 88<sup>th</sup> Annual Meeting, Washington, D.C.*, 09-2104.

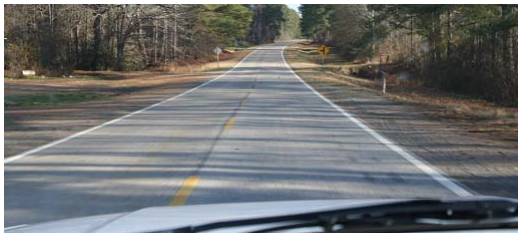
Xu, B., Ranjithan, R.R., and Kim, Y.R. (2002). "New Relationships Between Falling Weight Deflectometer Deflections and Asphalt Pavement Layer Condition Indicators," *Transportation Research Record: Journal of the Transportation Research Board*, 1806, 48-56.

## APPENDIX A-PHOTOS OF TEST SECTIONS

### A.1 Windshield Surveys of Test Sections

Photos were taken of the test sections at approximate intervals of 240 to 365 m (800 to 1,200 ft) and can be seen in the following figures. The photos were taken to allow one to observe the overall test section with both time and distance.

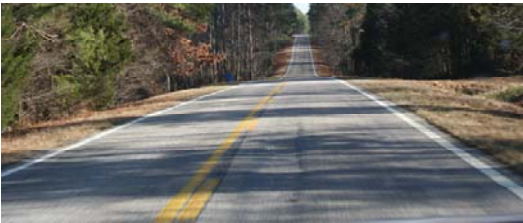
#### A.1.1 Windshield Survey of Hwy 17



(a) Begin Job Heading North 1 of 16



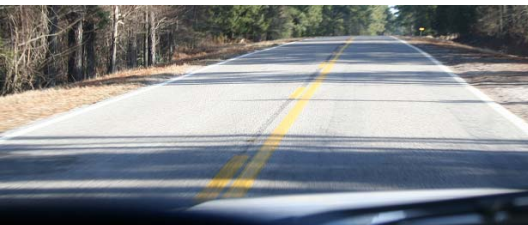
(b) Photo 2 of 16



(c) Photo 3 of 16



(d) Photo 4 of 16



(e) Photo 5 of 16



(f) Photo 6 of 16



(g) Photo 7 of 16



(h) Photo 8 of 16

**Figure A.1. Windshield Survey of Southern Half of Hwy 17 During Test Phase 1: Jan 08**



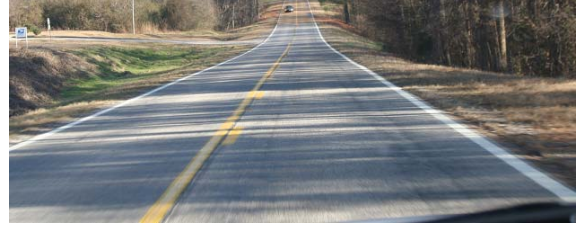
*(a) Middle Job Northbound 9 of 16*



*(b) Photo 10 of 16*



*(c) Photo 11 of 16*



*(d) Photo 12 of 16*



*(e) Photo 13 of 16*



*(f) Photo 14 of 16*



*(g) Photo 15 of 16*



*(h) End Job Photo 16 of 16*

***Figure A.2. Windshield Survey of Northern Half of Hwy 17 During Test Phase 1: Jan 08***



*(a) Begin Job Heading North 1 of 16*



*(b) Photo 2 of 16*



*(c) Photo 3 of 16*



*(d) Photo 4 of 16*



*(e) Photo 5 of 16*



*(f) Photo 6 of 16*



*(g) Photo 7 of 16*



*(h) Photo 8 of 16*

***Figure A.3. Windshield Survey of Southern Half of Hwy 17 During Test Phase 2: Aug 08***



*(a) Middle Job Northbound 9 of 16*



*(b) Photo 10 of 16*



*(c) Photo 11 of 16*



*(d) Photo 12 of 16*



*(e) Photo 13 of 16*



*(f) Photo 14 of 16*



*(g) Photo 15 of 16*



*(h) End Job Photo 16 of 16*

**Figure A.4. Windshield Survey of Northern Half of Hwy 17 During Test Phase 2: Aug 08**



*(a) Begin Job Heading North 1 of 16*



*(b) Photo 2 of 16*



*(c) Photo 3 of 16*



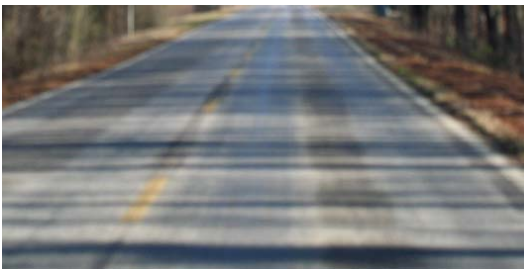
*(d) Photo 4 of 16*



*(e) Photo 5 of 16*



*(f) Photo 6 of 16*



*(g) Photo 7 of 16*



*(h) Photo 8 of 16*

***Figure A.5. Windshield Survey of Southern Half of Hwy 17 During Test Phase 3: Jan 09***



*(a) Middle Job Northbound 9 of 16*



*(b) Photo 10 of 16*



*(c) Photo 11 of 16*



*(d) Photo 12 of 16*



*(e) Photo 13 of 16*



*(f) Photo 14 of 16*



*(g) Photo 15 of 16*



*(h) End Job Photo 16 of 16*

***Figure A.6. Windshield Survey of Northern Half of Hwy 17 During Test Phase 3: Jan 09***



### A.1.2 Windshield Survey of Hwy 35

No windshield survey photos were shown for Hwy 35 during test Phase 3 since the photos were of poor quality and provided no insight to the report. It is believed that a setting on the camera was inadvertently switched, thus making the photos of low resolution.



(a) Begin Job Heading South 1 of 16



(b) Photo 2 of 16



(c) Photo 3 of 16



(d) Photo 4 of 16



(e) Photo 5 of 16



(f) Photo 6 of 16



(g) Photo 7 of 16



(h) Photo 8 of 16

**Figure A.7. Windshield Survey of Northern Half of Hwy 35 During Test Phase 1: Jan 08**



*(a) Middle Job Northbound 9 of 16*



*(b) Photo 10 of 16*



*(c) Photo 11 of 16*



*(d) Photo 12 of 16*



*(e) Photo 13 of 16*



*(f) Photo 14 of 16*



*(g) Photo 15 of 16*



*(h) End Job Photo 16 of 16*

***Figure A.8. Windshield Survey of Southern Half of Hwy 35 During Test Phase 1: Jan 08***



*(a) Begin Job Heading South 1 of 16*



*(b) Photo 2 of 16*



*(c) Photo 3 of 16*



*(d) Photo 4 of 16*



*(e) Photo 5 of 16*



*(f) Photo 6 of 16*



*(g) Photo 7 of 16*



*(h) Photo 8 of 16*

***Figure A.9. Windshield Survey of Northern Half of Hwy 35 During Test Phase 2: Aug 08***



*(a) Middle Job Northbound 9 of 16*



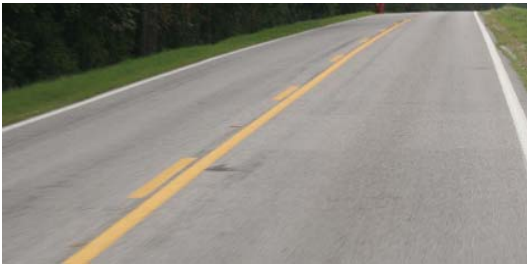
*(b) Photo 10 of 16*



*(c) Photo 11 of 16*



*(d) Photo 12 of 16*



*(e) Photo 13 of 16*



*(f) Photo 14 of 16*



*(g) Photo 15 of 16*



*(h) End Job Photo 16 of 16*

**Figure A.10. Windshield Survey of Southern Half of Hwy 35 During Test Phase 2: Aug 08**

## A.2 Visual Assessments of Test Locations

A photo was taken at each test location during each test phase. These photos were taken to provide a visual representation of the pavement at test locations. The research team and MDOT personnel also performed distress surveys at these locations. The following figures show each test location over the duration of testing.

### A.2.1 Hwy 17 Visual Assessment Photos



(a) Phase 1-Northbound-Jan 2008



(b) Phase 2-Northbound-Aug 2008



(c) Phase 3-Northbound-Jan 2009



(d) Phase 1-Southbound-Jan 2008

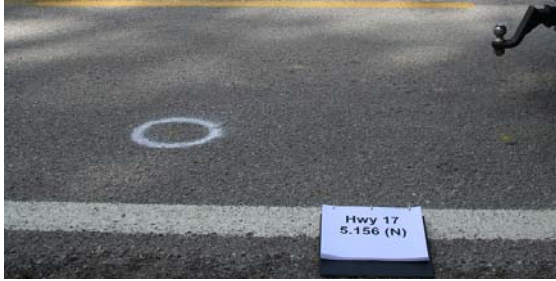


(e) Phase 2-Southbound-Aug 2008

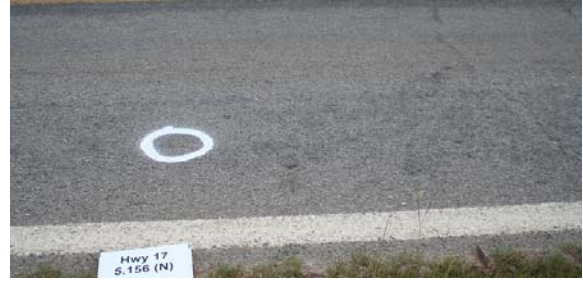


(f) Phase 3-Southbound-Jan 2009

**Figure A.11. Visual Assessment Photos of Hwy 17 Coordinate 5.061**



*(a) Phase 1-Northbound-Jan 2008*



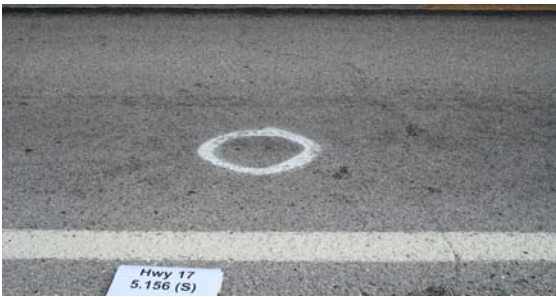
*(b) Phase 2-Northbound-Aug 2008*



*(c) Phase 3-Northbound-Jan 2009*



*(d) Phase 1-Southbound-Jan 2008*



*(e) Phase 2-Southbound-Aug 2008*



*(f) Phase 3-Southbound-Jan 2009*

***Figure A.12. Visual Assessment Photos of Hwy 17 Coordinate 5.156***



*(a) Phase 1-Northbound-Jan 2008*



*(b) Phase 2-Northbound-Aug 2008*



*(c) Phase 3-Northbound-Jan 2009*



*(d) Phase 1-Southbound-Jan 2008*



*(e) Phase 2-Southbound-Aug 2008*



*(f) Phase 3-Southbound-Jan 2009*

***Figure A.13. Visual Assessment Photos of Hwy 17 Coordinate 5.251***



*(a) Phase 1-Northbound-Jan 2008*



*(b) Phase 2-Northbound-Aug 2008*



*(c) Phase 3-Northbound-Jan 2009*



*(d) Phase 1-Southbound-Jan 2008*



*(e) Phase 2-Southbound-Aug 2008*



*(f) Phase 3-Southbound-Jan 2009*

***Figure A.14. Visual Assessment Photos of Hwy 17 Coordinate 5.346***

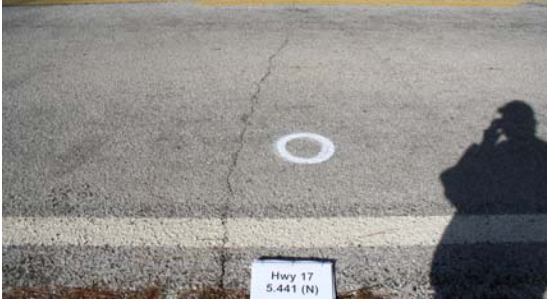




*(a) Phase 1-Northbound-Jan 2008*



*(b) Phase 2-Northbound-Aug 2008*



*(c) Phase 3-Northbound-Jan 2009*



*(d) Phase 1-Southbound-Jan 2008*



*(e) Phase 2-Southbound-Aug 2008*

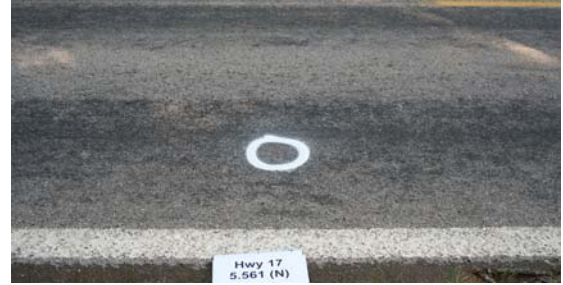


*(f) Phase 3-Southbound-Jan 2009*

***Figure A.15. Visual Assessment Photos of Hwy 17 Coordinate 5.441***



*(a) Phase 1-Northbound-Jan 2008*



*(b) Phase 2-Northbound-Aug 2008*



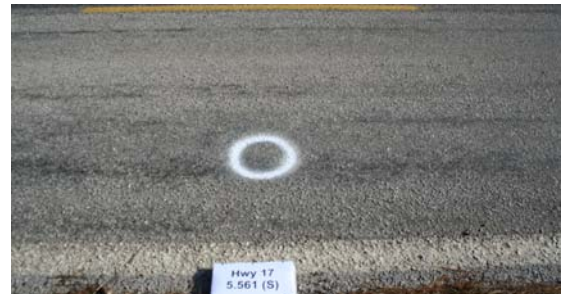
*(c) Phase 3-Northbound-Jan 2009*



*(d) Phase 1-Southbound-Jan 2008*



*(e) Phase 2-Southbound-Aug 2008*

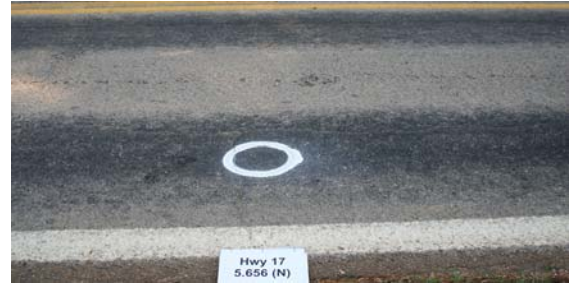


*(f) Phase 3-Southbound-Jan 2009*

***Figure A.16. Visual Assessment Photos of Hwy 17 Coordinate 5.561***



*(a) Phase 1-Northbound-Jan 2008*



*(b) Phase 2-Northbound-Aug 2008*



*(c) Phase 3-Northbound-Jan 2009*



*(d) Phase 1-Southbound-Jan 2008*



*(e) Phase 2-Southbound-Aug 2008*



*(f) Phase 3-Southbound-Jan 2009*

***Figure A.17. Visual Assessment Photos of Hwy 17 Coordinate 5.656***



*(a) Phase 1-Northbound-Jan 2008*



*(b) Phase 2-Northbound-Aug 2008*



*(c) Phase 3-Northbound-Jan 2009*



*(d) Phase 1-Southbound-Jan 2008*

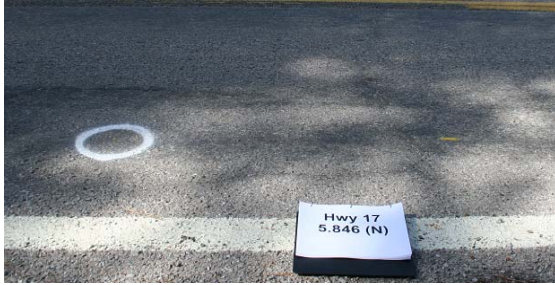


*(e) Phase 2-Southbound-Aug 2008*



*(f) Phase 3-Southbound-Jan 2009*

***Figure A.18. Visual Assessment Photos of Hwy 17 Coordinate 5.751***



*(a) Phase 1-Northbound-Jan 2008*



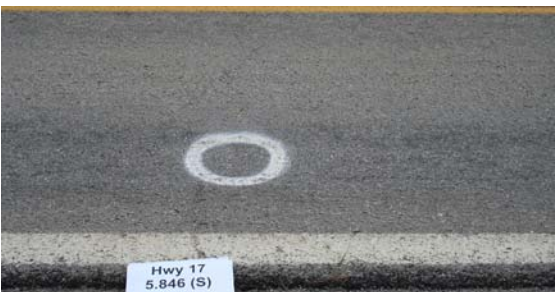
*(b) Phase 2-Northbound-Aug 2008*



*(c) Phase 3-Northbound-Jan 2009*



*(d) Phase 1-Southbound-Jan 2008*



*(e) Phase 2-Southbound-Aug 2008*

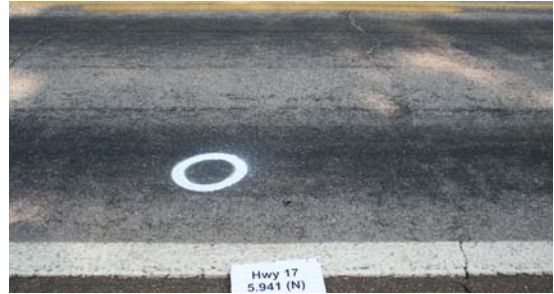


*(f) Phase 3-Southbound-Jan 2009*

***Figure A.19 Visual Assessment Photos of Hwy 17 Coordinate 5.846***



*(a) Phase 1-Northbound-Jan 2008*



*(b) Phase 2-Northbound-Aug 2008*



*(c) Phase 3-Northbound-Jan 2009*



*(d) Phase 1-Southbound-Jan 2008*



*(e) Phase 2-Southbound-Aug 2008*



*(f) Phase 3-Southbound-Jan 2009*

***Figure A.20. Visual Assessment Photos of Hwy 17 Coordinate 5.941***



*(a) Phase 1-Northbound-Jan 2008*



*(b) Phase 2-Northbound-Aug 2008*



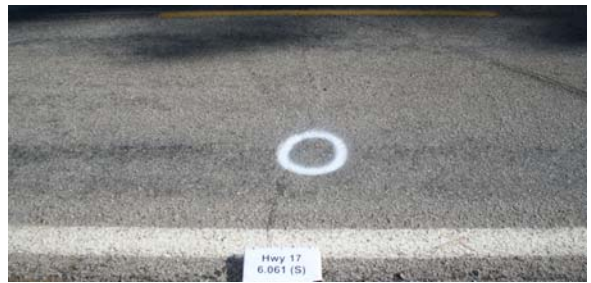
*(c) Phase 3-Northbound-Jan 2009*



*(d) Phase 1-Southbound-Jan 2008*



*(e) Phase 2-Southbound-Aug 2008*



*(f) Phase 3-Southbound-Jan 2009*

***Figure A.21. Visual Assessment Photos of Hwy 17 Coordinate 6.061***



*(a) Phase 1-Northbound-Jan 2008*



*(b) Phase 2-Northbound-Aug 2008*



*(c) Phase 3-Northbound-Jan 2009*



*(d) Phase 1-Southbound-Jan 2008*



*(e) Phase 2-Southbound-Aug 2008*



*(f) Phase 3-Southbound-Jan 2009*

**Figure A.22. Visual Assessment Photos of Hwy 17 Coordinate 6.156**





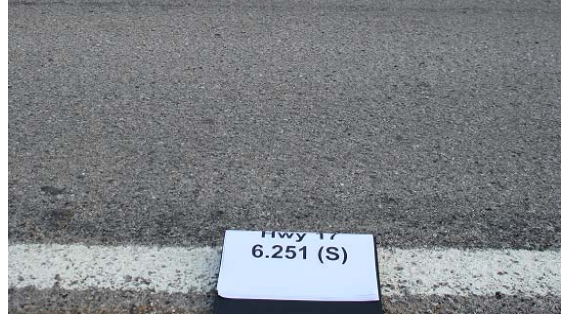
*(a) Phase 1-Northbound-Jan 2008*



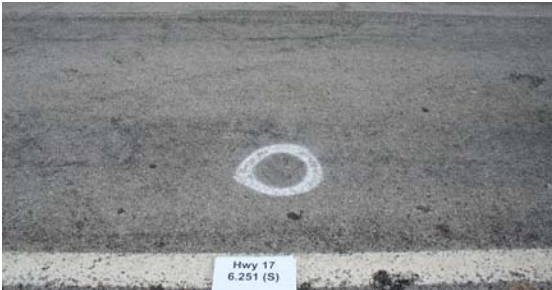
*(b) Phase 2-Northbound-Aug 2008*



*(c) Phase 3-Northbound-Jan 2009*



*(d) Phase 1-Southbound-Jan 2008*



*(e) Phase 2-Southbound-Aug 2008*

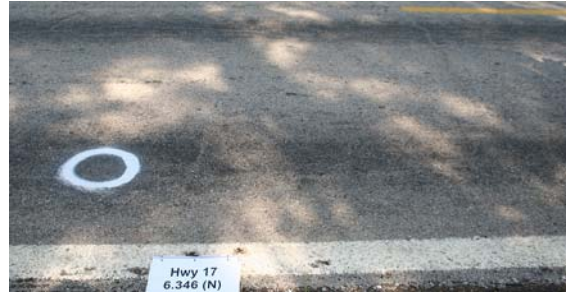


*(f) Phase 3-Southbound-Jan 2009*

***Figure A.23 Visual Assessment Photos of Hwy 17 Coordinate 6.251***



*(a) Phase 1-Northbound-Jan 2008*



*(b) Phase 2-Northbound-Aug 2008*



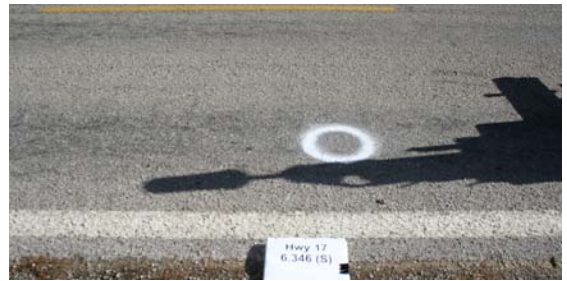
*(c) Phase 3-Northbound-Jan 2009*



*(d) Phase 1-Southbound-Jan 2008*



*(e) Phase 2-Southbound-Aug 2008*



*(f) Phase 3-Southbound-Jan 2009*

***Figure A.24. Visual Assessment Photos of Hwy 17 Coordinate 6.346***



*(a) Phase 1-Northbound-Jan 2008*



*(b) Phase 2-Northbound-Aug 2008*



*(c) Phase 3-Northbound-Jan 2009*



*(d) Phase 1-Southbound-Jan 2008*



*(e) Phase 2-Southbound-Aug 2008*



*(f) Phase 3-Southbound-Jan 2009*

***Figure A.25. Visual Assessment Photos of Hwy 17 Coordinate 6.441***



*(a) Phase 1-Northbound-Jan 2008*



*(b) Phase 2-Northbound-Aug 2008*



*(c) Phase 3-Northbound-Jan 2009*



*(d) Phase 1-Southbound-Jan 2008*



*(e) Phase 2-Southbound-Aug 2008*



*(f) Phase 3-Southbound-Jan 2009*

***Figure A.26. Visual Assessment Photos of Hwy 17 Coordinate 6.561***



*(a) Phase 1-Northbound-Jan 2008*



*(b) Phase 2-Northbound-Aug 2008*



*(c) Phase 3-Northbound-Jan 2009*



*(d) Phase 1-Southbound-Jan 2008*



*(e) Phase 2-Southbound-Aug 2008*

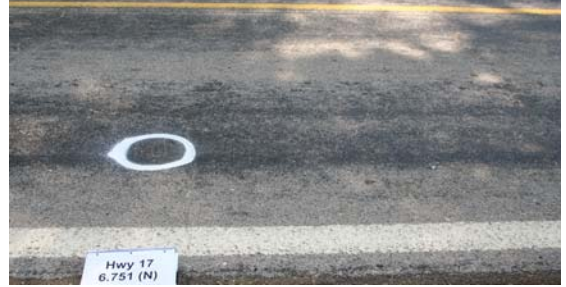


*(f) Phase 3-Southbound-Jan 2009*

**Figure A.27. Visual Assessment Photos of Hwy 17 Coordinate 6.656**



*(a) Phase 1-Northbound-Jan 2008*



*(b) Phase 2-Northbound-Aug 2008*



*(c) Phase 3-Northbound-Jan 2009*



*(d) Phase 1-Southbound-Jan 2008*



*(e) Phase 2-Southbound-Aug 2008*



*(f) Phase 3-Southbound-Jan 2009*

***Figure A.28. Visual Assessment Photos of Hwy 17 Coordinate 6.751***



*(a) Phase 1-Northbound-Jan 2008*



*(b) Phase 2-Northbound-Aug 2008*



*(c) Phase 3-Northbound-Jan 2009*



*(d) Phase 1-Southbound-Jan 2008*



*(e) Phase 2-Southbound-Aug 2008*



*(f) Phase 3-Southbound-Jan 2009*

***Figure A.29. Visual Assessment Photos of Hwy 17 Coordinate 6.846***



*(a) Phase 1-Northbound-Jan 2008*



*(b) Phase 2-Northbound-Aug 2008*



*(c) Phase 3-Northbound-Jan 2009*



*(d) Phase 1-Southbound-Jan 2008*



*(e) Phase 2-Southbound-Aug 2008*



*(f) Phase 3-Southbound-Jan 2009*

***Figure A.30. Visual Assessment Photos of Hwy 17 Coordinate 6.941***





*(a) Phase 1-Northbound-Jan 2008*



*(b) Phase 2-Northbound-Aug 2008*



*(c) Phase 3-Northbound-Jan 2009*



*(d) Phase 1-Southbound-Jan 2008*



*(e) Phase 2-Southbound-Aug 2008*

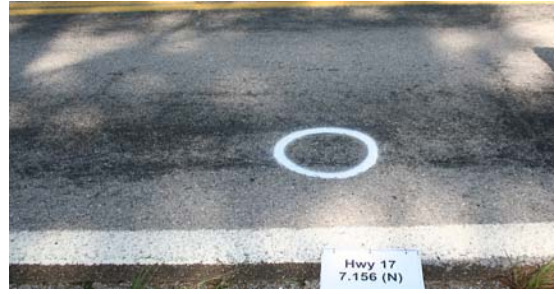


*(f) Phase 3-Southbound-Jan 2009*

***Figure A.31. Visual Assessment Photos of Hwy 17 Coordinate 7.061***



(a) Phase 1-Northbound-Jan 2008



(b) Phase 2-Northbound-Aug 2008



(c) Phase 3-Northbound-Jan 2009



(d) Phase 1-Southbound-Jan 2008



(e) Phase 2-Southbound-Aug 2008



(f) Phase 3-Southbound-Jan 2009

**Figure A.32. Visual Assessment Photos of Hwy 17 Coordinate 7.156**



*(a) Phase 1-Northbound-Jan 2008*



*(b) Phase 2-Northbound-Aug 2008*



*(c) Phase 3-Northbound-Jan 2009*



*(d) Phase 1-Southbound-Jan 2008*



*(e) Phase 2-Southbound-Aug 2008*



*(f) Phase 3-Southbound-Jan 2009*

***Figure A.33. Visual Assessment Photos of Hwy 17 Coordinate 7.251***



*(a) Phase 1-Northbound-Jan 2008*



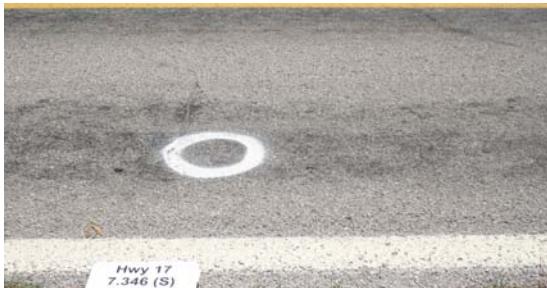
*(b) Phase 2-Northbound-Aug 2008*



*(c) Phase 3-Northbound-Jan 2009*



*(d) Phase 1-Southbound-Jan 2008*



*(e) Phase 2-Southbound-Aug 2008*

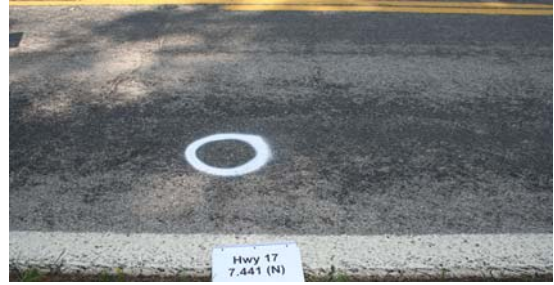


*(f) Phase 3-Southbound-Jan 2009*

***Figure A.34. Visual Assessment Photos of Hwy 17 Coordinate 7.346***



*(a) Phase 1-Northbound-Jan 2008*



*(b) Phase 2-Northbound-Aug 2008*



*(c) Phase 3-Northbound-Jan 2009*



*(d) Phase 1-Southbound-Jan 2008*



*(e) Phase 2-Southbound-Aug 2008*



*(f) Phase 3-Southbound-Jan 2009*

***Figure A.35. Visual Assessment Photos of Hwy 17 Coordinate 7.441***



*(a) Phase 1-Northbound-Jan 2008*



*(b) Phase 2-Northbound-Aug 2008*



*(c) Phase 3-Northbound-Jan 2009*



*(d) Phase 1-Southbound-Jan 2008*



*(e) Phase 2-Southbound-Aug 2008*

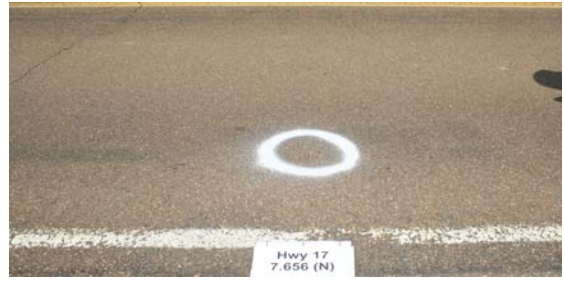


*(f) Phase 3-Southbound-Jan 2009*

***Figure A.36. Visual Assessment Photos of Hwy 17 Coordinate 7.561***



*(a) Phase 1-Northbound-Jan 2008*



*(b) Phase 2-Northbound-Aug 2008*



*(c) Phase 3-Northbound-Jan 2009*



*(d) Phase 1-Southbound-Jan 2008*



*(e) Phase 2-Southbound-Aug 2008*



*(f) Phase 3-Southbound-Jan 2009*

***Figure A.37. Visual Assessment Photos of Hwy 17 Coordinate 7.656***



*(a) Phase 1-Northbound-Jan 2008*



*(b) Phase 2-Northbound-Aug 2008*



*(c) Phase 3-Northbound-Jan 2009*



*(d) Phase 1-Southbound-Jan 2008*



*(e) Phase 2-Southbound-Aug 2008*



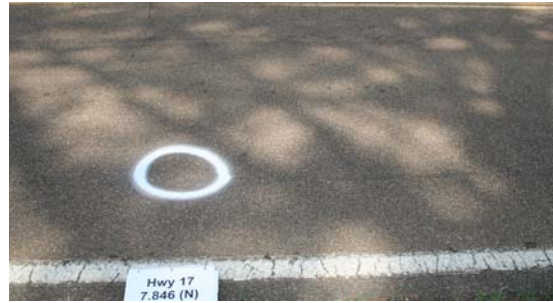
*(f) Phase 3-Southbound-Jan 2009*

***Figure A.38. Visual Assessment Photos of Hwy 17 Coordinate 7.751***





*(a) Phase 1-Northbound-Jan 2008*



*(b) Phase 2-Northbound-Aug 2008*



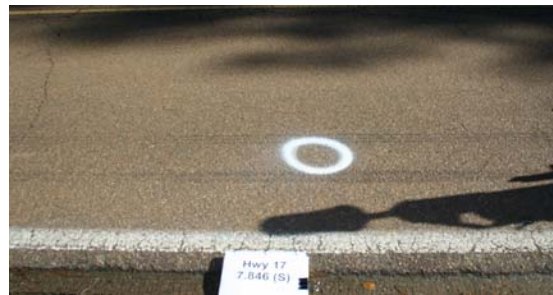
*(c) Phase 3-Northbound-Jan 2009*



*(d) Phase 1-Southbound-Jan 2008*

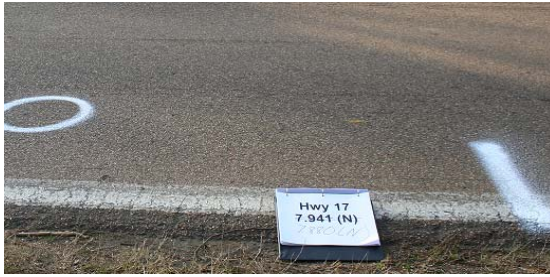


*(e) Phase 2-Southbound-Aug 2008*



*(f) Phase 3-Southbound-Jan 2009*

***Figure A.39. Visual Assessment Photos of Hwy 17 Coordinate 7.846***



*(a) Phase 1-Northbound-Jan 2008*



*(b) Phase 2-Northbound-Aug 2008*



*(c) Phase 3-Northbound-Jan 2009*



*(d) Phase 1-Southbound-Jan 2008*



*(e) Phase 2-Southbound-Aug 2008*



*(f) Phase 3-Southbound-Jan 2009*

**Figure A.40. Visual Assessment Photos of Hwy 17 Coordinate 7.880**

## A.2.2 Hwy 35 Visual Assessment Photos



*(a) Phase 1-Northbound-Jan 2008*



*(b) Phase 2-Northbound-Aug 2008*



*(c) Phase 3-Northbound-Jan 2009*



*(d) Phase 1-Southbound-Jan 2008*



*(e) Phase 2-Southbound-Aug 2008*



*(f) Phase 3-Southbound-Jan 2009*

***Figure A.41. Visual Assessment Photos of Hwy 35 Coordinate 17.868***



*(a) Phase 1-Northbound-Jan 2008*



*(b) Phase 2-Northbound-Aug 2008*



*(c) Phase 3-Northbound-Jan 2009*



*(d) Phase 1-Southbound-Jan 2008*



*(e) Phase 2-Southbound-Aug 2008*



*(f) Phase 3-Southbound-Jan 2009*

***Figure A.42. Visual Assessment Photos of Hwy 35 Coordinate 18.678***



*(a) Phase 1-Northbound-Jan 2008*



*(b) Phase 2-Northbound-Aug 2008*



*(c) Phase 3-Northbound-Jan 2009*



*(d) Phase 1-Southbound-Jan 2008*



*(e) Phase 2-Southbound-Aug 2008*



*(f) Phase 3-Southbound-Jan 2009*

***Figure A.43. Visual Assessment Photos of Hwy 35 Coordinate 18.868***



*(a) Phase 1-Northbound-Jan 2008*



*(b) Phase 2-Northbound-Aug 2008*



*(c) Phase 3-Northbound-Jan 2009*



*(d) Phase 1-Southbound-Jan 2008*



*(e) Phase 2-Southbound-Aug 2008*



*(f) Phase 3-Southbound-Jan 2009*

***Figure A.44. Visual Assessment Photos of Hwy 35 Coordinate 19.678***



*(a) Phase 1-Northbound-Jan 2008*



*(b) Phase 2-Northbound-Aug 2008*



*(c) Phase 3-Northbound-Jan 2009*



*(d) Phase 1-Southbound-Jan 2008*



*(e) Phase 2-Southbound-Aug 2008*



*(f) Phase 3-Southbound-Jan 2009*

***Figure A.45. Visual Assessment Photos of Hwy 35 Coordinate 19.868***



*(a) Phase 1-Northbound-Jan 2008*



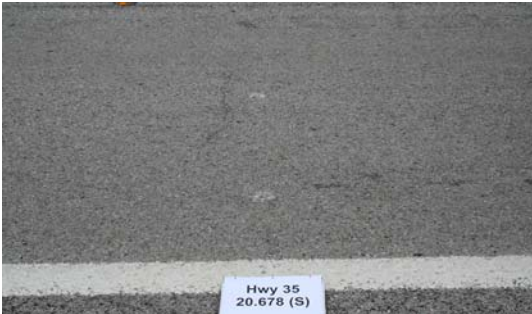
*(b) Phase 2-Northbound-Aug 2008*



*(c) Phase 3-Northbound-Jan 2009*



*(d) Phase 1-Southbound-Jan 2008*



*(e) Phase 2-Southbound-Aug 2008*



*(f) Phase 3-Southbound-Jan 2009*

***Figure A.46. Visual Assessment Photos of Hwy 35 Coordinate 20.678***